Current ripple simulation in DC traction voltage system of an electric bus: 2

Filip Gard
Linda Nilsson

Division of Industrial Electrical Engineering and Automation
Faculty of Engineering, Lund University

Lund Institute of Technology

Master thesis in cooperation with Volvo Buses

Current ripple simulation in DC traction voltage system of an electric bus: 2

Authored by:
Filip Gard || elt12fga@student.lu.se
Linda Nilsson || elt12lni@student.lu.se
Supervisors:
Per Widek || per.widek@volvo.com
Philip Abrahamsson || philip.abrahamsson@iea.lth.se

June 12, 2017

Abstract

Current ripple can cause a lot of problems as it spreads in the DC-side of the TVS of electric and electric hybrid vehicles. Fully knowing the properties of the TVS can be used to build a simulation model to determine the spreading of current ripple beforehand, which in turn is useful for calculating component placement, optimal filter sizes, and component lifetime. Being the second in line of an ongoing chain of thesis projects at Volvo buses, this master thesis proposes methods of measurement, simulation model adjustments, and usage of the finished model. Using an LCR meter, the impedance of several components was measured and modeled in LTSpice based on curve fitted parameters. Comparing the simulated properties to current and voltage levels measured in real vehicles, the accuracy of the models of different buses is presented and validated.

Acknowledgements

A big thank you to our advisor Philip Abrahamsson at the Department of Industrial Electrical Engineering and Automation at Lund University's Faculty of Engineering. Also a big thank you to the entire team at Volvo, especially to our supervisor Per Widek, Oskar Lingnert, and Jens Groot.

For always lending their expertise and time, thank you to Getachew Darge and Lars Lindgren at the Department. A special thank you to Ville Akujärvi, without who the Power Amplifier measurements would never have been performed.

Last but not least, thank you to our examiner Mats Alaküla, senior advisor at Volvo GTT and Professor at the Department of Industrial Electrical Engineering and Automation at Lund University.

Table of Contents

#VOLVO: Some information, such as figures and values marked with #VOLVO are of specific value to Volvo and not for public. Therefore the figures are replaced and the values are concealed.

1.   Introduction

The transport sector is one of the big contributors to global warming and climate change as a result of its carbon dioxide emissions, which account for a third of all greenhouse emissions in Sweden and 14 percent globally. Since transport of people and goods is a prerequisite for growth and welfare in the community it is required that the system in place be replaced. For Sweden, the ambition is to have a vehicle fleet which does not depend on fossil fuels by the year 2030. A more energy efficient, renewable transport system will then be needed in order to combat the increasing emissions of greenhouse gases to the atmosphere. [4]
One way to get there is by electrifying many of the vehicles. Volvo Buses have successfully implemented electric hybrid buses in London and electric buses in Gothenburg and are expanding all over the world. The electrified vehicles, however, are complex and development is expensive. By taking a predictive approach, in which the electrical behavior of buses can be simulated and accounted for before a new bus is actually built, this can change for the better. [16]

1.1 Problem formulation

In an electric or electric hybrid bus, loads such as an EMD, a DC/DC converter, or an air compressor are fed power from the electric storage through the Traction Voltage System (TVS). Connecting the 600 Volt DC-side of the TVS with such a load is a Power Electronic Converter (PEC), which consists of switching IGBTs. With every switching period, a PEC will generate current ripple in its surrounding electric circuit. The frequency of this ripple will therefore be tied to the switching frequency and the modulation of each individual PEC and the amplitude of the ripple, as a previous thesis concluded, depends on the size of the load. Attenuating this current ripple completely is not an easy task and as different applications in the bus are running at the same time, a cacophony of current ripple will spread throughout the 600 Volt DC link that connects them. This has the potential to cause extensive and expensive damage to all components affected, since they might not be designed to handle current ripple of other frequencies and magnitudes than their own. Issues such as thermal fatigue and decreased component lifespan are among the problems which can be caused by current ripple. However, some countermeasures do exist. Different input stages can be applied to the DC-side of each converter in order to attenuate current ripple and cancel out noise. Such input stages typically consist of a DC-link capacitor and a Common Mode (CM) choke. Fully knowing the composition of the 600 Volt DC system in today's buses is essential when optimizing the, size, placement, and lifetime of future components and reducing the time-to-market for new bus models [3]. That is what this master thesis is dedicated to.

1.2 Purpose and aim

During the fall semester of 2016, a master thesis project was carried out with the purpose of building a simulation model for the 600 Volt DC system using LTSpice.[12] The idea then was to split the model into parts, which could then be connected together in new ways in order to determine the behavior of the TVS in both existing and future bus models. Some of the many benefits of a predictive model such as that is the possibility to be able to specify certain requirements to the suppliers and to verify that the electrical system of a new model

works satisfactory before putting it together. As a result of this, vehicle performance, component lifetime, and development costs can be greatly reduced. However, because the master thesis project performed during last fall did not completely meet the requirements with regards to model accuracy; two new thesis projects were formed, this being one of them. The purpose of this project is to further increase the accuracy of the already existing simulation model through meticulous component measurements and adjustments based on data from a bus in operation. These models are then to be verified against the electrical behavior of several different bus models, with the end goal being to end up with a margin of error no larger than 10 percent in component current ripple amplitude. Since the real world TVS is vulnerable not only to a large current ripple, but to certain frequencies as well, it is also verified whether the model can be used to find these resonant frequencies. In the end, the aim is for the simulation model to be used by the entire department at Volvo and updated regularly as components are exchanged for newer versions. For this to be possible, the simulation model has to be both user friendly and flexible.

1.3 Scope and limitations

This thesis, like its predecessor, is limited to the DC-side of the TVS of the electric and electric hybrid buses as well as the new TWIN MOTOR BUS1 and TWIN MOTOR BUS2 buses. Charging of the vehicle, neither while moving nor at standstill, is included in the evaluation of the current ripple. The cables are also excluded with the exception of updating the simulation model based on values provided by the parallel thesis project. By taking part in vehicle measurements performed by Volvo, data which the simulation model is to be verified against is acquired. The worst case component current ripple amplitude of the simulation model should not extend a margin of error greater than 10 percent with regards to the measured current ripple in a real vehicle. Much like in the previous thesis project, some simplifications in the TVS model can be made in order to make it as simple and intuitive as possible. It should also be determined whether such a simplified model could be used to find the resonant frequencies of the TVS. A report containing methodology, results, and conclusions is provided to Volvo at the end of the project. Lastly, as the end product is to be used and updated regularly, the finished model must be highly flexible with regards to component parameters and placement. A manual for how to operate the model is therefore included in the report.

1.4 Thesis outline

In the first chapter, the work leading up to this thesis is briefly presented along with the main underlying motivation and a short description of the planning and execution of the project. In chapter 2 – Theory, most of the theory involved in component modeling and measurements is explained before diving into the TVS of the different buses in chapter 3 – Traction voltage system. There it is explained how the major components are interconnected in the different buses. Zooming in even further, chapter 3 also goes into detail on every one of the major components and explains their equivalent circuits. In chapter 4 – Component measurements and impedance analysis, the system sensitivity to various component parameter changes is presented to determine the focus of the component measurements, which also are presented in

chapter 4. Chapter 5 – Simulation model structure describes how the simulation models for the different buses are updated based on the measurements and curve fitting adjustments. In the following chapter, chapter 6 – Verification, are the comparisons of the simulated current ripple and the current ripple found in the real buses as well as ripple frequency dependency. The conclusion with regards to model accuracy and measurement validity is presented in chapter 7 – Conclusion. Some recommendations for future work are also presented along with a few of the applications for the model.

1.5 Methods

Building on the previous thesis project model, the first steps were to establish which component parameters had a noteworthy influence on the current ripple and to get a good grasp on how that ripple could be affected. This was done by studying the previous thesis work, but also by performing a sensitivity analysis of the simulation system as it was at the beginning of the project. Once components of interest had been established, the work of measuring their true values began. This was attempted using three different measurement methods: the LCR meter, a current transformer in conjunction with a multimeter, and a custom built measurement rig henceforth referred to as the power amplifier measurement. Based on the results from these measurements, the simulation models for the electric and electric hybrid buses were adjusted accordingly, using a curve fitting script in MATLAB and the built in functionality of LTSpice which allows for components to be given equivalent parasitic parameters. The load sources of the model were changed based on the true load behavior of the buses with regards to current to be able to make a realistic comparison. By adjusting the load sources even further the frequency behavior of the model could be tested as well. The simulation models for the new TWIN MOTOR BUS1 and TWIN MOTOR BUS2 were built from scratch using the same component models as in the electric and electric hybrid models. In the case of the electric hybrid bus, the electric bus, and the TWIN MOTOR BUS1, these simulation models were then verified based on the measurements performed on the real vehicles. Finally, a user guide thoroughly explaining how to perform the recommended measurements and adjust the model accordingly was written and provided to Volvo along with this report.

2.   Theory

2.1   Fundamental electrical and CM filter properties

Electrical components and wires can pick up noise of different natures. For the two-conductor setup, the noise presents itself as common mode or differential mode disturbances, both of which can impact the system negatively if not cancelled properly. For this purpose, a choke can be used. As no component is ideal, however, a choke meant to cancel noise can still affect the system in other ways due to its parasitic characteristics.

2.1.1   Impedance

In theory, components such as conductors are often modeled as ideal. In practical applications, however, this is rarely the case, either for conductors or other components. While properties such as inductance in an inductor or capacitance in a capacitor are wanted, these components also have an internal resistance and, in the case of the capacitor, an internal inductance as well (and vice versa, the point here is that parasitic elements have to be accounted for when modeling components accurately). For non-ideal components or RLC-circuits, the proportionality constant impedance consists of a combination of all of these.

Impedance can be expressed as:

$$Z = \frac{U}{I}$$ Equation 1

Here, I is the current passing through the component and U the voltage across its terminals. The impedance Z can in turn be split into two subcomponents: pure resistance as well as the frequency dependent reactance. How resistance and reactance are related to resistance, inductance, and capacitance can be seen in Table 1Table 1 How resistance, reactance and impedance are related.

Table 1 How resistance, reactance and impedance are related

Circuit element	Resistance (R)	Reactance (X)	Impedance (Z)
Resistor	R	0	$Z_R = R = R \angle 0^o$
Inductor	0	ωL	$Z_L = j\omega L = \omega L \angle +90^o$
Capacitor	0	$-\frac{1}{\omega C}$	$Z_C = \frac{1}{j\omega C} = \frac{1}{\omega C} \angle -90^o$

For an ideal resistor, the impedance Z will therefore be equal to R, whereas the impedance of an inductor will be $j\omega L$. Here, ω can be written as:

$$\omega = 2\pi f$$ Equation 2

As seen in Table 1 How resistance, reactance and impedance are related, inductive and capacitive elements in series also have the property of affecting the phase of an AC-signal. It

is said that the instantaneous voltage across an inductor "leads" the current by 90 $^\circ$ while the voltage across a capacitor "lags" the current by 90 $^\circ$. The instantaneous voltage across a pure resistor is not affected at all, and is therefore "in phase" with the current, see Figure 1. The voltage across a series RLC-circuit will thus be made up of a combination of all three voltages. Since these voltages are not in phase with each other, however, the total voltage across the RLC-circuit (or non-ideal component) has to be described as the phasor sum. The result is the voltage triangle based on Pythagoras theorem:

$$V_s = \sqrt{V_R^2 + (V_L - V_C)^2}$$ Equation 3

Where V_s must be positive.
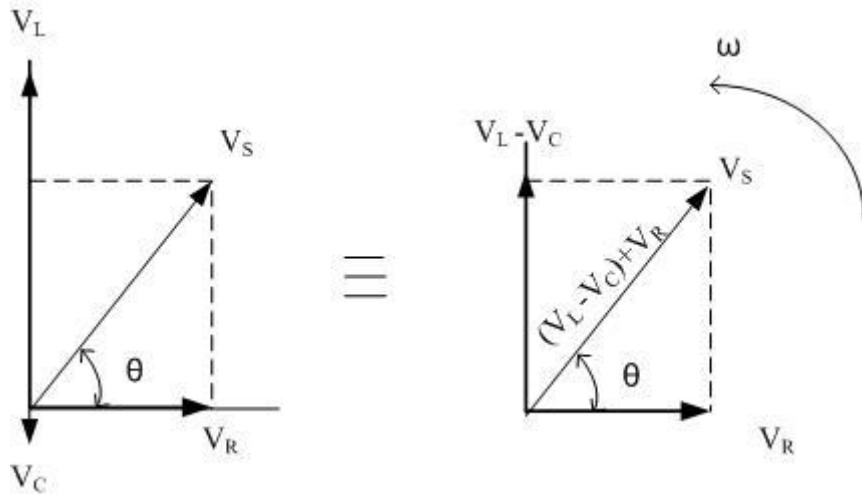
Figure 1 Voltage triangle

Knowing the expressions for resistance and reactance seen in Table 1, the voltages in the voltage triangle can be substituted using resulting in the fundamental expression for series impedance:

$$Z = \sqrt{R^2 + (X_L - X_C)^2} = \sqrt{R^2 + (\omega L - \frac{1}{\omega C})^2}$$ Equation 4

Much like the voltage triangle, the impedance triangle can be drawn as in Figure 2. The phase angle Φ in such a figure is the same angle as the phase difference θ between the instantaneous current and voltage in Figure 1 above. The angle of Φ in the impedance triangle depends on the relationship between X_L and X_C. At the frequency where they are of equal size, resonance occurs (more on that later).
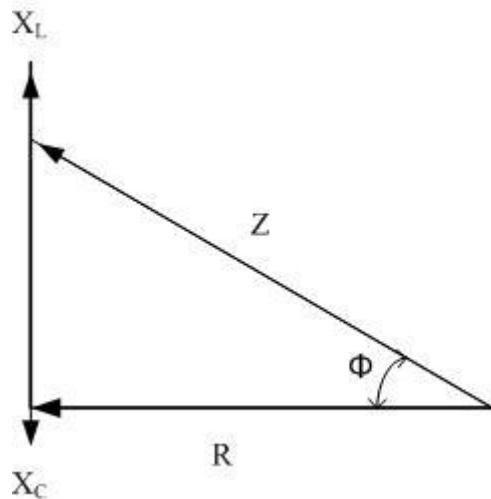
Figure 2 Impedance triangle

Of course, most of the derivations in this chapter are based on the RLC series circuit. Depending on how each physical component is constructed, it may need to be modeled differently in order to represent it accurately. The general principle still holds, however.[7]

Linear Technology, creators of LTSpice, recommends the modeling of capacitors and inductors seen in Figure 3 and Figure 4, respectively. [10][11]
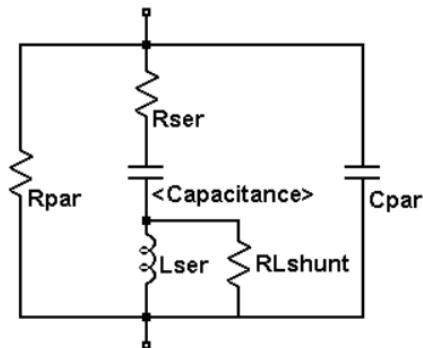

Figure 3 Equivalent circuit of a capacitor
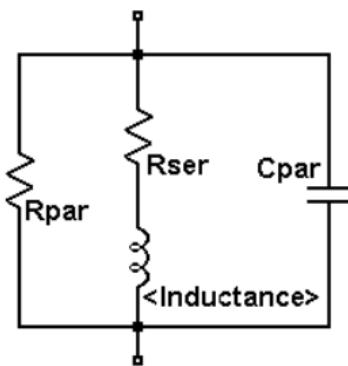
Figure 4 Equivalent circuit of an inductor

2.1.2 Frequency and current dependency in passive components

Physical objects and systems are affected differently by external forces and vibrations based on the frequency of these. For certain frequencies, these vibrations may give rise to oscillations of higher amplitude due to the storing of vibrational energy in the system. These frequencies are known as a system's **resonant frequencies**. There are resonant systems everywhere in nature, but this thesis focuses mainly on resonance and frequency behavior in electrical circuits, which takes the shape of current peaks. As mentioned in chapter 3.1.1, the resonant frequency of a series RLC circuit will occur when $X_L=X_C$. For other frequencies, the circuit will behave as seen in Figure 5 and be capacitive when $X_C>X_L$ and inductive when $X_L>X_C$. In other words, a capacitor with an internal inductance will, for some frequencies, act as an inductor and vice versa. From a simulation modeling perspective, this can be problematic as alternating currents of different frequencies will be affected differently by the circuit. Adjusting for this can be done by modeling not only the main property of major components, but their parasitic elements as well. For capacitors and inductors, this can once again be seen in Figure 3 and Figure 4.
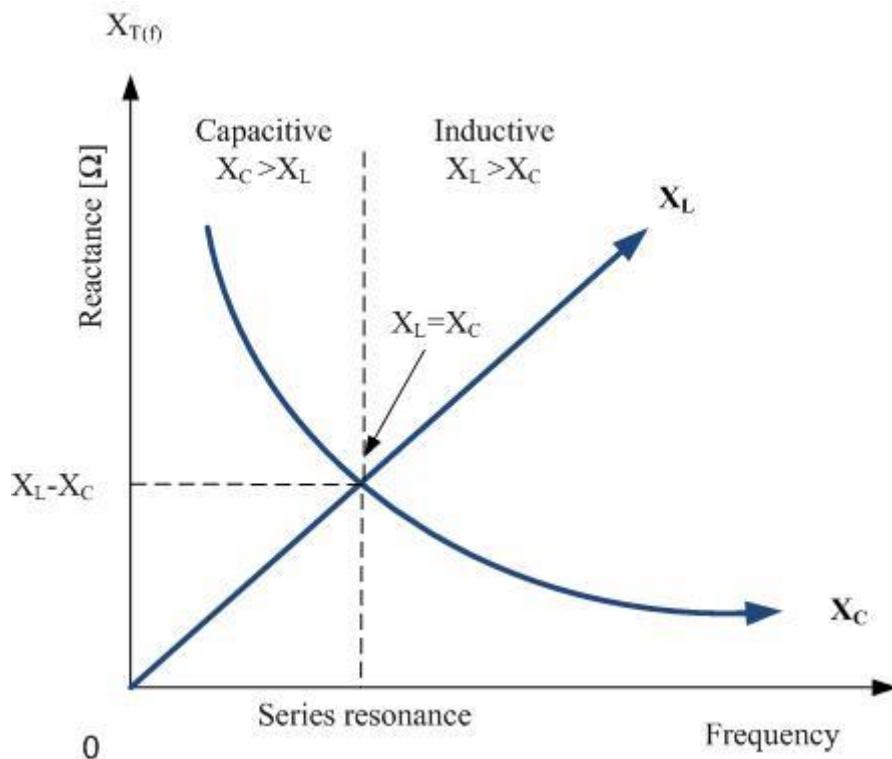

Figure 5 Resonance behavior of electrical components.

At the resonant frequency, the impedance consists solely of the resistance of the circuit. Resistance, however, can also be affected by the frequency of a signal due to the **skin effect**. The skin effect is the result of AC carrying conductors giving rise to a magnetic field not only around it, but inside the conductor itself. These tiny whirls of magnetic fields will counteract

the current flowing in the middle of the conductor and force it to flow mostly along the edges of the conductor (assuming cylindrical shape). The depth at which the current still flows is called the skin depth and it depends on the frequency of the current and the material of the conductor according to equation 5. Because less of the conductor cross section area is being utilized, the resistance of the conductor will rise as a function of frequency. The approximate resulting current flow can be seen in Figure 6.
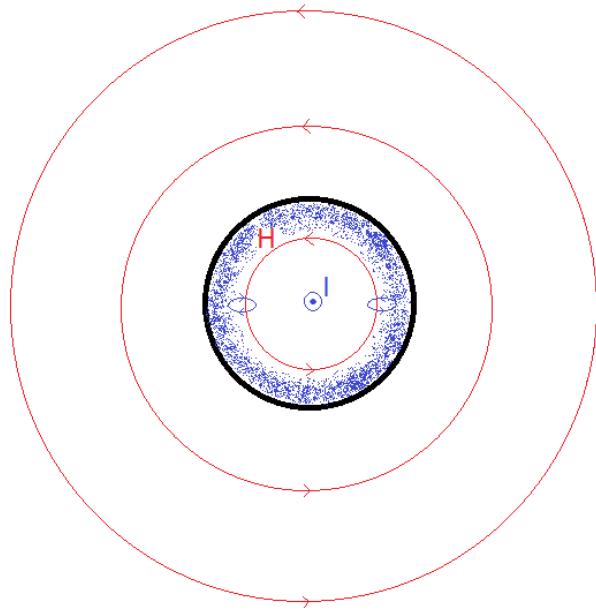

Figure 6 The skin effect visualized. The magnetic field created by the current flow gives rise to eddy currents flowing within the conductor itself. Such eddy currents will limit the current flow to the edges of the conductor, decreasing its cross-section area.

$$\delta = \sqrt{\frac{2}{\omega * \mu_r * \mu_0 * \sigma}}$$
Equation 5

Magnetic fields which affect the properties of a conductor can have other places of origin than the conductor itself, however. Another conductor carrying an alternating current, as seen in Figure 7, can just like the skin effect limit the current flow in certain regions of a conductor, and thereby increase its resistance, by inducing eddy currents in said conductor. This commonly happens when two or more conductors carrying an alternating current are close together and is called the **proximity effect**. In the case of a wound inductor, the different windings will also affect each other due to the proximity effect. Since the current of the nearby conductors will be flowing in the same direction in such an inductor, the current density will be the highest on the far sides of the conductors seen in Figure 7, as opposed to when the current is flowing in different directions in the two conductors. While the cabling of the buses is largely covered by another thesis, the proximity effect in these components still has to be accounted for. [1][6][17]

As current flows through an inductor consisting of windings wound around a core made of a ferromagnetic material, there is also the effect of **core saturation** to consider. A core gets saturated as the magnetic domains of the material it consists of all align themselves with an applied external field. Depending on its application, this effectively sets a lower limit to the size of a ferromagnetic core, as saturation can be avoided by having a large enough core and therefore a large amount of magnetic domains to magnetize. From a circuit perspective, an inductor with a saturated core will have its inductance affected by the current and alternating currents flowing through a saturated core could be a cause of harmonics in the system. As seen in Figure 8, the inductance typically drops rather drastically at the point of saturation. The saturation effect is also noticeable for lower current levels with an increase in temperature, as this causes the magnetic domains to align with an external field more easily. For these reasons, inductors with ferromagnetic cores which are to be used in a TVS must be dimensioned with the current ripple levels in mind (if only there was some way to predict these beforehand).[5][14]
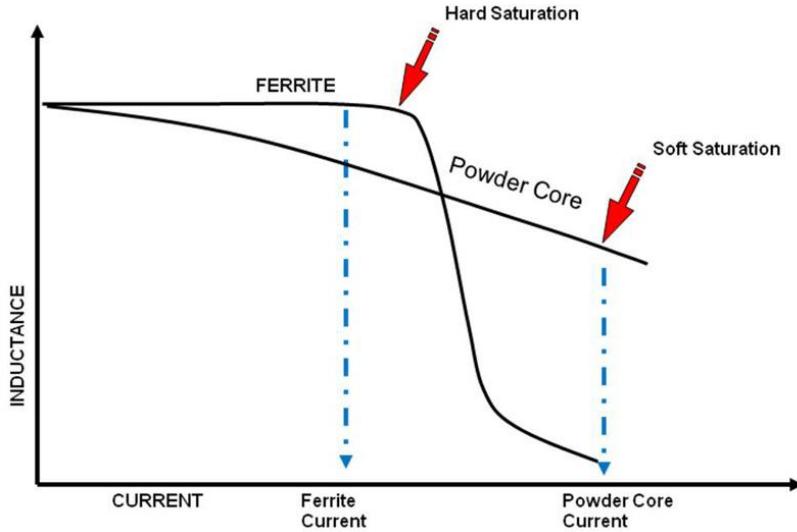
Figure 8 Inductance as a result of saturation in a typical ferrite core.

2.1.3   Common mode noise

Common mode, or CM, noise is picked up by both signal conductors and can be the result of stray transmitter signals, as seen in Figure 9. The voltage level V_{com} of the common mode noise will be of the same phase and magnitude and its current will propagate in the same direction in both conductors. The voltage difference V_{diff} of common mode noise will therefore be 0 at all times between the two conductors, as seen in Figure 10.[13]
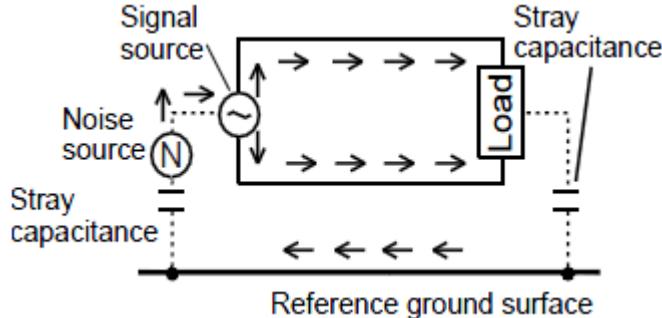

Figure 9 CM noise entering an electric system.

2.1.4   Differential mode noise

Noise that gives rise to currents flowing in opposite directions in the two conductors is known as differential mode noise, henceforth referred to as DM noise or DM currents. DM noise enters the system in the same way as the signal from a signal source, as seen in Figure 11.[13]
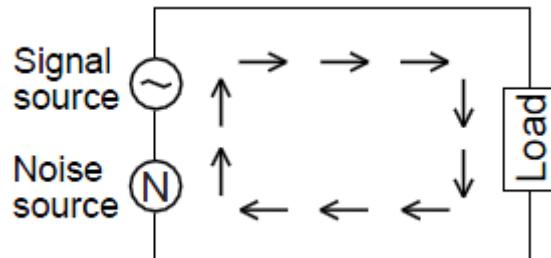

Figure 11 DM noise entering an electrical system.

2.1.5   The CM choke

In order to cancel CM signals, a common mode choke can be used. A choke can be made by winding the two conductors around a common ferrite core as in Figure 12Figure 12. If the conductors are wound in the opposite directions as seen from the same side, i.e. clockwise and anti-clockwise, the choke is a CM choke. As the current passes through one of the conductors, a magnetic field is generated inside the core. If two fields are generated in the same core at the same time, the fields interact with each other. Two opposite fields counteract as the meet, while two fields generated in the same direction add together. For common mode noise, the result is the latter in a CM choke. The CM noise currents each generate a magnetic field in the core which will be circulating in the same direction. This causes the currents to see a high inductance as they enter the choke, which will ideally result in both noise currents canceling. Currents flowing in different directions through the common mode filter, i.e. DM signals will instead cause the magnetic fields of the core to be facing in opposite directions, as seen in Figure 12. If the windings around the core are equal in number of windings the fields will then cancel each other out instead. This theoretically results in a very low or zero inductance for currents passing through the windings.
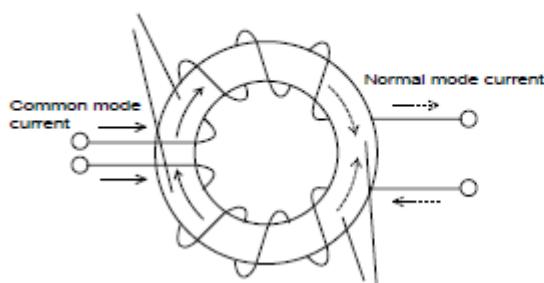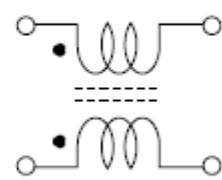

16

However, CM chokes are, like most electrical components, non-ideal. If the windings are not perfectly balanced, for instance, the magnetic fields in the core will not cancel fully. This results in a stray inductance, which typically corresponds to between 2-10 % of the CM inductance. The windings also carry with them a small series resistance as well as a parallel resistance and capacitance. In any electric vehicle, knowing these properties is essential in order to accurately simulate the current ripple of the TVS. [9][15]

2.2   Measurement methods

An LCR meter can be used for various component measurements and provides high accuracy over a broad spectrum of frequencies. It can be set to perform frequency sweeps and store the results automatically and the voltage level can be given a DC bias if needed. It cannot, however, be used in conjunction with an external source providing a larger current flow through the test object. For measuring current dependency over a broad frequency spectrum, a rig consisting of a custom built amplifier generally has to be used instead. Although it does not allow for frequency dependency to be measured, certain measurements can also be performed using a simple current transformer connected through a voltage transformer directly to the electric grid.

2.2.1   LCR-measuring

A typical LCR meter is an instrument used for measuring impedance and its components. The aforementioned impedance vector of an electrical component can be determined by measuring the RMS values of the AC flowing through it, the voltage across its terminals, and the phase difference between them. An LCR meter applying the automatic balance bridge method, as most LCR meters do, can be used to perform these measurements by connecting the target to the terminals of the LCR meter as seen in Figure 13.[8]
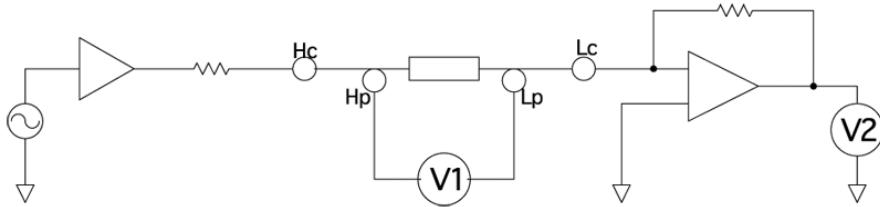
Figure 13 The automatic bridge method circuit design. Hc applies a measurement signal of wanted frequency, which Lc receives and converts into a voltage based on the detected resistance. Hp and Lp marks the high and low potentials of the measurement target.

When performing exact measurements on components with low impedance, residual components in the test fixture come into play. These are unwanted parasitic characteristics which affect the measured values. It can therefore be good practice to correct the measured values by finding these residual components and adjust the measured values accordingly. This is known as open correction and short correction, both of which most LCR meters are designed to handle. In Figure 14, the equivalent circuit for the residual components of a measurement target is shown. [8]
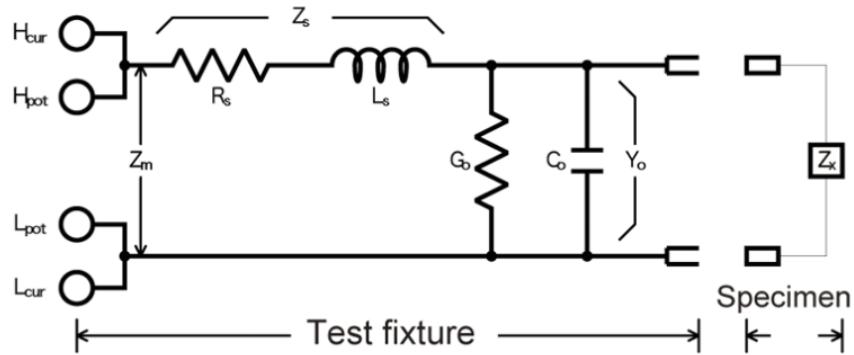
Figure 14 Equivalent circuit for the residual components of the test fixture.

Where Z_m is the measured value, Z_s is the short residual impedance, Y_0 is the residual admittance and Z_x is the true value.

Equation 6 describes the relationship of the measured and residual values.

$$Z_m = Z_s + \frac{1}{Y_0 + \frac{1}{Z_x}} \qquad \text{Equation 6}$$

Practically, an LCR meter can be used to perform measurements on a variety of components such as capacitors, inductors and coils, transformers, piezoelectric elements, and contactless IC cards. The signal frequency can typically be swept ranging from DC to a few hundred kHz and the measured values can be stored on an external drive. However, LCR meters can rarely handle external sources connected to the same sample and as the LCR meter usually does not give off currents higher than a few hundred milliampere, finding the current dependency of the measured component parameters is not possible.

2.2.2 Current transformer

Using a voltage transformer paired with a current transformer, some simple impedance measurements can be performed using an oscilloscope or a multimeter. With the voltage transformer connected to the electric grid and the current transformer connected between the voltage transformer and the specimen, the current flowing through the specimen can be increased significantly. The impedance can then be found using equation 1. In order to determine the ratio of, for instance, resistance and inductance of the measured impedance, it is required to perform some additional measurements as well. Either the phase shift in Figure 2 can be measured directly using an oscilloscope, or the purely resistive part in equation 4 can be found by connecting the specimen to a power box feeding only DC, since ω then becomes zero.
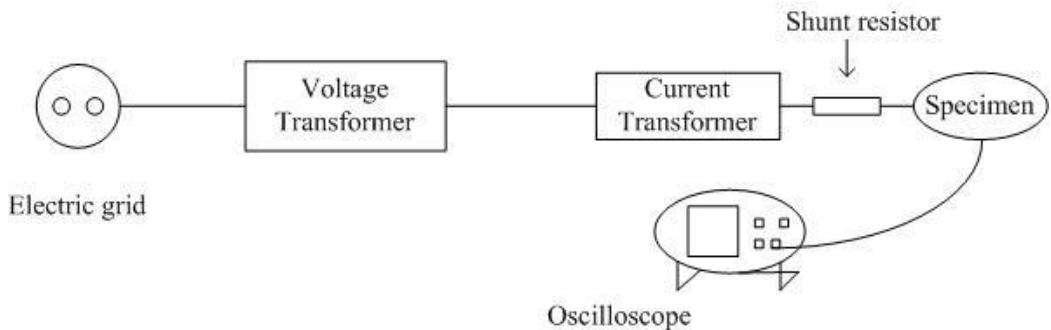
Figure 15 Current transformer setup

This method can be useful when determining the current dependency of the specimen parameters. However, the frequency of the current will be set to the frequency of the grid when using this method. In other words, it is not possible to find the current dependency in conjunction with the frequency dependency of the component parameters.

2.2.3   Power Amplifier measurements

The custom built power amplifier measurement setup shown in Figure 16 was originally designed to measure the properties of wound transformers and inductors with saturated cores, but it can also be used to find both the current and frequency dependency of a load. This, by default, takes all of the issues mentioned in chapter 2.1 into account. Using a computer as controller, a waveform generator can be set to output specific current amplitudes at specific frequencies. As the output levels are set by the waveform generator, a synchronization pulse is sent to a trigg detector, which in turn tells the computer to start the data acquisition. This signal can then be amplified by a power amplifier to generate higher current levels. The current supplied to the load is measured with a precision shunt resistor via a voltage difference amplifier. The load voltage can be measured by first scaling the direct voltage down to levels between ±10 Volt using a LEM LV 25-P. The voltage and current signals can then be acquired by the NI-9223 and stored in the computer. When calculating the impedance based on the current and voltage levels acquired, the scaling factors of the shunt resistor and the LEM have to be taken into consideration.
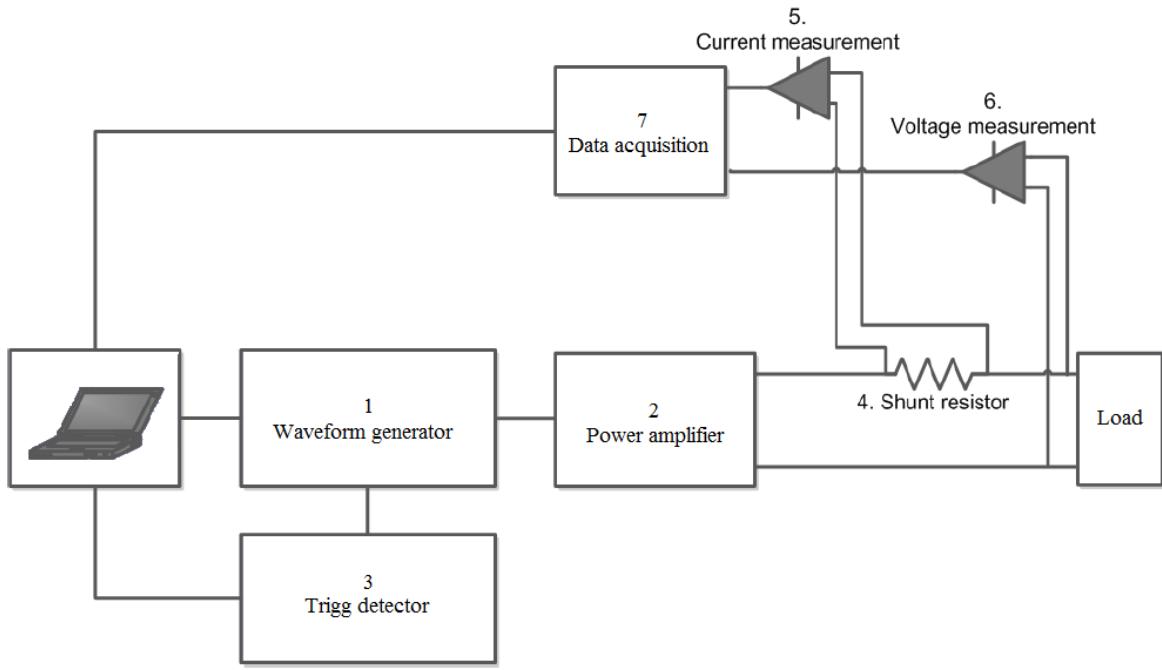
Figure 16 The power amplifier measurement setup

Equipment referenced in Figure 16:
1. Rigol DG1022
2. AE Techron 7796
3. National Instrument USB-6008
4. Ohmite TGHGC0500FE
5. INA117
6. LEM LV 25-P
7. National Instrument NI-9223 @ 1 MS/s

2.2.4   Battery measurements using a current injection transformer

A budget solution to performing measurements on batteries operating at higher voltages is by injecting sinusoidal currents to the battery using a current injection transformer and measuring the voltage and current at the battery terminals. The results of such measurements have been verified using standard Electrochemical Impedance Spectroscopy (EIS) devices by Chalmers University of Technology. For further explanations and measurement setup, see their report. [18]

3.   Traction Voltage System

3.1   Types of Traction Voltage Systems

The Traction Voltage System, TVS, consists of several different subsystems coupled together with cables. All of Volvos bus model are equipped with versions of these utility providing subsystems. What varies between the different bus models, however, is often only the placement of the components and the quantity of components. A further introduction of the different subsystems can be found in Subsystem specification.

3.1.1   Electric hybrid

Figure 17 shows a simplified block diagram of the 600V DC-system for Volvos electric hybrid bus.
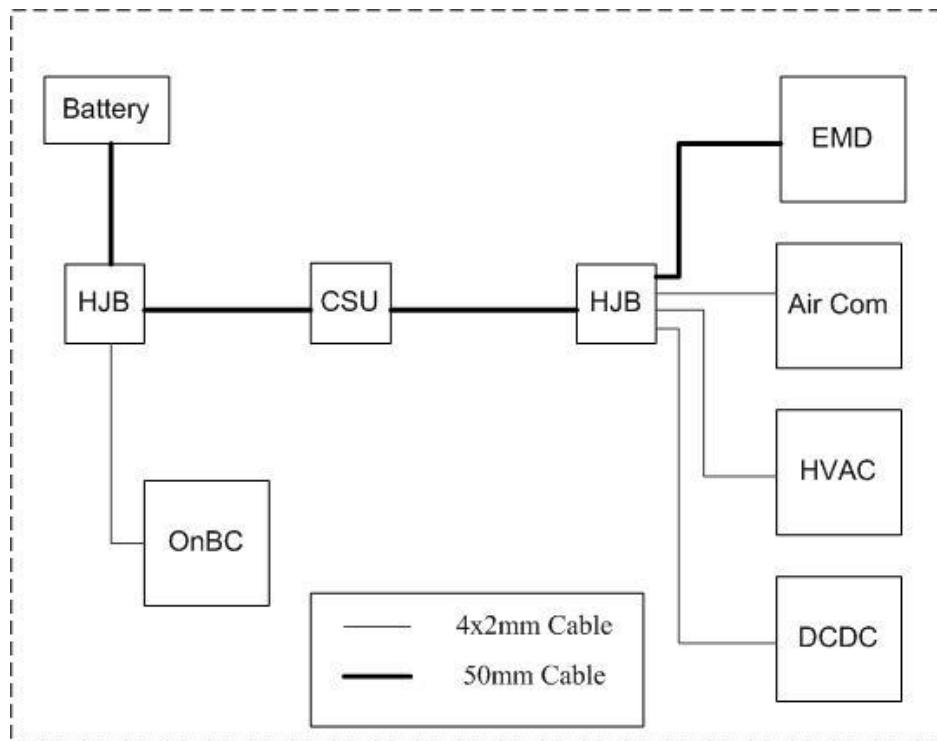
Figure 17 The DC-system for the electric hybrid bus.

3.1.2   Electric

Figure 18 shows a simplified block diagram of the 600V DC-system for Volvos electric bus. As may be expected, the amount of batteries in the electric model is increased in order to allow for the bus to travel longer distances on a single charge. Volvos electric bus platform in figure 2 is currently in use on bus line 55 in Gothenburg, Sweden.
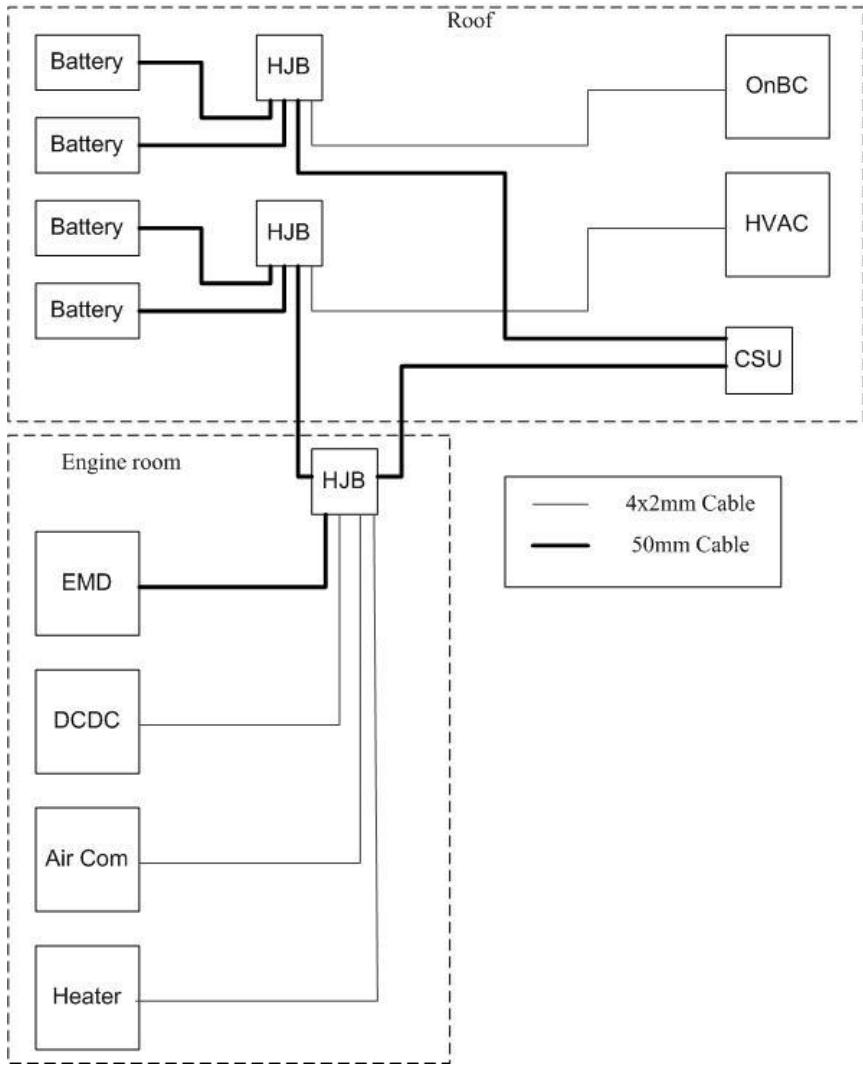
Figure 18 The DC-system for the electric bus.

3.1.3 TWIN MOTOR BUS1

The TWIN MOTOR BUS1 looks and behaves rather differently compared to its predecessors. It is powered only by electricity and sports a carbon chassis so strong that no other structural members are needed. This is not always for the best, however, as the thinner walls and lower floor means less room for components and wiring. Conceptually, the idea is also for the TWIN MOTOR BUS1 to be able to disassemble and assemble in a different fashion, such as adding one or several joints and floor passenger area segments. Because of its unique structure, the driving wheels of the bus have to be powered by different electric machines in order for the bus to make the tight corners. From a current ripple perspective, this can potentially result in new situations depending on how the electric motor drives are controlled.

A block diagram of the electrical system for the basic structure of the TWIN MOTOR BUS1 can be seen in Figure 19.
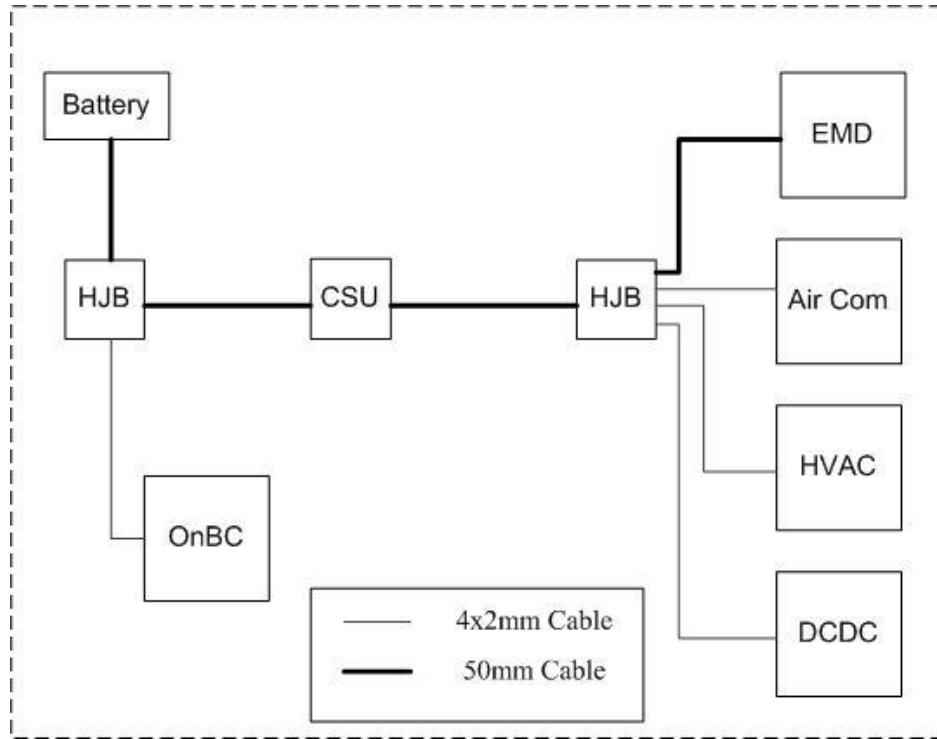
Figure 19 The DC-system for the TWIN MOTOR BUS1 #VOLVO

3.1.4 TWIN MOTOR BUS2

The TWIN MOTOR BUS2 is also powered completely by electricity. Figure 20 shows a simplified block diagram of the 600V DC-system for Volvos Twin Motor bus2.
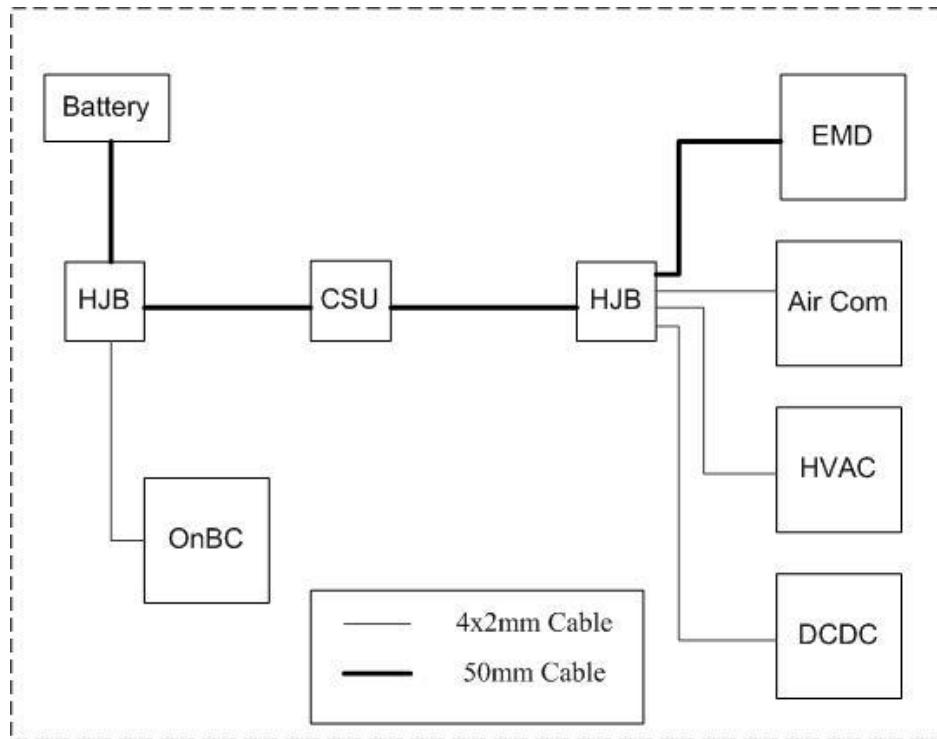

Figure 20 The DC-system for the Twin Motor bus2 #VOLVO

#VOLVO: Some information, such as figures and values marked with #VOLVO are of specific value to Volvo and not for public. Therefore the figures are replaced and the values are concealed.

3.2   Subsystem specification

A number of basic requirements are found in all of Volvos buses. An engine or a **motor** driving the vehicle forward and an energy storage system will cover the most fundamental functions. In the case of the electric or electric hybrid model driving in electric mode, the energy storage system consists of a **battery**. However, the ride would be a rather unpleasant one without the other functions of the TVS. Lights, the control panel and the steering servo are examples of functions powered by a low voltage system operating at 24 V. Connecting this low voltage system to the 600 V system is a **DCDC** converter. Climate control and ventilation is managed by the **HVAC** and an **air compressor** fills up tanks of pressurized air, which can be used to operate the doors and kneel the bus. As there is no combustion engine to provide heat to the passenger section in the winter, an electric **heater** is sometimes used in fully electric vehicles as well. Lastly, an **onboard charger** is used to connect the TVS to a charging station during a low power charge. The different subsystems are connected together by cables in junction boxes as seen previously in the chapter. With the exception of the junction boxes, all of these subsystems are equipped with filter components which affect the properties of the TVS and the spreading of current ripple. Building on the previous project, the load subsystems are equipped with current sources which represent their respective PECs.

3.2.1   MDS- Motor Drive System

Perhaps the biggest difference between a conventional vehicle and an electric is the propulsion system. Electric machines as traction motors can be used for both propulsion and braking, and provides high torque even at low speeds. Because the machine can work both as a motor and a generator, the energy storage system can be replenished when applying the brakes. The electric machines in both the electric and the electric hybrid are permanently magnetized synchronous machines. The PEC's in their respective models are equipped with different filter components. Motor specifications can be seen in Table 2 and Table 3. For 600 V, the base speed presented is based on the maximum power of #VOLVO kW in the case of the electric hybrid bus and #VOLVO kW in the case of the electric bus, according to the supplier.

Table 2 Specification values for the EMD typ b

Converter type	#VOLVO
Switching Frequency	#VOLVO
Converter load type	#VOLVO
Converter load power	#VOLVO
Electric Machine base speed	#VOLVO

Table 3 Specification values for the EMD typ c

Converter type	#VOLVO
Switching Frequency	#VOLVO
Converter load type	#VOLVO

#VOLVO: Some information, such as figures and values marked with #VOLVO are of specific value to Volvo and not for public. Therefore the figures are replaced and the values are concealed.

Converter load power	#VOLVO
Electric Machine base speed	#VOLVO

3.2.2 DCDC – Direct Current Converter

The DCDC converter is used to supply the low voltage side loads with power. Lights, panels, steering servo, etc. make up a total maximum load of #VOLVO kW, as seen in Table 4. The lowest voltage applied to reach full power can be used to calculate the converters duty cycle.

Table 4 Specification values for the DCDC

Converter type	#VOLVO
Switching Frequency	#VOLVO
Converter load type	#VOLVO
Converter load power	#VOLVO
Lowest voltage applied for full performance	#VOLVO

3.2.3 Air compressor

The air compressed by the air compressor is used to kneel the bus, brake, and operate the doors is also driven by an electric machine. The specifications for the PMSM used in this application can be seen in Table 5. The lowest voltage applied to reach full power can be used to calculate the converters duty cycle.

Table 5 Specification values for the Air Compressor

Converter type	#VOLVO
Switching Frequency	#VOLVO
Converter load type	#VOLVO
Converter load power	#VOLVO
Electric Machine base speed	#VOLVO
Lowest voltage applied to reach base speed	#VOLVO

3.2.4 HVAC - Heat Ventilation and Air Conditioning

The HVAC system is used to control the climate of the bus with regards to temperature and ventilation. It is powered by an induction machine, which operates as shown in Table 6. The lowest voltage applied to reach full power can be used to calculate the converters duty cycle.

Table 6 Specification values for the HVAC

Converter type	#VOLVO
Switching Frequency	#VOLVO
Converter load type	#VOLVO
Converter load power	#VOLVO

Electric Machine base speed	#VOLVO
Lowest voltage applied to reach base speed	#VOLVO

3.2.5   Heater

Electric vehicles do not produce enough waste heat to keep the temperature of the passenger area at a comfortable level during winter. For this purpose, an electric heater is installed in Volvos fully electric vehicles. The heater operates at #VOLVO kW.

3.2.6   OnBC - On Board Charger

While the low power on board charger is only active while the vehicle is at standstill, its filter components still affect and are affected by the current ripple when the loads are active. Charging using the On Board Charger is not considered in this thesis.

3.2.7   Cable

Connecting the different components are the cables. The cables are dimensioned based on the power of the component they are connected to. Volvo's bus department uses 50 mm^2 cables for the batteries and the EMD, and 2x4 mm^2 cables for the other loads. Cable measurements are mainly performed as part of a separate thesis project.

3.2.8   ESS - Energy Storage System

In the existing bus models for Volvo's electric and electric hybrid vehicles, a SAFT battery is used as energy storage system. It has a nominal battery voltage of 633 Volt and a nominal capacity of #VOLVO Ah and consists of 16 Li-ion modules in series, each containing 12 battery cells. Larger batteries typically exhibit a circuit behavior based on the characteristics of the battery cells for lower frequencies and the battery rig for higher frequencies.

3.2.9   HJB – Hybrid Junction Box

The hybrid junction box serves as a merge point for cables and contains fuses. It contains no other components and is not included in this thesis for evaluation.

3.2.10   CSU – Charging Switch Unit

The charging switch unit connects the TVS to the charging rails. Other than the cables connected to it, it does not contain any impactful components and is not included in this thesis for evaluation either.

4. Component measurements and impedance analysis

As a first step of getting to know the system and identifying components of interest, a sensitivity analysis was performed on the existing model.

As a certain frequency behavior was expected, LCR measurements were performed in order to find the impedance as a function of frequency ranging from 100 Hz to 300 kHz. A curve fitting script in MATLAB was used in order to find the equivalent series and parallel parameters of the different components. The starting values provided to the script were found by using the LCR meter's function to measure equivalent parameter values.

Measurements using a current transformer operating at grid frequency were performed as an early attempt at finding the current dependency of the common mode choke values. The inductance and series resistance were found either by measuring the DC resistance and calculating the inductance using Pythagoras' theorem or by measuring the phase shift directly.

The Power Amplifier measurements were performed at the institute of industrial production at LTH. Using their custom built rig seen in Figure 16, the impedance was measured as a function of both frequency and current.

All measurements were performed on the DM properties of the components.

4.1 Sensitivity analysis

As the preexisting model was somewhat uncertain with regards to both component values and model design, a simple sensitivity analysis was performed on the existing simulation model in order to provide insight into how component changes affected the ripple. Together with an estimation of which components were most likely to differ from their given values and which components were available, the focus of the measurements was determined. The components to measure based on the sensitivity analysis and availability are presented in Table 7.

Table 7 Result from the sensitivity analysis

Subsystem	Component(s) to measure
EMD type b	CM choke (DM properties) DC-link capacitor
EMD type c	CM choke (DM properties) DC-link capacitor
DCDC	CM choke (DM properties)
Air compressor	CM choke (DM properties)
HVAC	CM choke (DM properties)
OnBC	CM choke (DM properties)
Battery	Entire rig
Cables	Entire cable (separate thesis project)

4.2   LCR measurements

Using the LCR meter, both the impedance and its reactive and resistive components were measured as a function of frequency. Entering these values into the curve fitting script as starting values provided equivalent component values which in turn yielded the total impedance wanted for all frequencies. Schematics for all of the components see chapter 0.

4.2.1   EMD type B

In the hybrid bus EMD, measurements were performed on the CM choke and the DC-link capacitors. The measured impedance as a function of frequency of the EMD type b capacitor is shown in Figure 22 along with the fitted lines based on the impedance of the capacitor model seen in Figure 3. Figure 25 shows the measured impedance as a function of frequency of the CM choke as well as the fitted curves based on the impedance of the circuit seen in Figure 4. The measured values from Figure 23 were used as reference to the curve fitting. Table 9 shows the values of the equivalent series and parallel components for the CM choke. The values for the equivalent components of the capacitor are shown in Table 8. The values for the capacitor were measured by utilizing the DC-bias function of the LCR meter.

Table 8 Result of the curve fitting for the DC-link capacitance in EMD typ b

DC_link Capacitance	C	Rser	Lser	Rpar	Cpar	RLshunt
	#VOLVO	#VOLVO	#VOLVO	#VOLVO	#VOLVO	#VOLVO
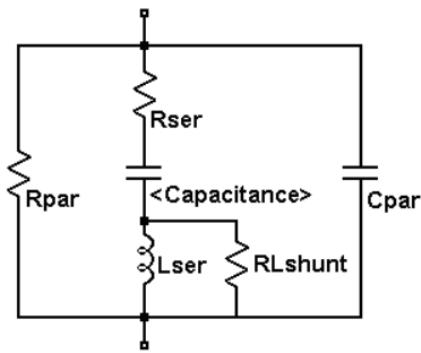
Figure 21 (Figure 3 Equivalent circuit of a capacitor

Impedance as a function of frequency for the DC-link Capacitor in EMD$_B$
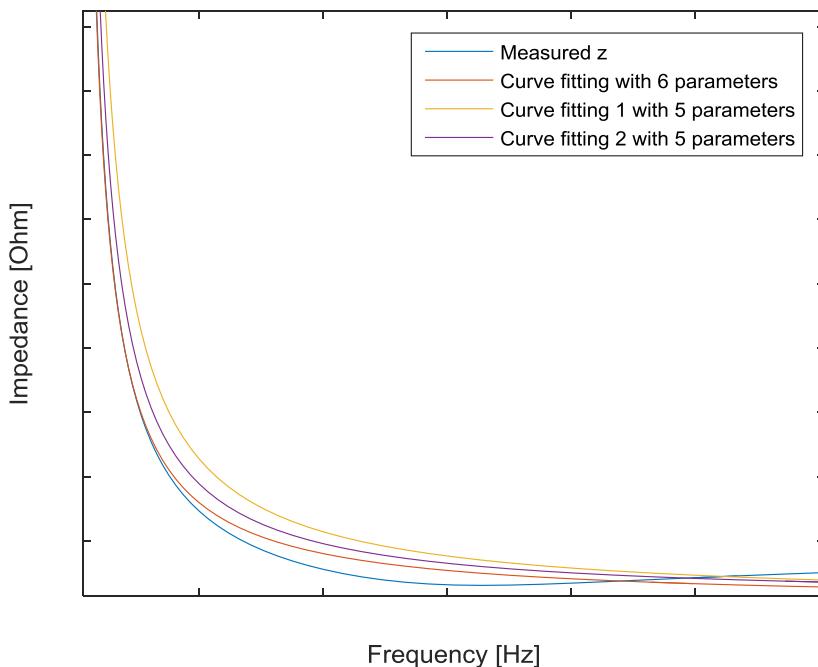
Figure 22 Curve fitting of the DC-link capacitance in EMD type b

Leakage inductance of the EMD type B choke

×10⁻⁶

Inductance [H]

Frequency [Hz]

Series resistance of the EMD type B choke

Resistance [Ohm]

Frequency [Hz]
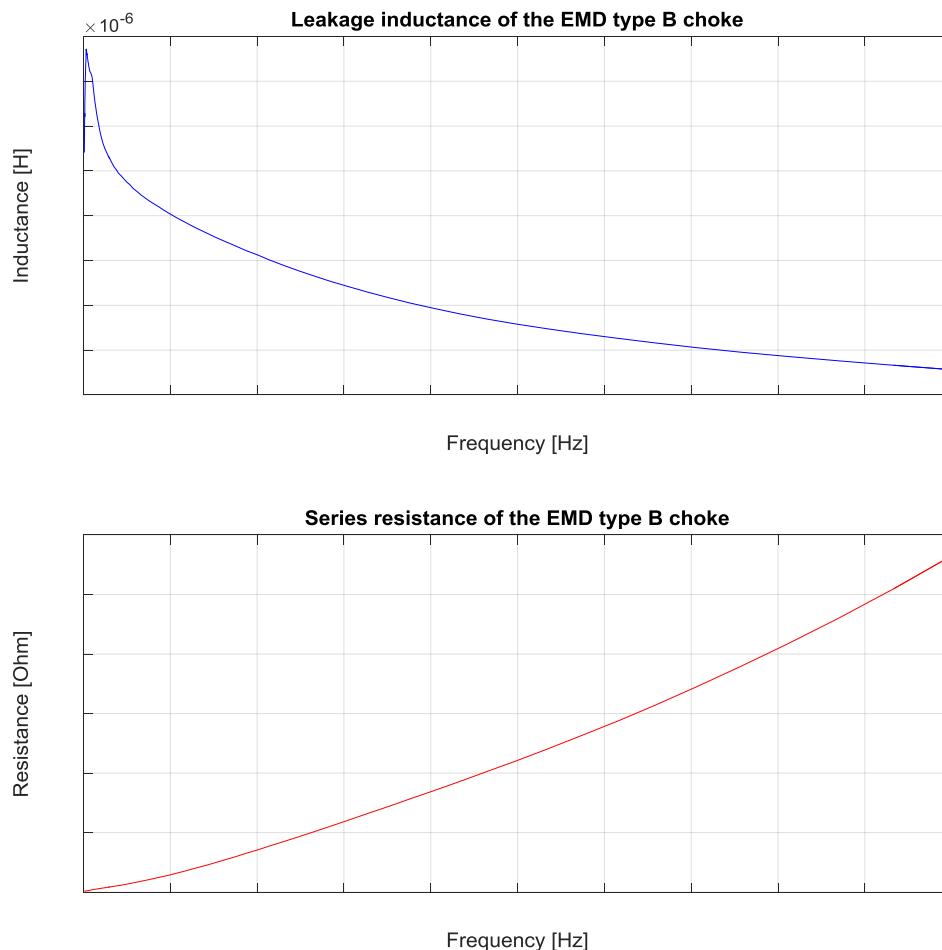
Figure 23 The Inductance and Resistance in the CM choke in EMD type b

Table 9 Result of the curve fitting for the CM-choke in EMD type b

CM-choke	L	Rser	Cpar	Rpar
	#VOLVO	#VOLVO	#VOLVO	#VOLVO
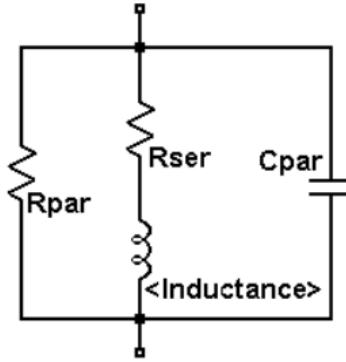
Figure 24 (Figure 4 Equivalent circuit of an inductor

Impedance as a function of frequency for the CM-choke in EMD$_B$
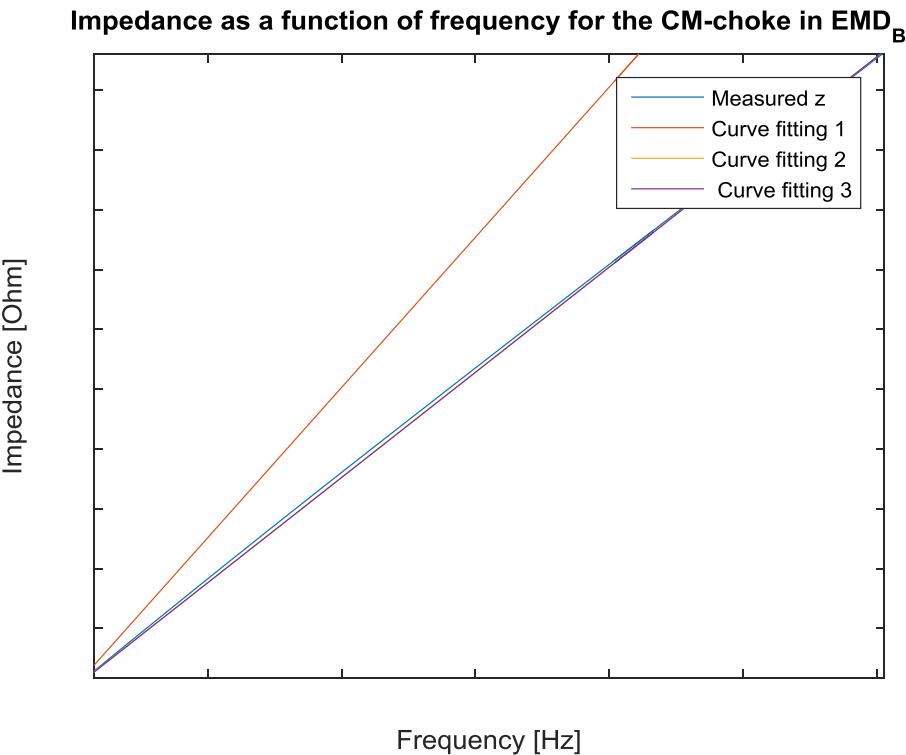
Figure 25 Curve fitting of the CM-choke in EMD type b

4.2.2 EMD type C

For the EMD type c, measurements were performed to find the impedance as a function of frequency of the CM choke and DC-link capacitor. The impedance of the CM choke is plotted in Figure 27 along with the curve fitting impedance based on the equivalent circuit of an inductor seen in Figure 4. The equivalent circuit parameters are shown in Table 11. The measured DC-link capacitor impedance and its fitted curves are shown in Figure 26. Its impedance is based on the equivalent circuit of a capacitor seen in Figure 3 with the values presented in Table 10. The values for the capacitor were measured by utilizing the DC-bias function of the LCR meter.

DC_link Capacitance	C	Rser	Lser	Rpar	Cpar	RLshunt
	#VOLVO	#VOLVO	#VOLVO	#VOLVO	#VOLVO	#VOLVO

Impedance as a function of frequency for the DC-link Capacitor in EMD$_c$

Figure 26 Curve fitting of the DC-link capacitance in EMD type c

Table 11 Result of the curve fitting for the CM-choke in EMD type c (equivalent circuit Figure 24)

CM-choke	L	Rser	Cpar	Rpar
	#VOLVO	#VOLVO	#VOLVO	#VOLVO

#VOLVO: Some information, such as figures and values marked with #VOLVO are of specific value to Volvo and not for public. Therefore the figures are replaced and the values are concealed.

Impedance as a function of frequency for the CM-choke in EMD$_C$
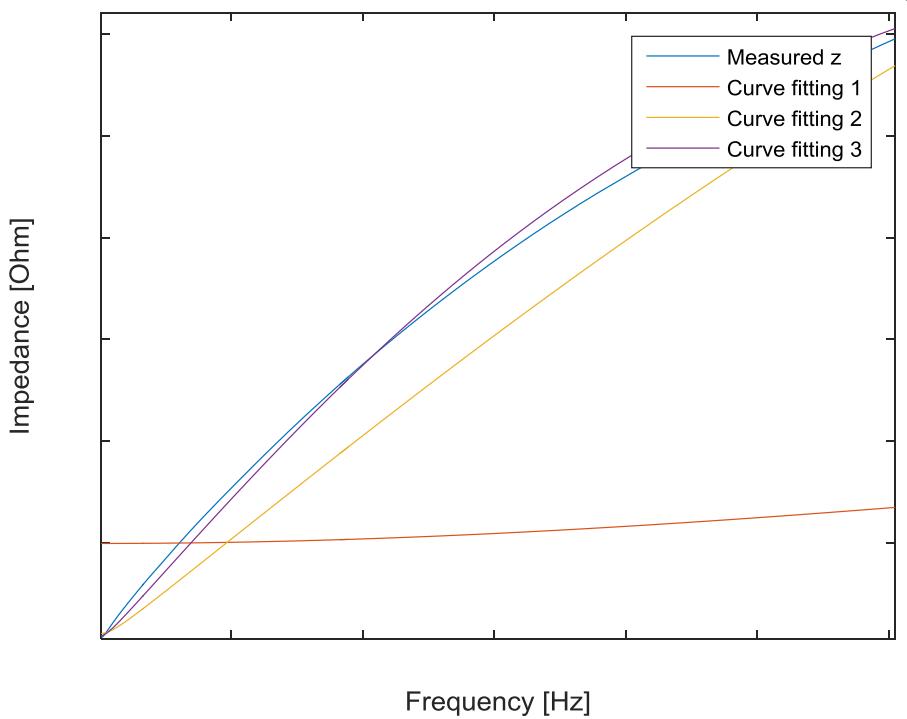
Figure 27 Curve fitting of the CM-choke in EMD typ c

4.2.3   DCDC

In the DCDC, only the CM choke was available without permanently destroying the circuit board. Impedance measurement results are shown in Figure 29 along with the curve fitting plots based on the equivalent circuit in Figure 4. The measured values in Figure 28 were used as reference values to the curve fitting. The equivalent circuit component values are shown in Table 12.

Leakage inductance of the DCDC choke

Series resistance of the DCDC choke
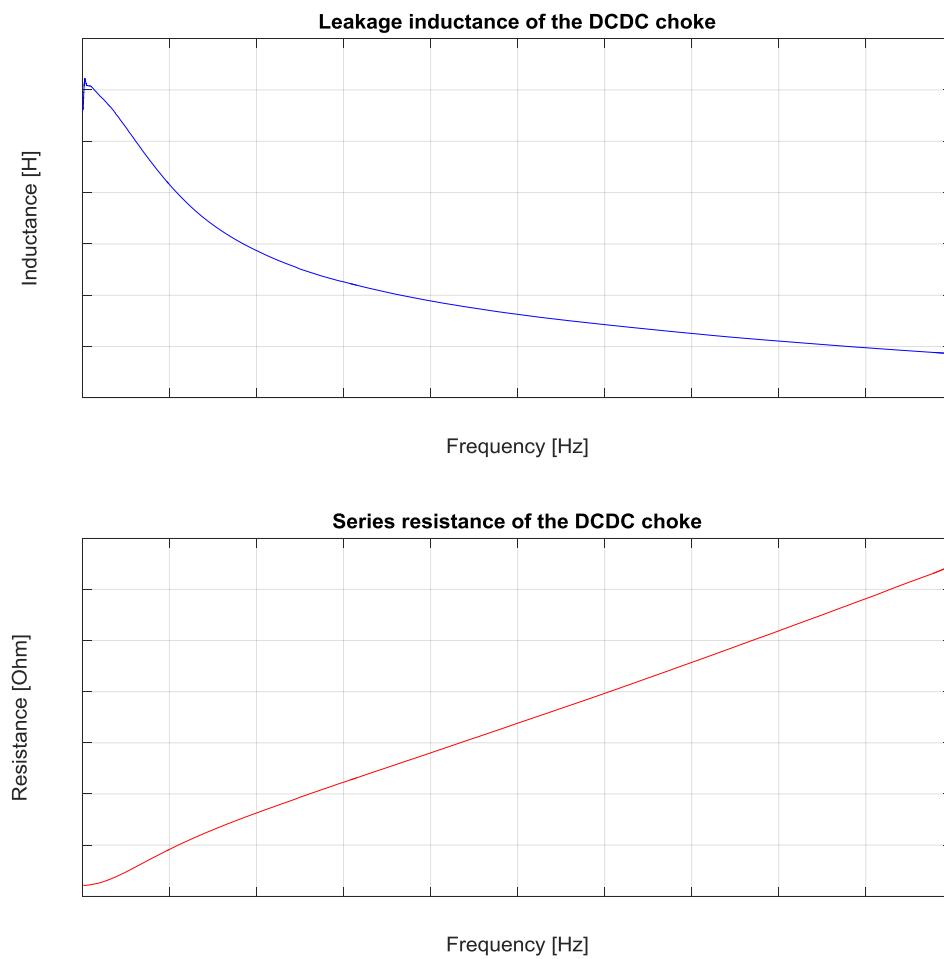
Figure 28 The Inductance and Resistance in the CM choke in DCDC

Table 12 Result of the curve fitting for the CM-choke in DCDC (equivalent circuit Figure 24)

CM-choke	L	Rser	Cpar	Rpar
	#VOLVO	#VOLVO	#VOLVO	#VOLVO

Impedance as a function of frequency for the CM-choke in DCDC
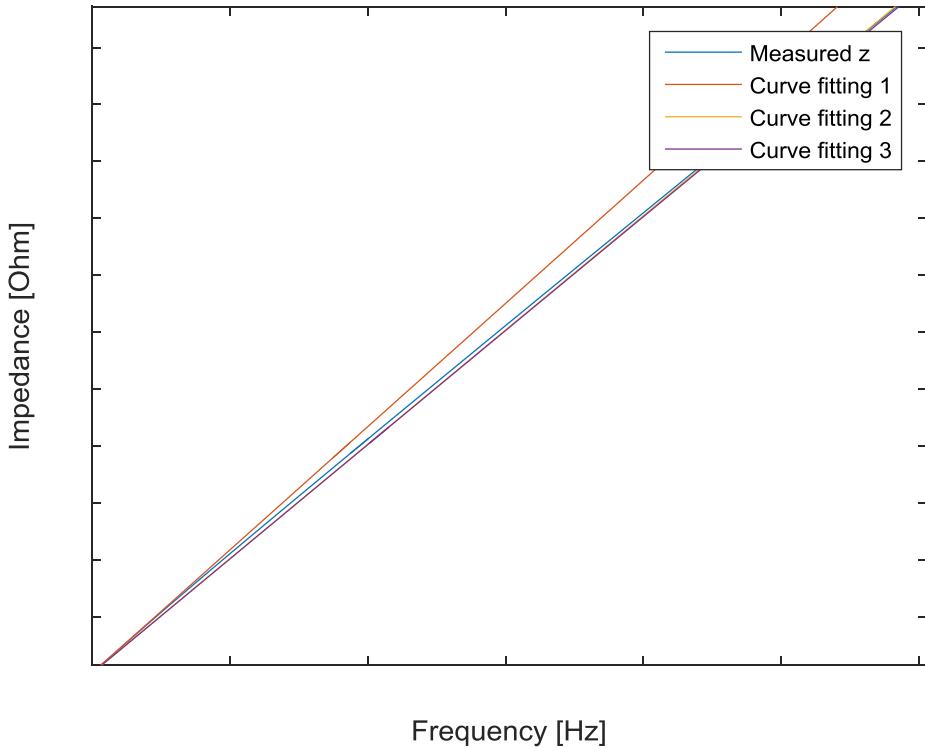
Figure 29 Curve fitting of the CM-choke in DCDC

4.2.4 Air compressor

Like in the DCDC, only the CM choke was available for measuring. Impedance measurement results are shown in Figure 31 along with the curve fitting plots based on the equivalent circuit in Figure 4. The measured values in Figure 30 were used as reference values to the curve fitting. The equivalent circuit component values are shown in Table 13.

Leakage inductance of the air compressor choke

Series resistance of the air compressor choke
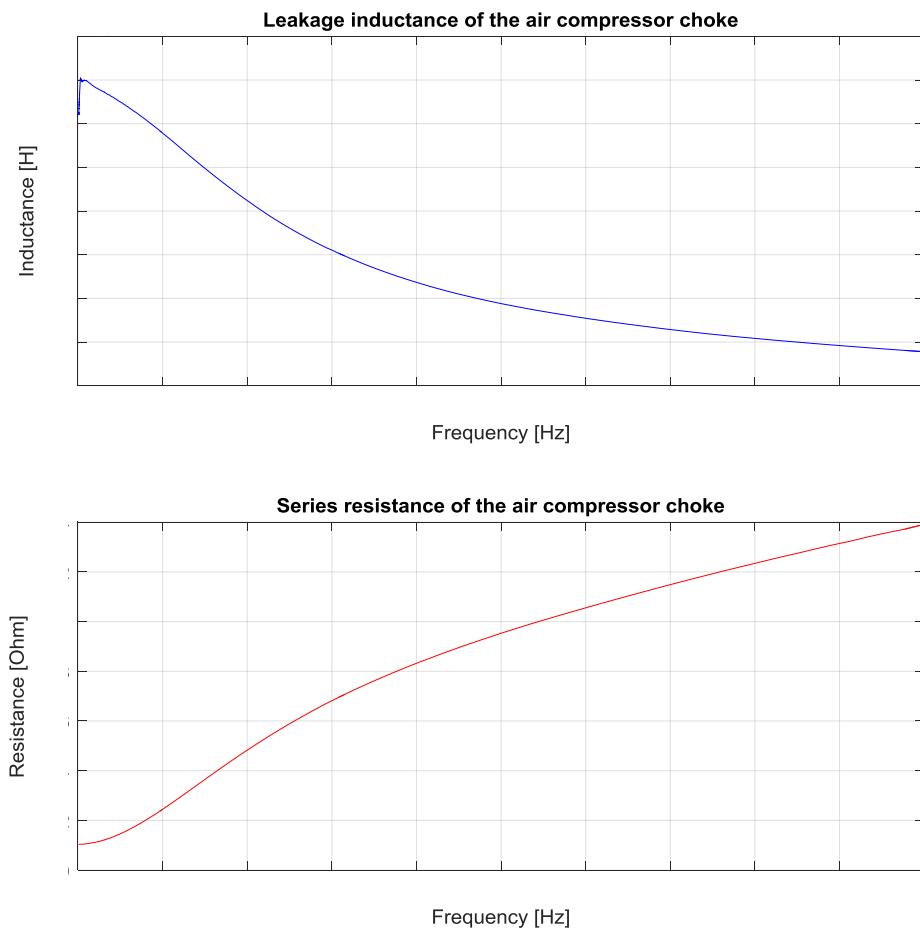
Figure 30 The Inductance and Resistance in the CM choke in Air Compressor

Table 13 Result of the curve fitting for the CM-choke in Air Compressor (equivalent circuit Figure 24)

CM-choke	L	Rser	Cpar	Rpar
	#VOLVO	#VOLVO	#VOLVO	#VOLVO

Impedance as a function of frequency for the CM-choke in Air Compressor,

Legend:
- Measured z
- Curve fitting 1
- Curve fitting 2
- Curve fitting 3

Impedance [Ohm] (y-axis)

Frequency [Hz] (x-axis)
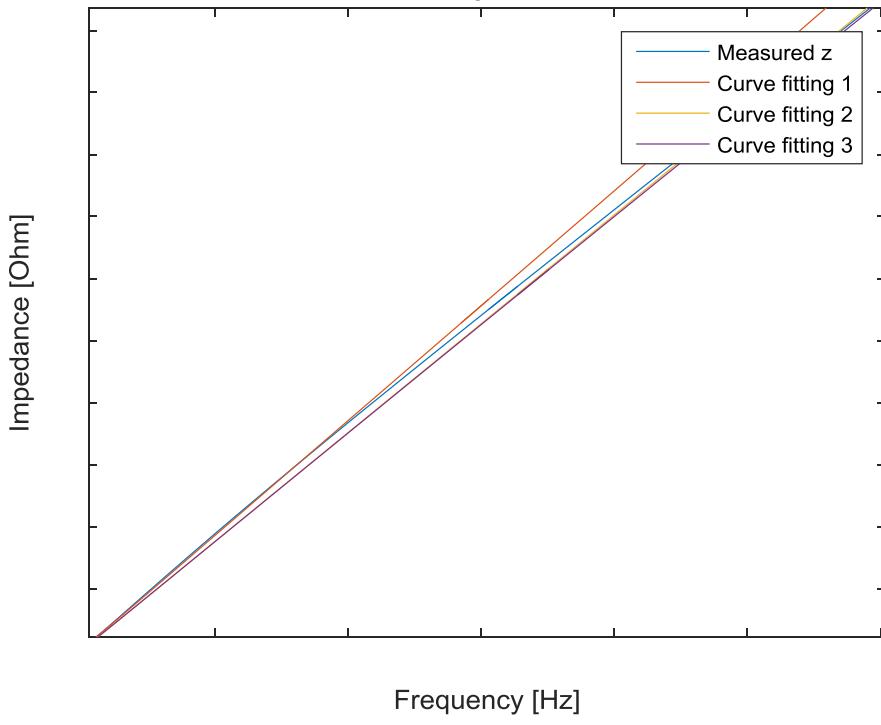
Figure 31 Curve fitting of the CM-choke in Air Compressor

4.2.5   HVAC

The CM choke was the only component available for measurement in the HVAC. Although some measurements were performed on the entire board, a circuit representation was not found as the initial values were impossible to measure without destroying the circuit. The measured impedance of the CM choke is shown in Figure 33 along with the curve fitting plots based on the equivalent circuit of an inductor seen in Figure 4. The measured values in Figure 32 were used as reference values to the curve fitting. The equivalent circuit component values are shown in Table 14.

Leakage inductance of the HVAC choke

Inductance [H]

Frequency [Hz]

Series resistance of the HVAC choke

Resistance [Ohm]
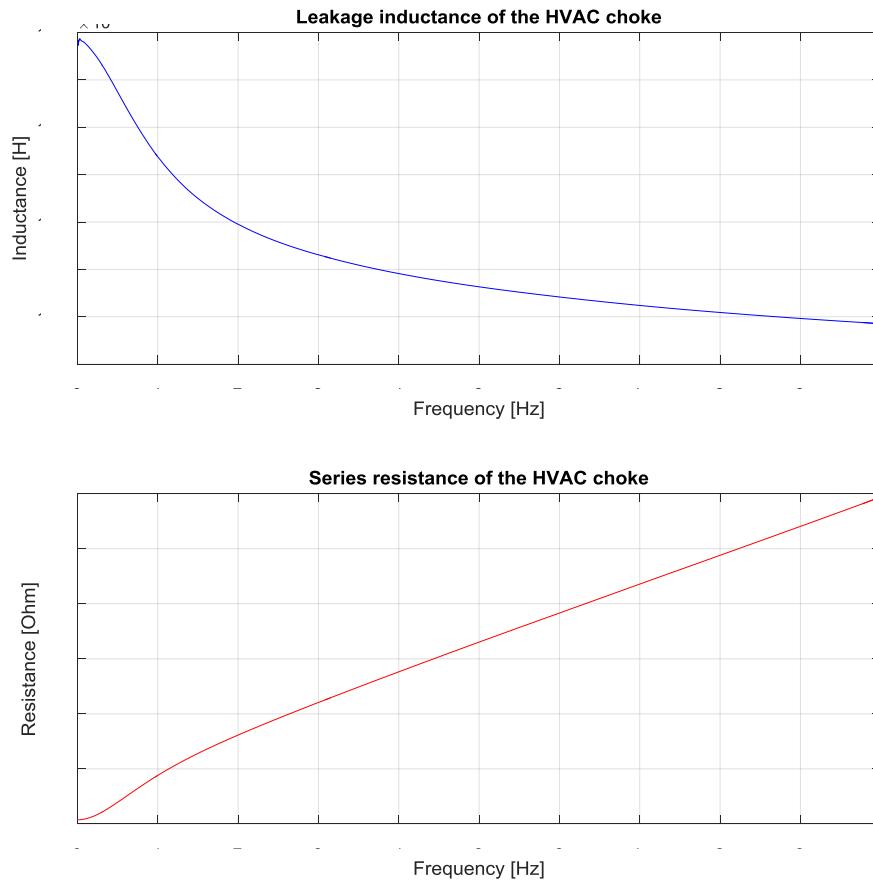
Frequency [Hz]

Figure 32 The Inductance and Resistance in the CM choke in HVAC

Table 14 Result of the curve fitting for the CM-choke in HVAC (equivalent circuit Figure 24)

CM	L	Rser	Cpar	Rpar
	#VOLVO	#VOLVO	#VOLVO	#VOLVO

#VOLVO: Some information, such as figures and values marked with #VOLVO are of specific value to Volvo and not for public. Therefore the figures are replaced and the values are concealed.

Impedance as a function of frequency for the CM-choke in HVAC
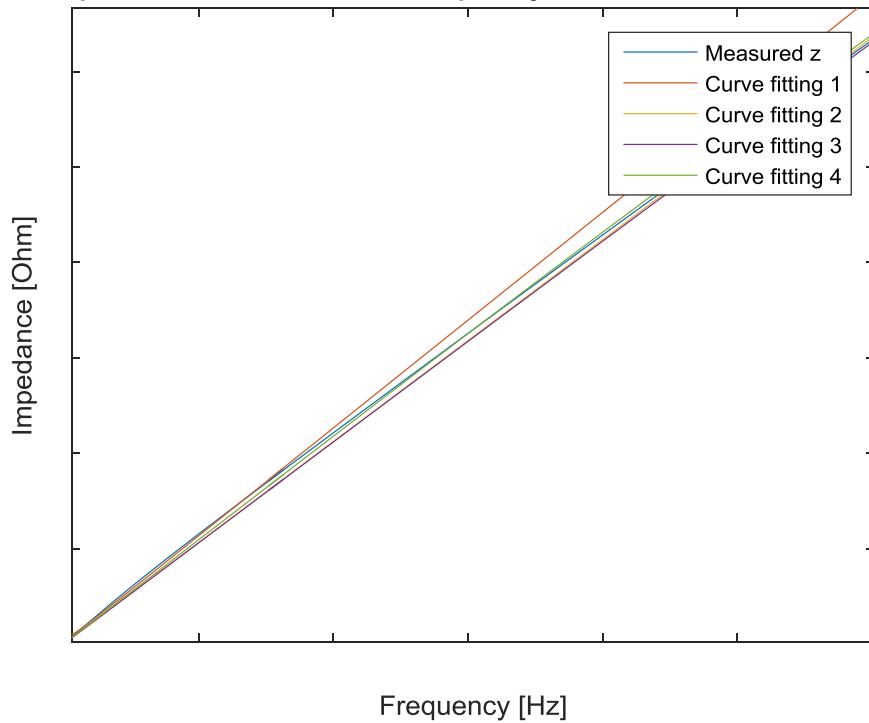
Figure 33 Curve fitting of the CM-choke in HVAC

4.2.6   OnBC

The impedance of the CM choke was also measured for the On Board Charger. Its impedance as a function of frequency can be seen in Figure 35. The fitted curves are shown in the same plot, their impedance based on the equivalent circuit of an inductor seen in Figure 4. The measured values in Figure 34 were used as reference values to the curve fitting. Its equivalent circuit component values are shown in Table 15.

Leakage inductance of the Onbc choke

Inductance [H]

Frequency [Hz]

Series resistance of the Onbc choke

Resistance [Ohm]

Frequency [Hz]
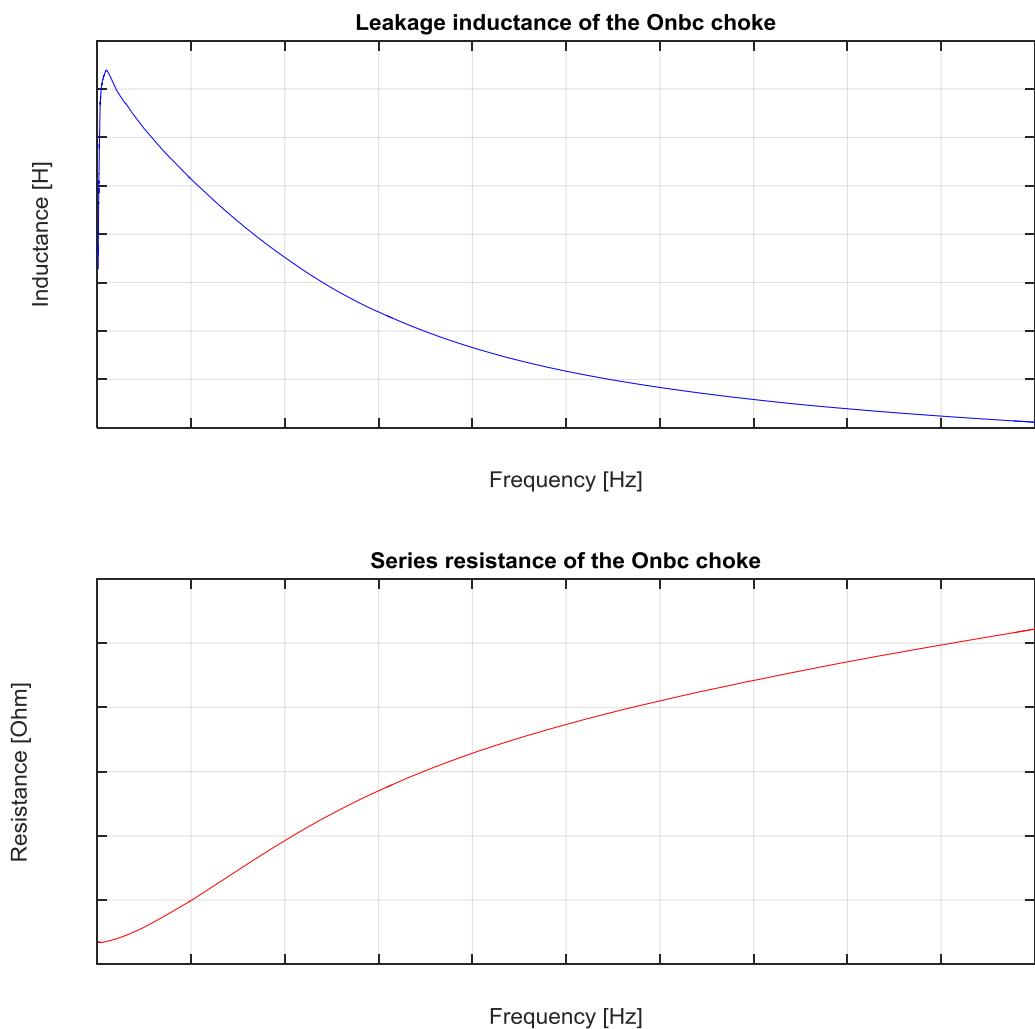
Figure 34 The Inductance and Resistance in the CM choke in OnBC

Table 15 Result of the curve fitting for the CM-choke in OnBC (equivalent circuit Figure 24)

CM	L	Rser	Cpar	Rpar
	#VOLVO	#VOLVO	#VOLVO	#VOLVO

#VOLVO: Some information, such as figures and values marked with #VOLVO are of specific value to Volvo and not for public. Therefore the figures are replaced and the values are concealed.
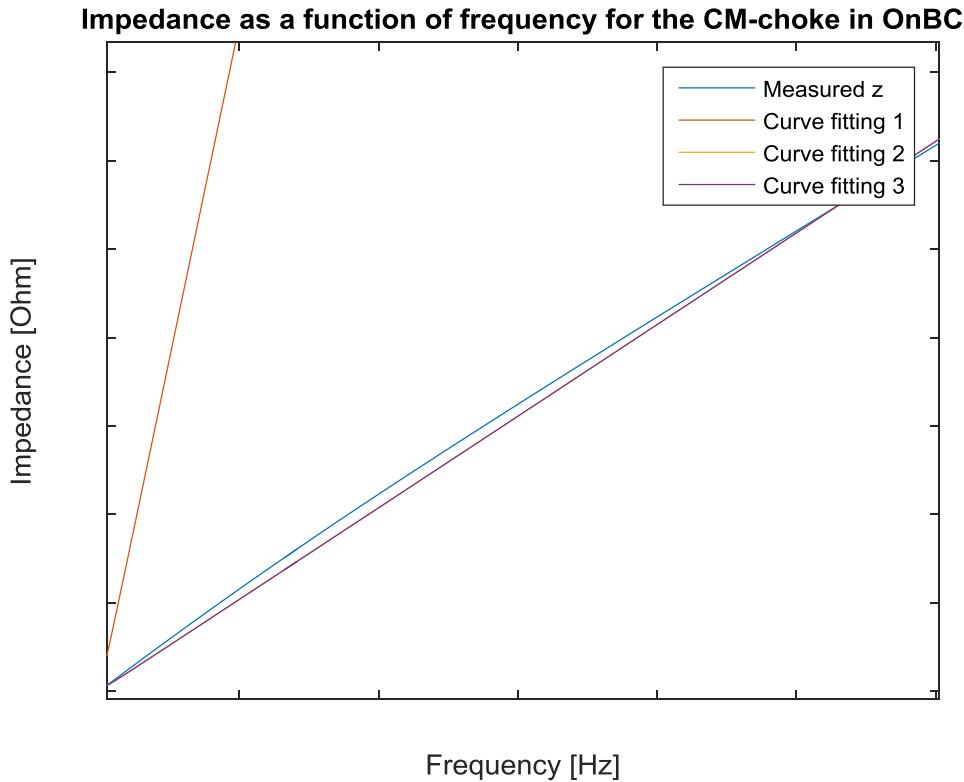
Figure 35 Curve fitting of the CM-choke in OnBC

4.2.7 Cables

Although some cable measurements were performed in order to provide placeholder values for the cables during the course of the project, the cable values provided by the parallel thesis project workers were eventually used in the model. The equivalent circuit model for the cables was modeled based on the T model. The values were not based on a frequency dependent model such as a curve fitting but instead selected based on the frequency of the most powerful load.

4.3 Current transformer measurements at grid frequency

The measurement setup shown in Figure 15, was used in an attempt to measure the current dependency of the impedance for all CM chokes. V_{top}, I_{top} and the resistance in the setup was measured and the impedance and inductance was calculated. The measurement results are shown in Table 16.

Table 16 Current transformer measurement results. *=img

	Z [Ω]	L [H]	R [Ω]
DCDC	#VOLVO	#VOLVO	#VOLVO
Air Compressor	#VOLVO	#VOLVO	#VOLVO
HVAC	#VOLVO	#VOLVO	#VOLVO
OnBC	#VOLVO	#VOLVO*	#VOLVO

#VOLVO: Some information, such as figures and values marked with #VOLVO are of specific value to Volvo and not for public. Therefore the figures are replaced and the values are concealed.

4.4   Power Amplifier measurement

Measurements using the Power Amplifier measurement rig were performed on all CM chokes. The available capacitors were excluded from the measurements, as the Power Amplifier measurement rig was not built to output a DC-bias. The Impedance as a function of both frequency and current for all components can be seen in Figure 36, Figure 37, Figure 38, Figure 39, Figure 40 and Figure 41.
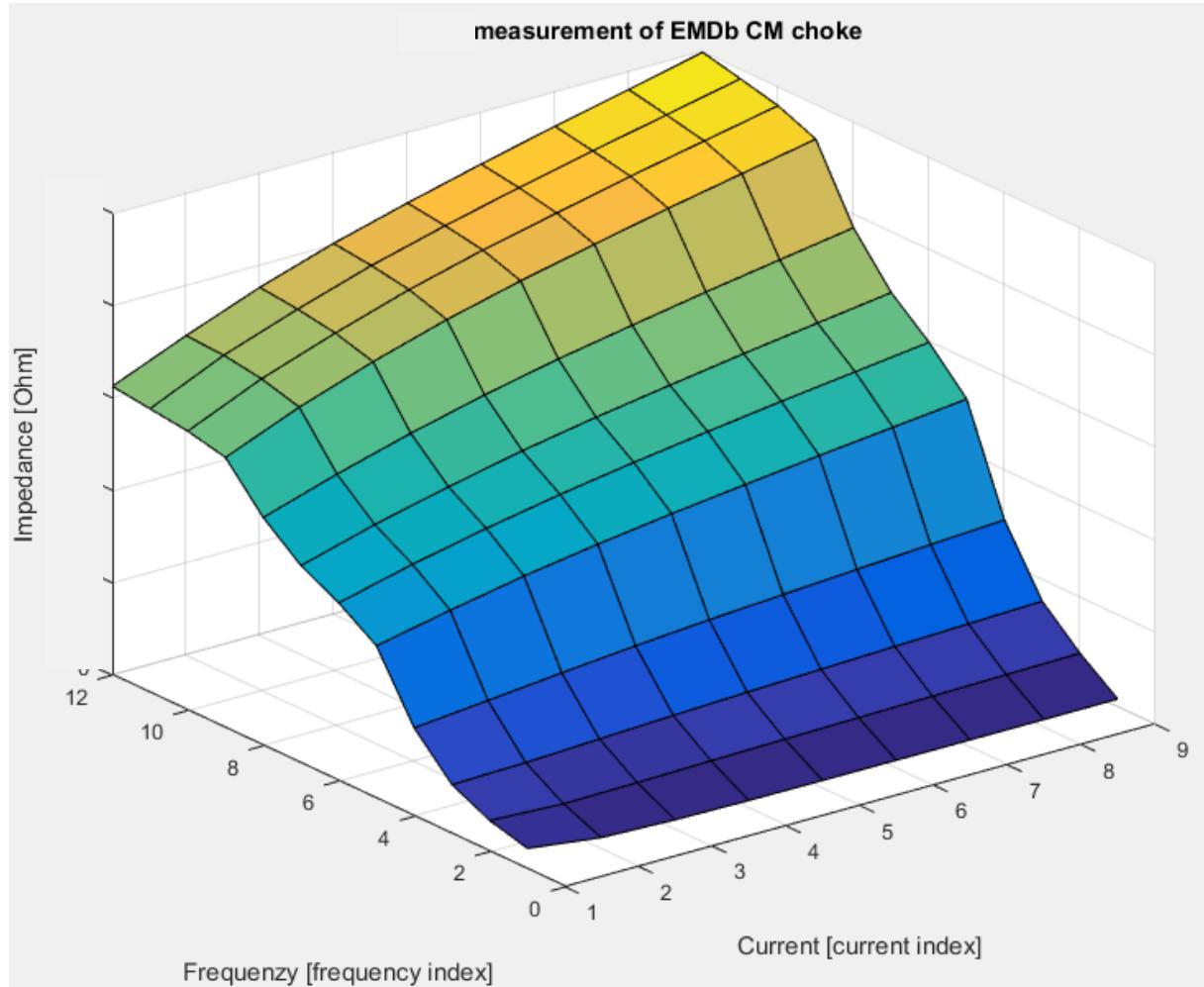
Figure 36 The measured impedance of the EMD type b CM choke as a function of frequency and current.

#VOLVO: Some information, such as figures and values marked with #VOLVO are of specific value to Volvo and not for public. Therefore the figures are replaced and the values are concealed.
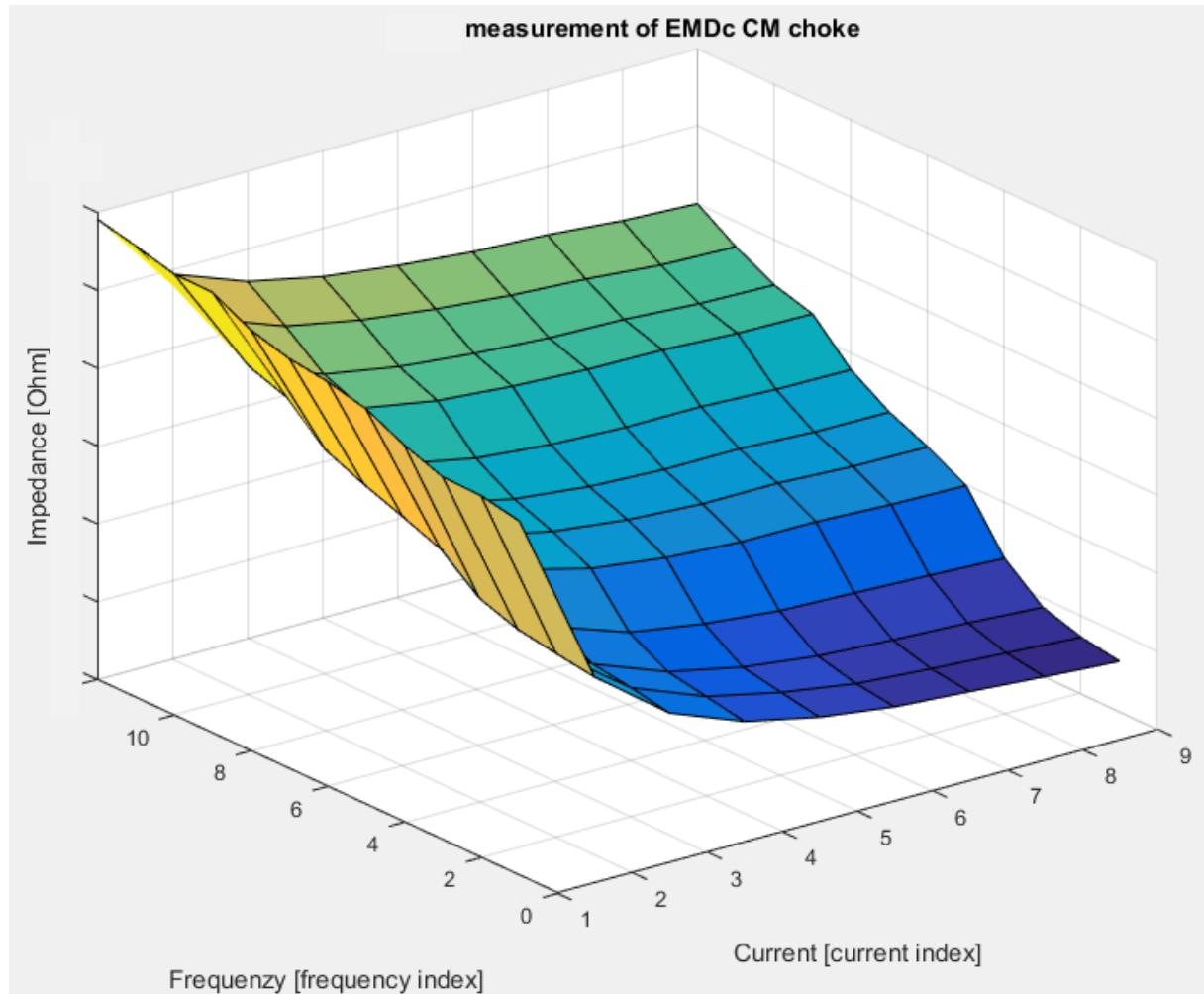
Figure 37 The measured impedance of the EMD type c CM choke as a function of frequency and current.
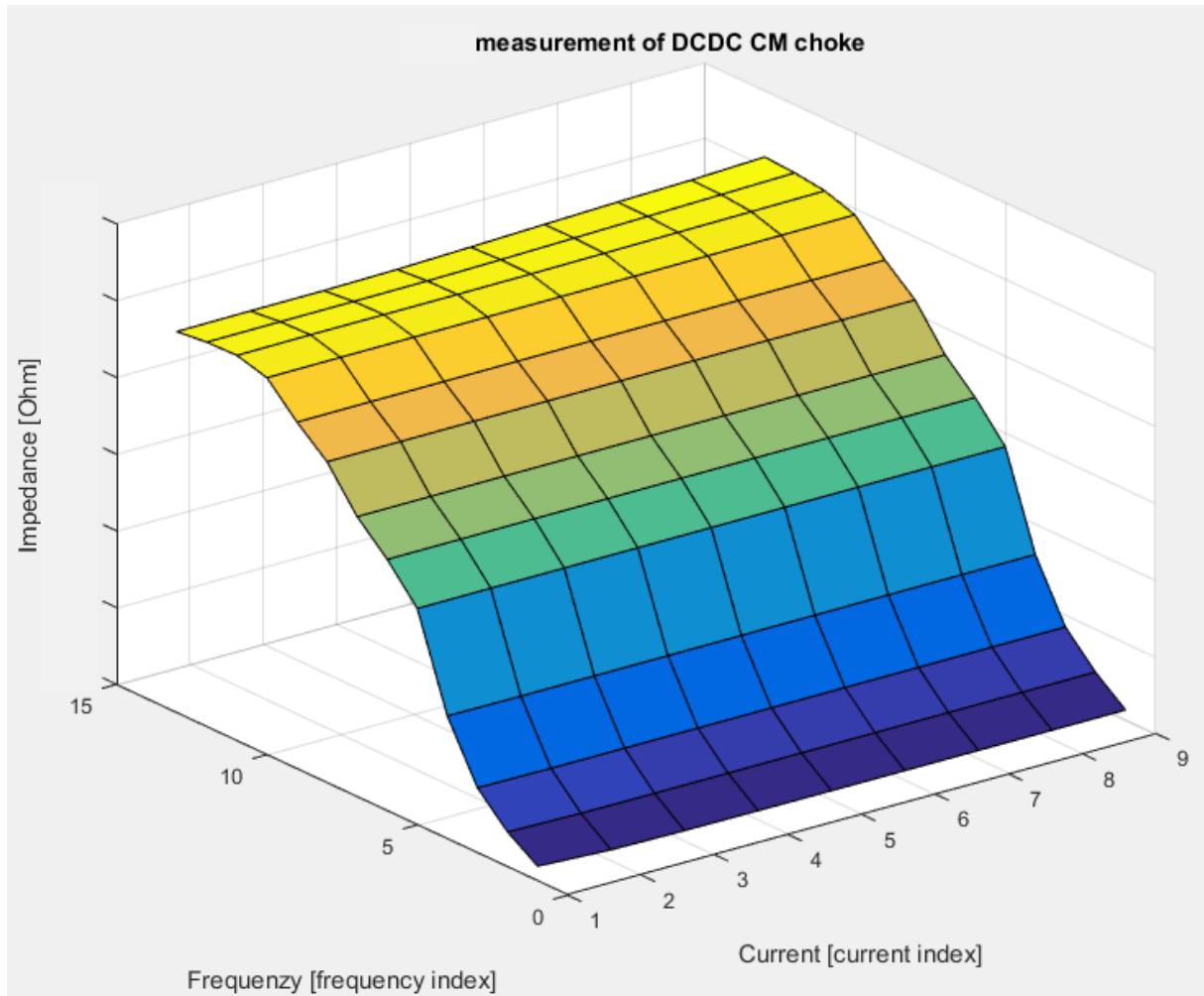
Figure 38 The measured impedance of the DCDC CM choke as a function of frequency and current.
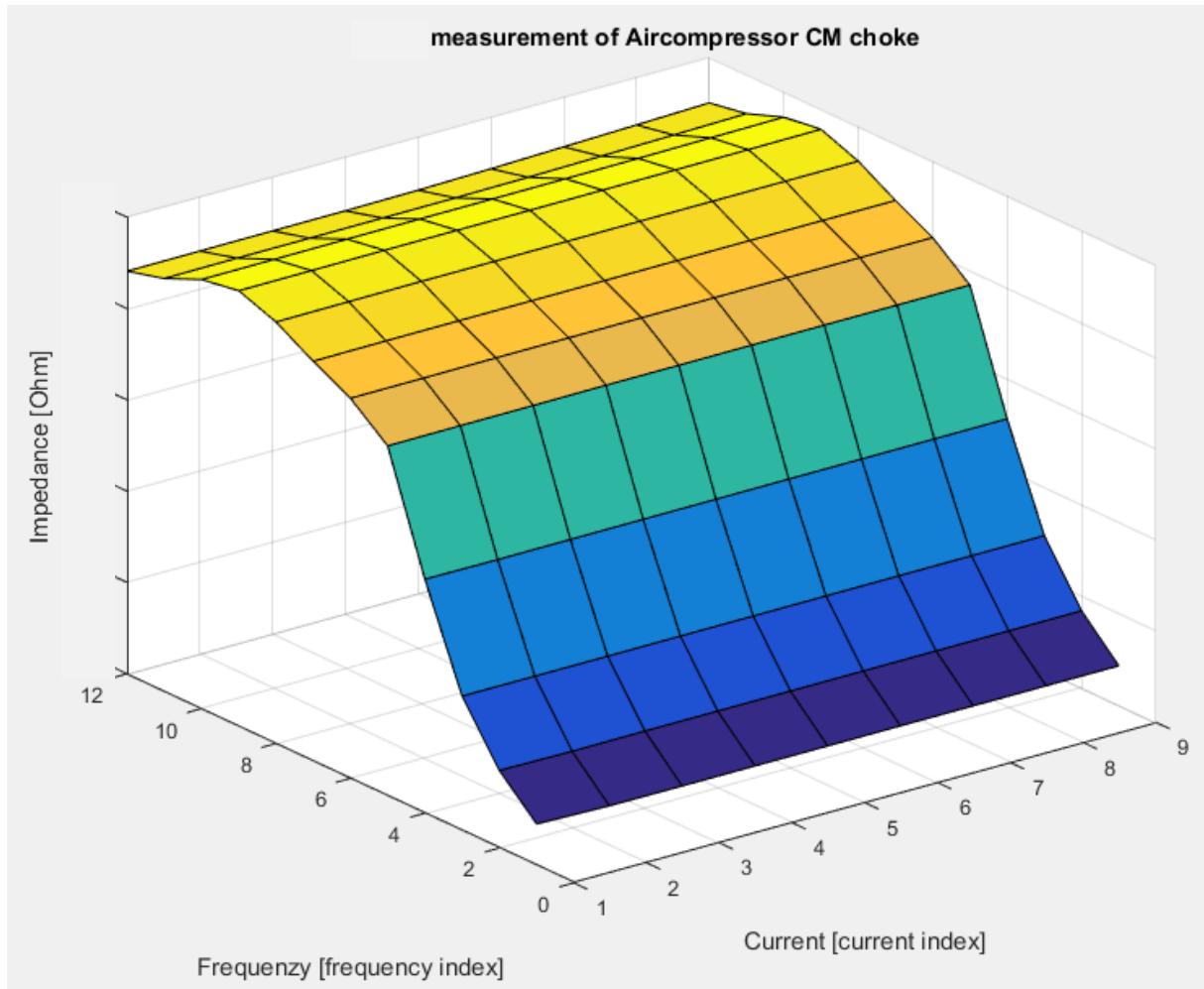
Figure 39 The measured impedance of the air compressor CM choke as a function of frequency and current.
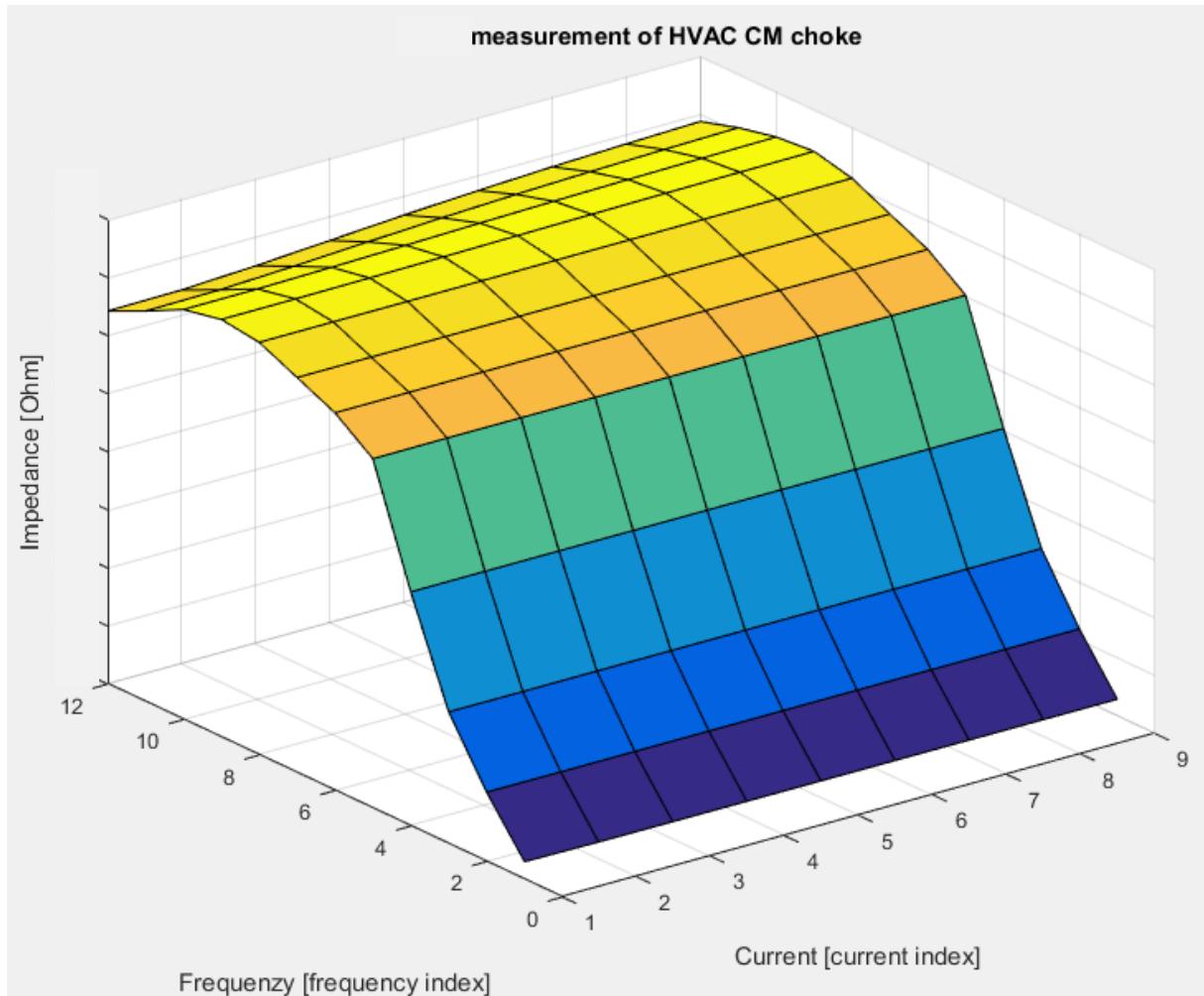
Figure 40 The measured impedance of the HVAC CM choke as a function of frequency and current.
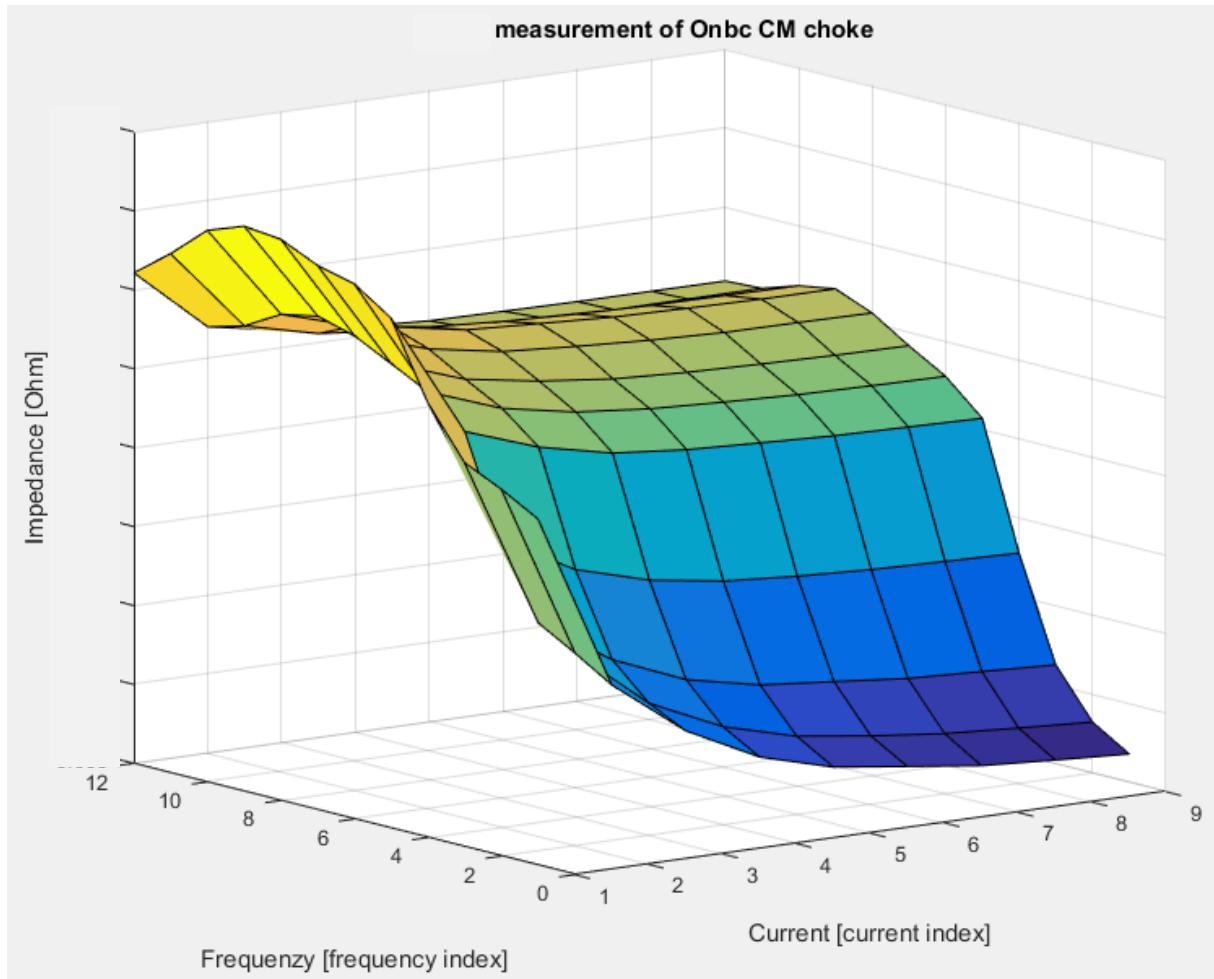
Figure 41 The measured impedance of the OnBC CM choke as a function of frequency and current.

As seen in chapter Power Amplifier measurement, the impedance of some of the major components is affected both by frequency and current. The rise of impedance as a function of frequency is likely due to the skin effect and the proximity effect, as they increase the resistance by limiting the current flow. The current dependency seen in the Power Amplifier measurements of the EMD type b, EMD type c, and on board charger, however, is slightly harder to explain. Core saturation could be a guess in the case of the EMD type c and the on board charger, as the impedance drops slightly with an increase in current. However, core saturation is not very likely due to the fact that the chokes are CM chokes, which should be able to handle DM signals such as the measurement signal of a higher magnitude without saturating. As for the EMD type b, the impedance rises with an increased current. The likeliest explanation to this is probably thermal dependency. During the measurement the component became so warm that it was left to cool off before proceeding. In conjunction with the increased resistance due to the higher frequency, the temperature will rise even higher and faster, causing an enhanced rise in impedance. The effect of this can even be seen in some of the other components, where the combination of a high frequency and a high current causes the impedance to increase slightly. In a real vehicle, the components are mounted on a heat

sink meant to drain the heat. If the increased temperature during the measurements was the source of the current dependency, perhaps the effect won't be as prominent in a real vehicle.

The frequency behavior of the impedance seen in the Power Amplifier measurements does not mirror the frequency behavior seen in the LCR measurements. This is likely due to the LEM LV 25-P used to scale the voltage down later being found to do so as a function of frequency for frequencies of about 3 kHz and higher. The current dependency for each frequency point can still be seen, however, as all current points of the same frequency were attenuated by an equal amount. While taking the frequency behavior into account in the model can be rather easily done using a curve fitting script, doing the same for current dependency is hard. If the current dependency is approximated to be constant independent of frequency, a rather crude solution is to simply scale the measured impedance curve based on the current dependency factor seen in the equation below.

$$Current\ dependency\ factor = \frac{Impedance\ at\ component\ ripple\ size}{Impedance\ at\ 100\ mA}$$

Performing measurements meant to find the reactive and resistive part of the different components by using a current transformer operating at grid frequency proved to be difficult. The reactive part of the impedance was often so small due to the low frequency of the signal that separating the impedance into its resistive and reactive components more often than not yielded highly unlikely results. The current transformer setup could be used to provide an estimation of the current dependency of the total impedance though, once again granted the current dependency is approximated to be constant independent of frequency. The results can then be used in conjunction with LCR measurements in order to provide an accurate model. However, modeling a new bus will create a catch 22 as the current ripple size is unknown until said bus has been constructed for real.

Another thing worth noting is that, while the LCR meter measurements are used as the foundation for the resulting simulation model, the reactive measurements for lower frequencies are probably not to be trusted for the same reason as explained above about the current transformer measurements. The frequency of the measurement signal is simply too low to provide a phase shift large enough to measure properly, as the somewhat loose conditions wL >> R and wL >> 1/wC, or 1/wC >> R and 1/wC >> wL respectively no longer hold. Also, no open and short correction of the values measured with the LCR meter was performed. The reason for this being that moving the test fixture around even slightly was estimated to introduce a larger error than what could be corrected for.

4.5 Battery measurements using a current injection transformer

Using a GAMRY measurement instrument, an attempt was made at measuring the impedance of a 12 Volt car battery using the current injection transformer setup mentioned in chapter Battery measurements using a current injection transformer. The measurements using the GAMRY instrument were performed as a test before moving on to larger batteries, but as the results proved unsatisfying, no further battery measurements were performed. The measured impedance of a 2 Ohm resistor when the current transformer was connected between the GAMRY instrument and the battery and when the GAMRY instrument was connected directly to the battery is shown in Figure 42. With the help of the people at the Volvo workshop, much of the battery measurement equipment was mounted on a wooden board and isolated as a safety precaution. Hopefully this will make the process of performing measurements on the batteries easier in the future.
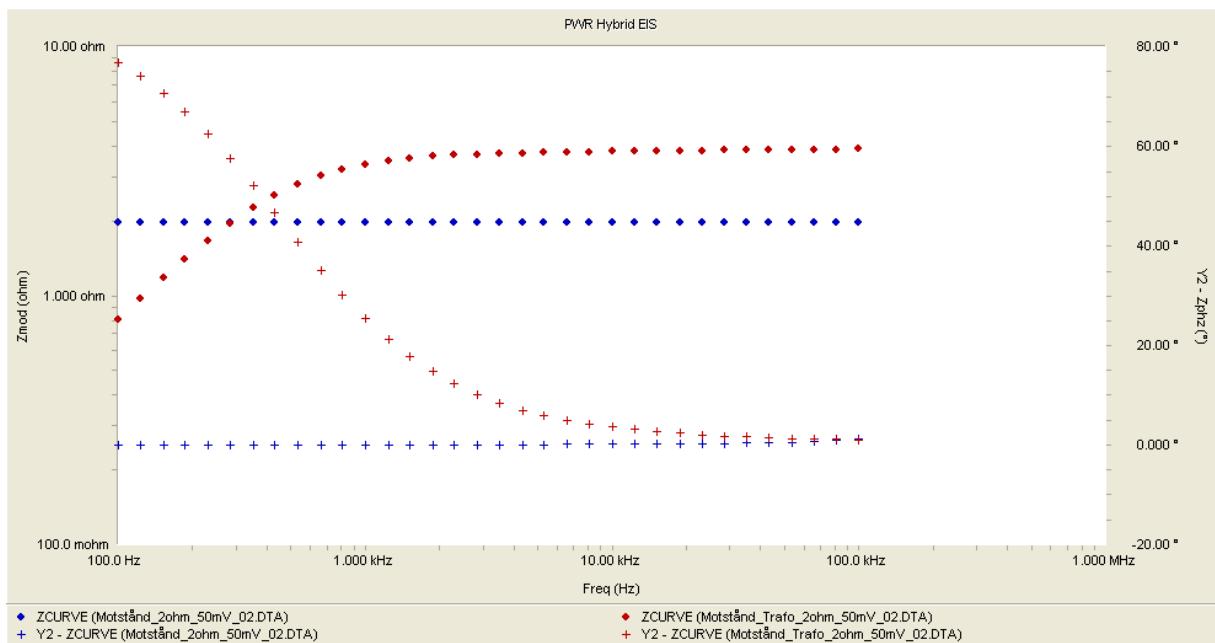
Figure 42 The difference in measured impedance of a 2 Ohm resistor when the GAMRY was connected through the current injection transformer (red) and when it was not (blue).

The brief battery measurements performed using the GAMRY did not yield very promising results. As seen in the impedance measurements when testing the instrument, the results differed depending on whether the current injection transformer was connected between the GAMRY and the specimen or not. This effect is likely due this some filtering of the measurements performed by the GAMRY itself, as its measurement probe and the injection probe are originally meant to be in the same node. As the current injection transformer setup is probably the simplest solution, an approach when using it with a different instrument should be looked into.

49

4.6 Vehicle measurements performed by Volvo

Looking into the vehicle measurements performed by Volvo, several unexpected tendencies were discovered. In order to give the simulation model a fighting chance in the verification, these tendencies were also modeled to some extent. The following section presents some of the results found, which to a large extent are based on measurements performed on the electric hybrid bus with only one component active at a time. According to results provided by the previous thesis project, the DC link current ripple produced by a PEC is at its worst when the duty cycle is at 50 % [12]. The pulsed current loads of the simulation models are therefore largely based on this case, if relevant.

4.6.1 EMD type b

Based on the vehicle measurements in the electric hybrid, the time when the EMD type b was at 50 % duty cycle was found by looking at the FFT of the DC link current ripple. This time was the matched to a mean current level, which in turn was used to model the worst case load model of the EMD type b. As the speed of the motor increases, the amplitude of the total current ripple seen in Figure 43 appears to increase as well. The frequencies which cause this behavior appear to match the frequencies of the peaks seen in Figure 44. Looking at the current ripple in Figure 45, the shape of the current ripple of the different frequencies can be seen.
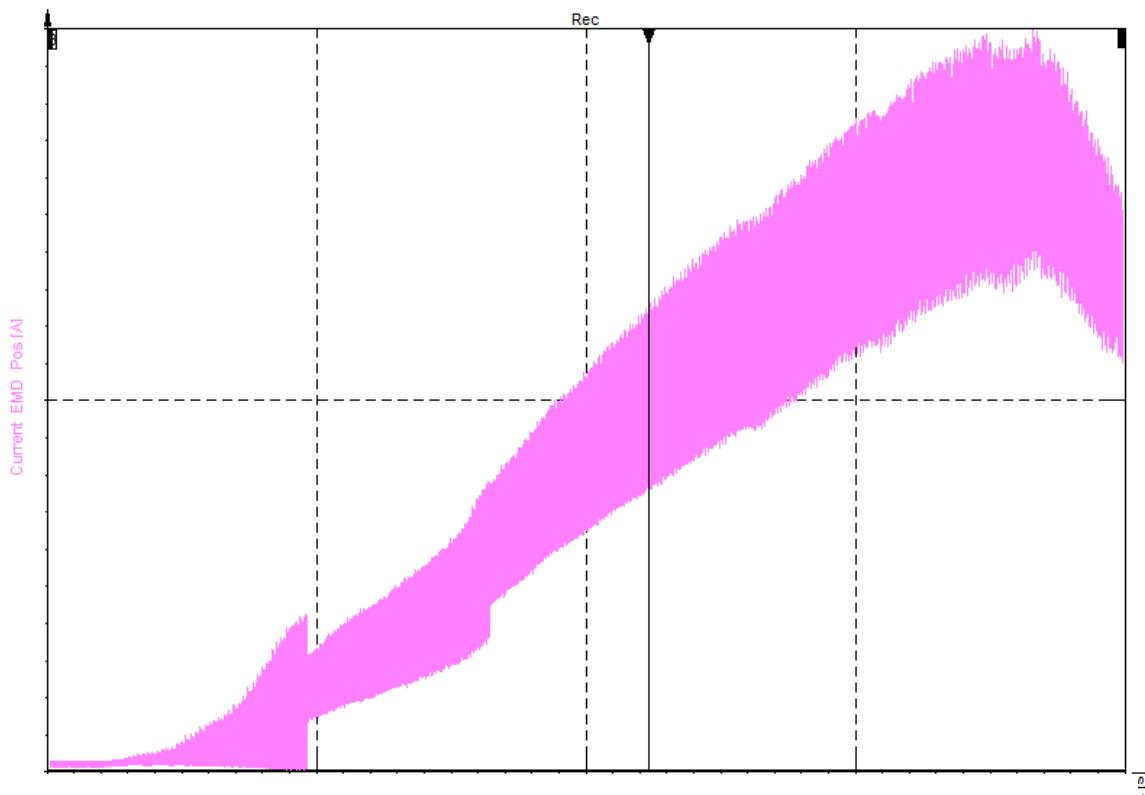
Figure 43 The total DC link current measured at the DC terminals of the EMD type b during acceleration at full torque in the electric hybrid. Only the EMD is active. The changes in switching frequency can be seen as steps in the current. The point at which the duty cycle reaches 50 % is marked by the vertical line.

FFT (df = 48,83 Hz)
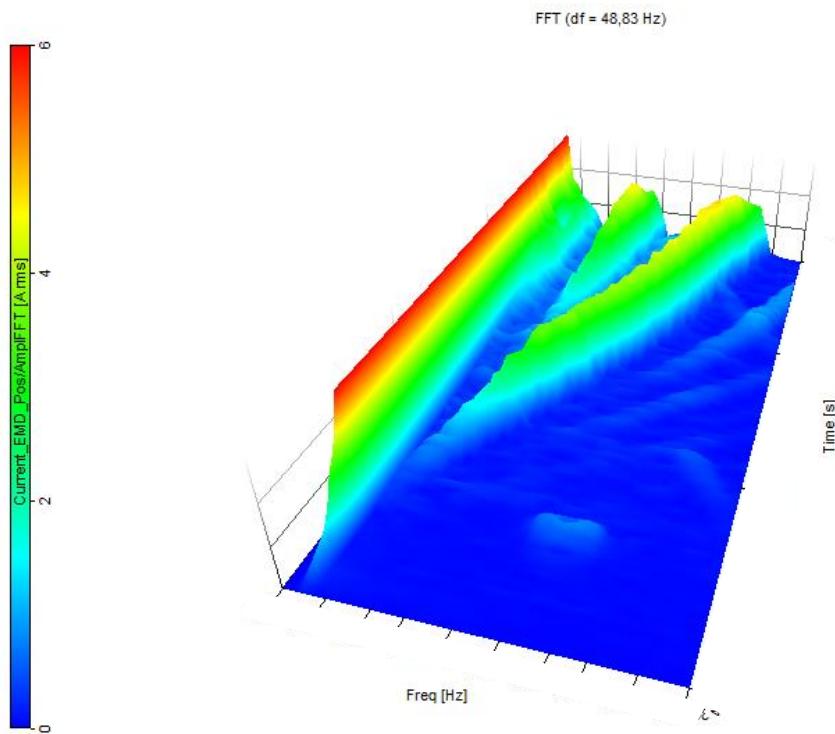
Figure 44 The low frequency DC link current measured at the DC terminals of the EMD as a function of frequency in the EMD type b in the electric hybrid. Only the EMD is active.

FFT (df = 48,83 Hz)
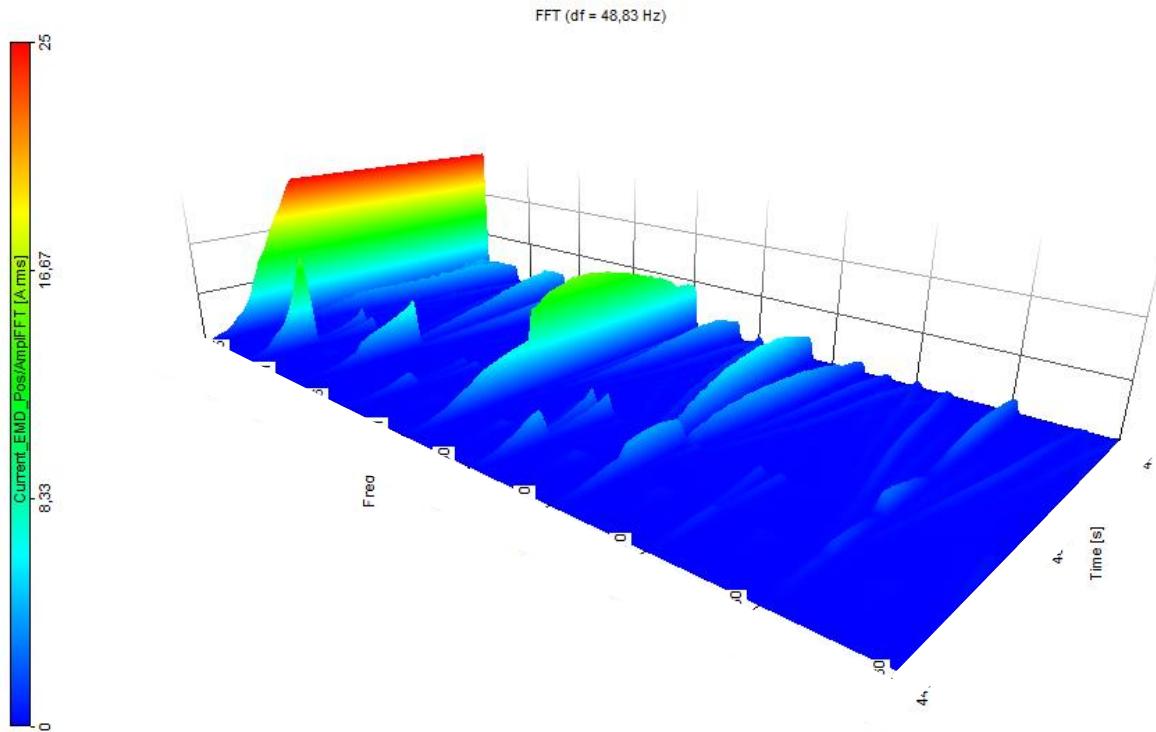
Figure 45 The DC link current measured at the DC terminals of the EMD as a function of frequency and time in EMD type b in the electric hybrid. Only the EMD is active.

4.6.2   EMD type c

The vehicle measurements of the electric bus provided a good estimation of the current level at 50 % duty cycle as well. This was used to model the worst case load model of the EMD type c. The current ripple amplitude measured in the EMD type c as a function of time and frequency can be seen in Figure 46.
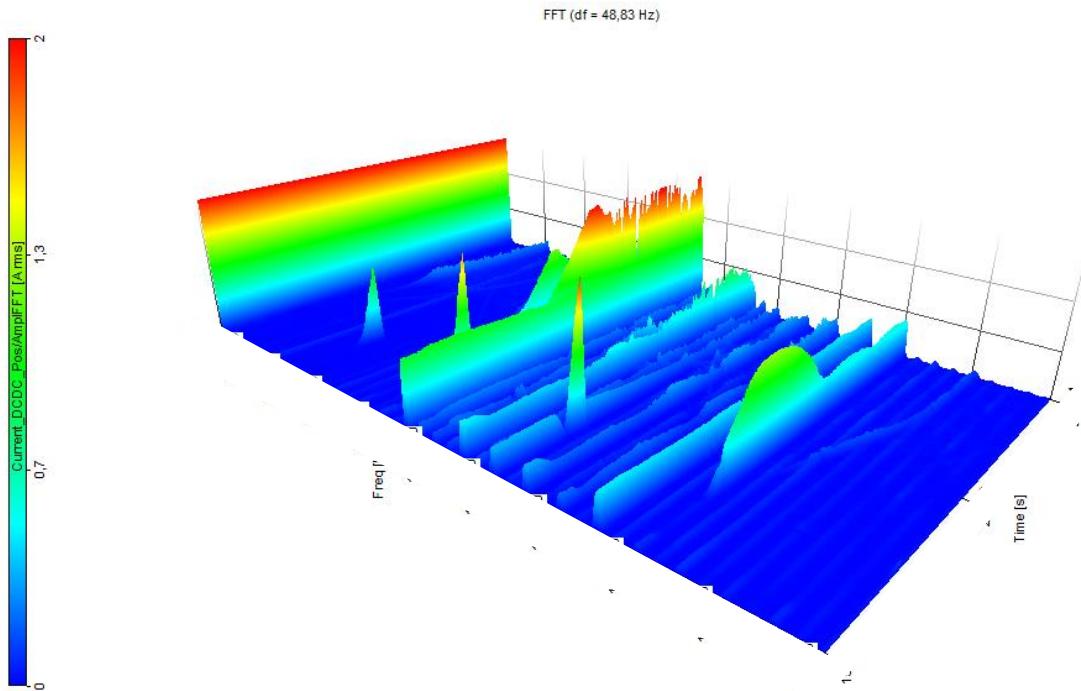
Figure 46 The DC link current measured at the DC terminals of the EMD as a function of frequency and time in EMD type c in the electric bus. Several components are active.

4.6.3   Dual EMD type c

Installing two electric motors in the same vehicle, as in the TWIN MOTOR BUS1, resulted in some previously unseen behavior. Theoretically, if the on-pulse of the PECs of the two EMDs were to be on at the same time, the current ripple as seen from the rest of the vehicle would increase. Depending on the duty cycle, the opposite should occur if the two motors were completely out of phase. In the case of 50 % duty cycle, this would theoretically mean no current ripple whatsoever, as the two pulses added together creates a constant DC level. For the same reason, the case when the two motors both operate at 25 % duty cycle can potentially take the appearance of 50 % duty cycle to the rest of the circuit if the two motors are out of phase. The distance between the motors also potentially has an effect on the current ripple, as the length of the cables determines the impedance.

The ripple measured in the two EMDs during acceleration differs between different measurements. In one instance, the two motors are operating in phase at the start of the acceleration. As the change in switching frequency occurs, one of the motors changes its switching frequency from #VOLVO to #VOLVO kHz sooner than the other. This results in an

#VOLVO: Some information, such as figures and values marked with #VOLVO are of specific value to Volvo and not for public. Therefore the figures are replaced and the values are concealed.

imbalance between the motors. As the second motor also changed its switching frequency, the motors were once again operating in phase. However, during the time of the acceleration, the current pulses would slowly drift apart, once again resulting in a slight imbalance between the two. In other measurements, the pulsed currents of the two motors drift in and out of phase in a different manner and the current ripple as a result is vastly different. In order to properly verify a model simulating the current ripple of the DC link of the TWIN MOTOR BUS1, it is therefore required looking at many different measurements and adjust the pulsed current loads representing the motors of the model appropriately.

4.6.4   DCDC

The DCDC was found to be giving off a DC link current ripple fundamental frequency of #VOLVO kHz rather than the previously thought #VOLVO kHz. The true shape of this ripple was unclear due to the relatively low sampling frequency, but as the DCDC converter is not used to power a motor, the estimation provided by the previous master thesis that the lowest voltage applied for full performance in conjunction with the battery voltage and the rated power can be used to calculate the duty cycle was used [12]. The mean current of the fully loaded DCDC was used together with its duty cycle in order to model the load.

4.6.5   Air compressor

Investigating the curve form of the DC link current ripple generated by the air compressor in the electric hybrid, it was found that the air compressor PEC likely operates at 52 % duty cycle. The previously estimated duty cycle was 83 %. The mean current level was used in conjunction with the duty cycle to approximate a model for the air compressor load. The zoomed in current ripple of the air compressor can be seen in Figure 47.
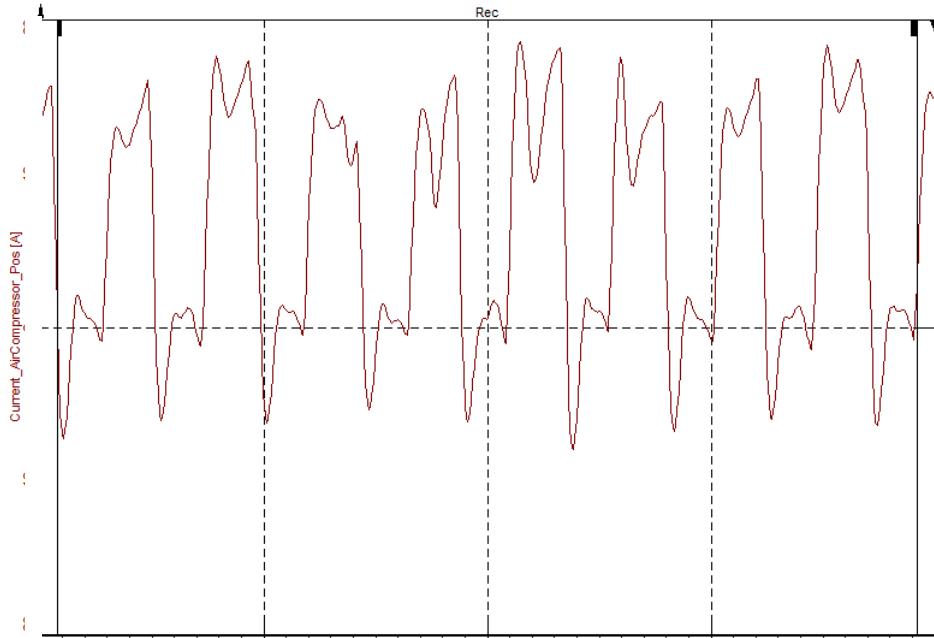
Figure 47 DC link current ripple as a function of time measured on the DC terminals of the air compressor PEC in the electric hybrid.

53

4.6.6   HVAC

The ripple in the HVAC is somewhat affected by the AC load. While this was previously established, a further investigation of the ripple waveform, Figure 48, in the electric hybrid shows that the PEC of the HVAC operates at a duty cycle of 51 %. The previously estimated duty cycle was 93 %. The HVAC load was modeled using the mean current level during operation and the duty cycle.
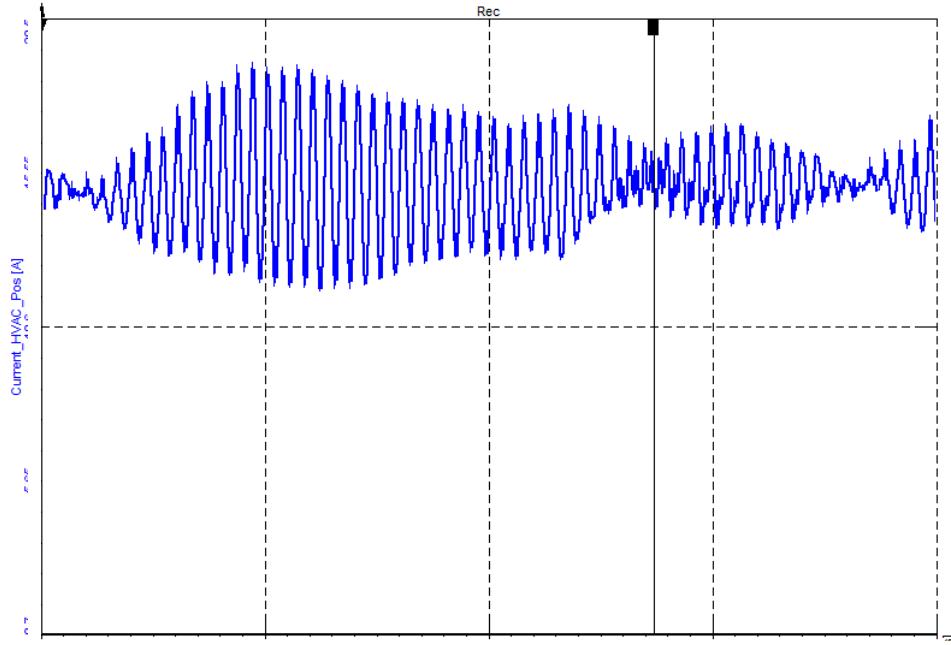
Figure 48 Current ripple as a function of time, in the HVAC in the electric hybrid.

4.6.7   Battery

The previous battery model was largely based on the impedance of a single battery cell, which was then multiplied by the amount of cells in a battery pack. However, recent studies performed by Chalmers indicate that the impedance of the cells is insignificant in comparison to the impedance of the battery rig for higher frequencies (usually at about 1 kHz and more, depending on the battery).

5. Simulation model structure

The circuit models are largely based on the preexisting models, which in turn rely on data from component owners at Volvo and their suppliers. The components for which measurements are performed are updated according to their respective equivalent circuits found in chapter 4.2Component measurements and impedance analysis. Some of the simulation model pulsed current loads are also updated based on new measurements provided by Volvo in order to more accurately represent the current and voltage levels. For the EMD in the electric hybrid bus, a special source is modeled in order to simulate the entire acceleration. This is only possible in the electric hybrid bus because no other load is active in the vehicle measurements. All component values not mentioned are provided by Volvo during this or the previous thesis project and remain unchanged.

5.1 Electric hybrid

Not much has changed in the electric hybrid model as the base structure is the same. The simulation model can be seen in Figure 49.
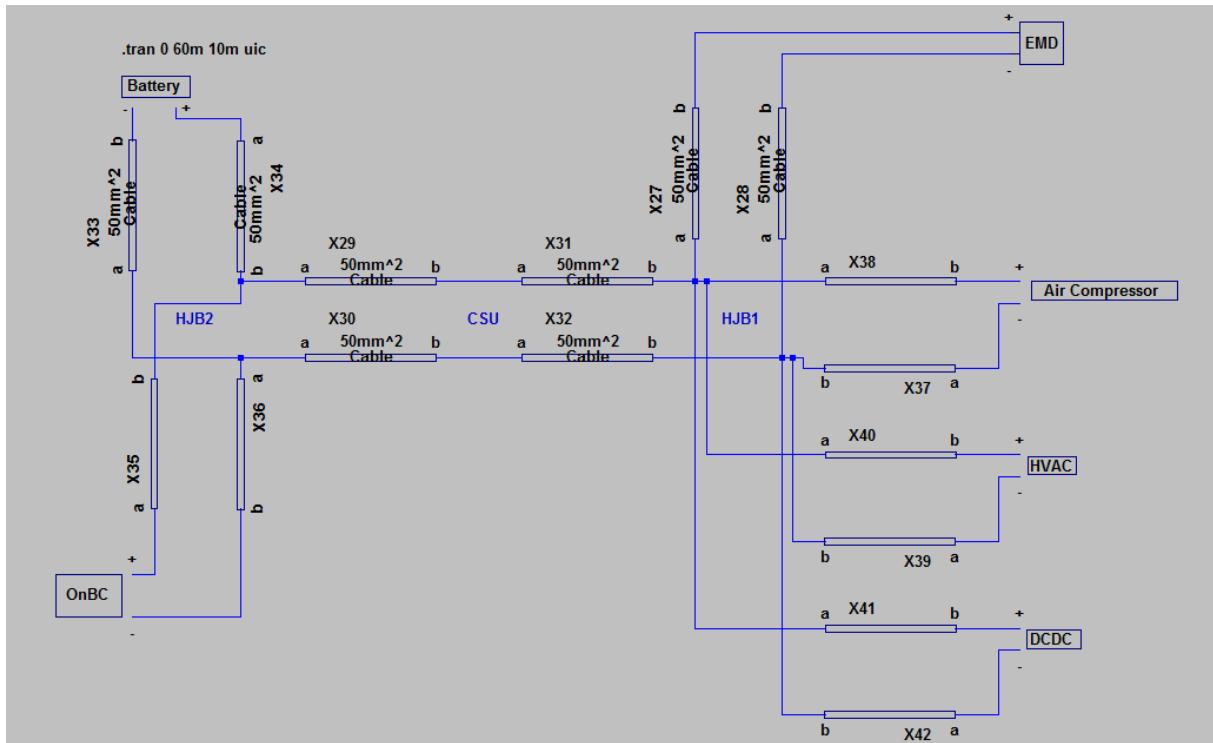
Figure 49 The simulation model of the electric hybrid

5.2 Electric

The structural simulation model for the electric bus can be seen in Figure 50.
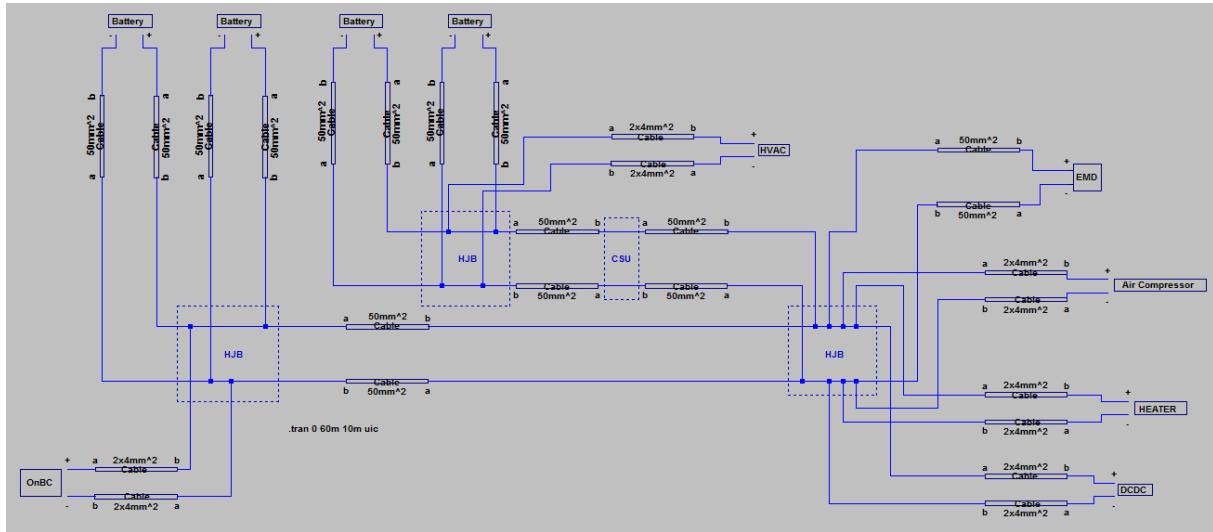
Figure 50 The simulation model of the electric bus

5.3 TWIN MOTOR BUS1

The model for the TWIN MOTOR BUS1 was made from scratch along with the TWIN MOTOR BUS1 model library. A special model was also made in order to be able replicate the behavior seen in the vehicle measurements in which the two motors drift apart and change switching frequency independently. The different simulation models can be seen in Figure 51 and Figure 52.
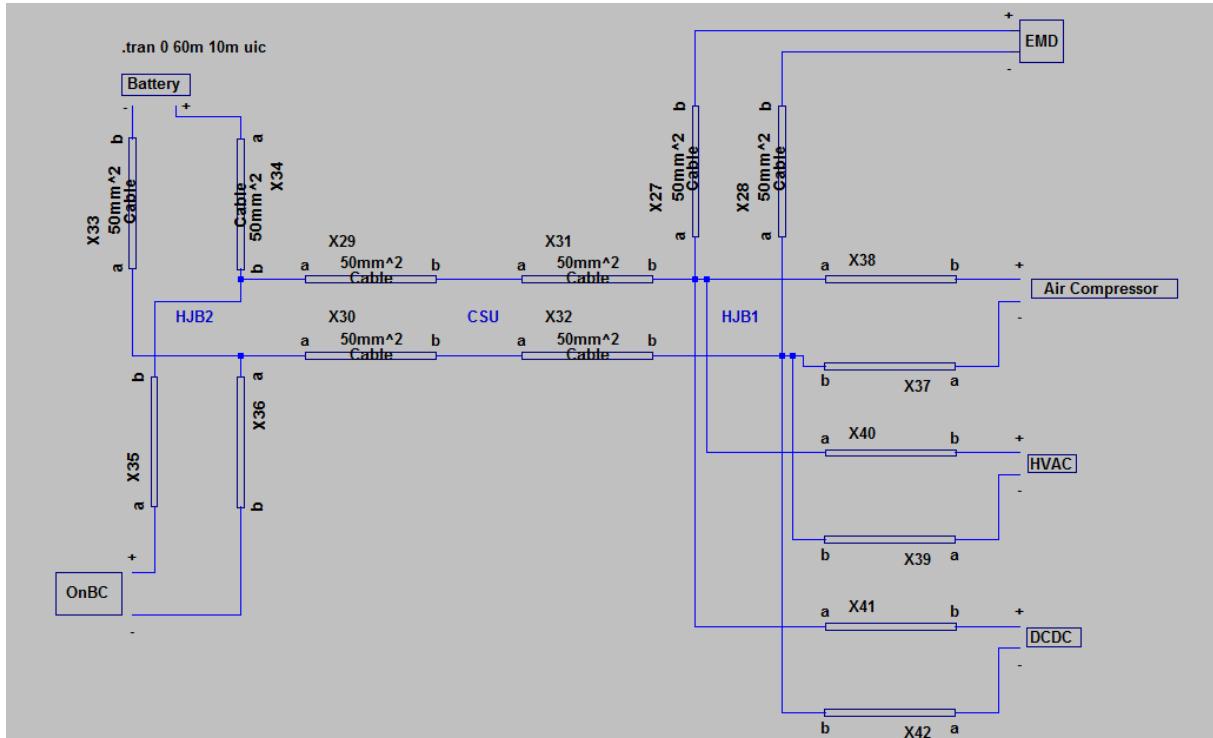
Figure 51 The simulation model of the TWIN MOTOR BUS1 #VOLVO
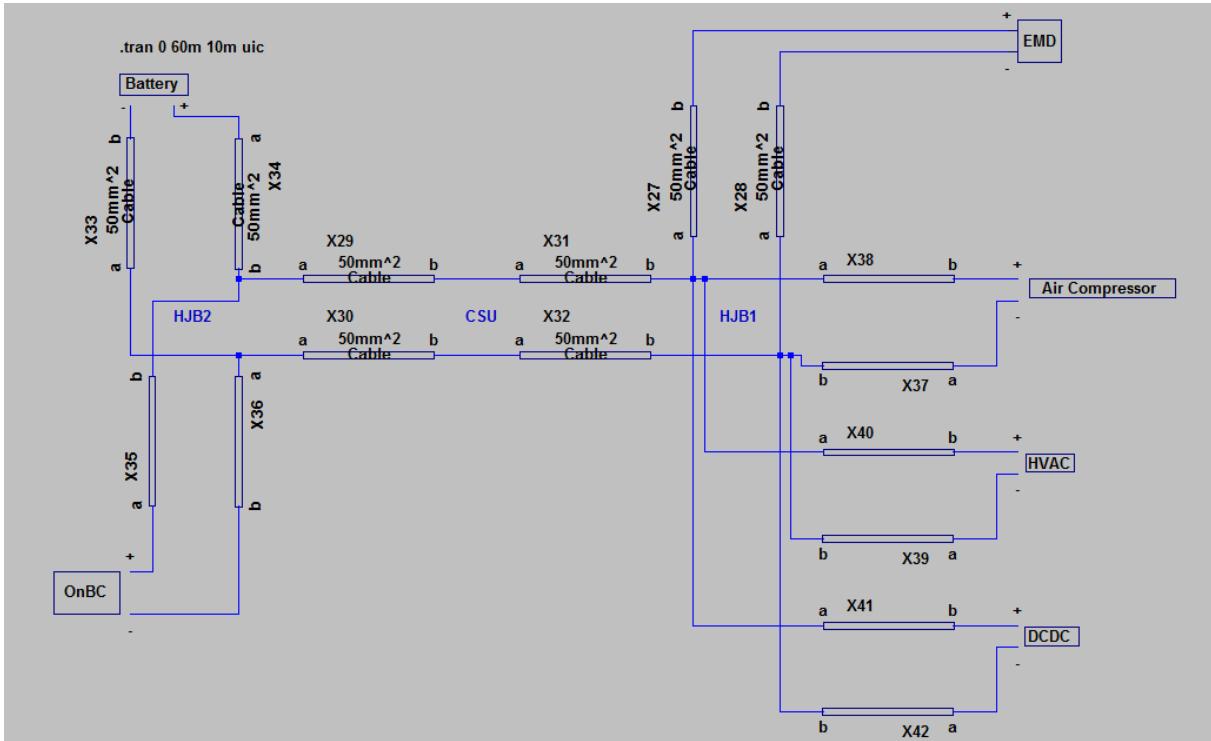
Figure 52 The simulation model, of the TWIN MOTOR BUS1, used to simulate the effects of dual motors #VOLVO

5.4 TWIN MOTOR BUS2

The structural simulation model of the TWIN MOTOR BUS2 can be seen in in Figure 53. The TWIN MOTOR BUS2 contains both the 70 mm^2 cable and the 95mm^2 cable (which has not been modeled yet). The Twin Motor bus2 model was made along with its model library.
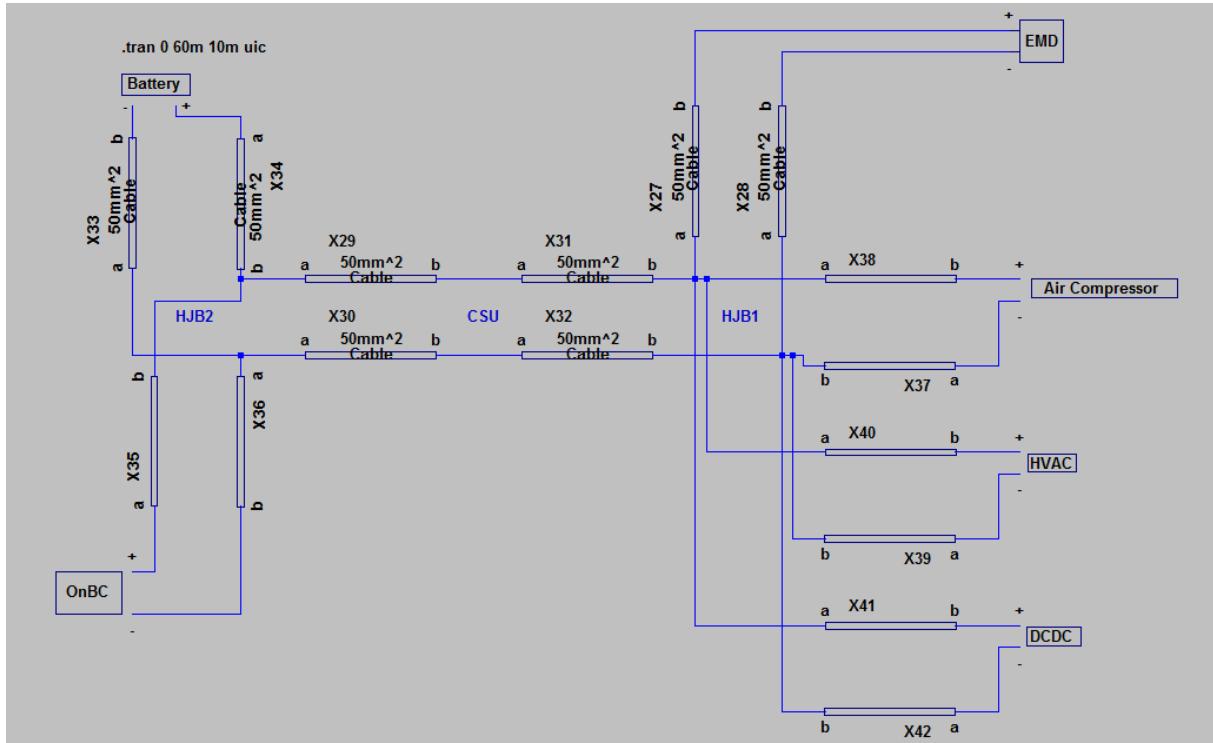
Figure 53 The simulation model of the TWIN MOTOR BUS2 #VOLVO

5.5 EMD type b

The structural simulation model of the EMD type b can be seen in Figure 54. Note that all of the equivalent component values of the inductor and the capacitor are presented in the previous chapter. The pulse height #VOLVO A of the pulsed load current comes from twice the average current at 50 % duty cycle. f_{sw} relates to the switching frequency of the EMD type b, which is set to be on 50 % of the time by the 0.5 factor.
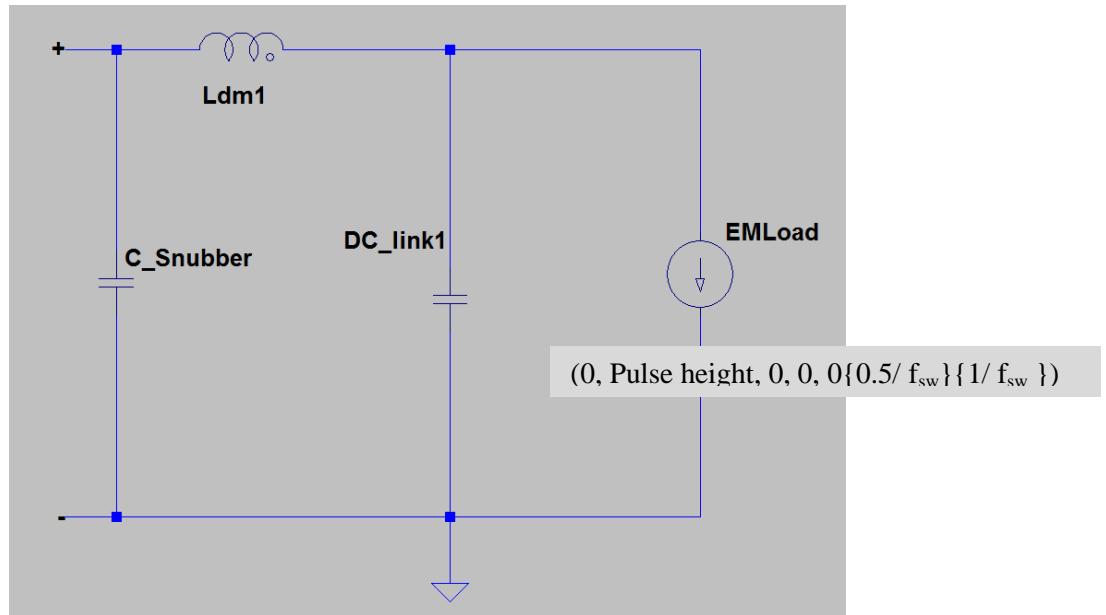
Figure 54 The simulation model of the EMD type b

5.6   EMD type c

Figure 55 shows the simulation model of the EMD type c used in the fully electric bus. All of the values of the measured components can be found in the previous chapter. The pulse height #VOLVO A of the pulsed load current comes from twice the average current at 50 % duty cycle. #VOLVO relates to the switching frequency of the EMD type b at 11.2 % duty cycle as an example of how to simulate the #VOLVO kHz current ripple in the DC link at the point just before the change in switching frequency occurs. In order to simulate the current ripple produced in the DC link by the EMD type c operating at 50 % duty cycle, the rightmost input values can be changed to #VOLVO s and #VOLVO s, respectively.
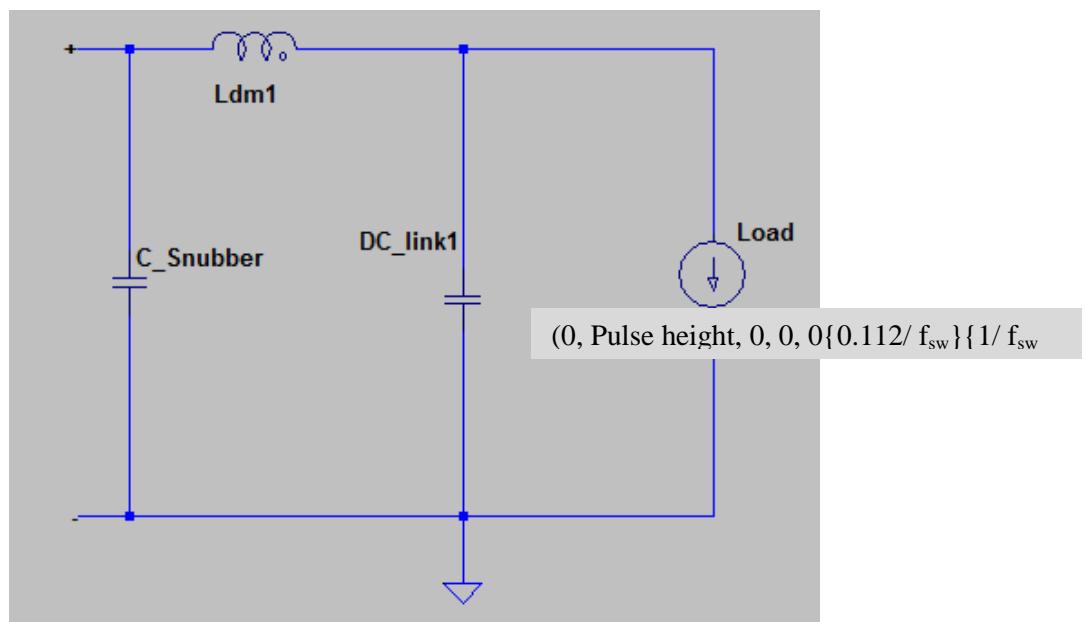
Figure 55 The simulation model of the EMD typ c #VOLVO

5.7   DCDC

In the DCDC model, Figure 56, the missing CM filter has been added in the model. The equivalent components of the CM choke are presented in the previous chapter. The duty cycle of the pulsed current load is 79.4 % according to the formula provided by the previous thesis project. The amplitude of the pulse is calculated by dividing the mean current of the fully loaded DCDC by #VOLVO.

$(0, \text{Pulse height}, 0, 0, 0\{0.794/ f_{sw}\}\{1/ f_{sw}$
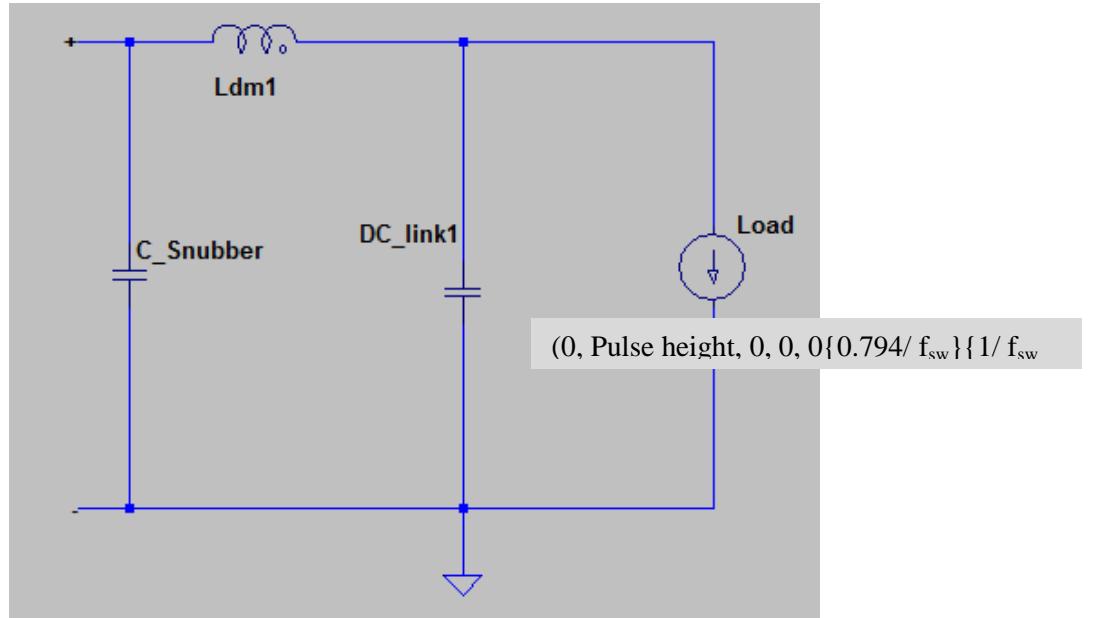
Figure 56. The simulation model of the DCDC #VOLVO

5.8   Air compressor

The simulation model of the air compressor subsystem can be seen in Figure 57. The CM choke is updated with the curve fitting parameters in the previous chapter. The pulsed current load is updated based on the current behavior of the air compressor measured in the electric hybrid bus, which in the previous chapter is estimated to be roughly 52 %. The height of the current pulse is the result of dividing the mean current by the duty cycle.
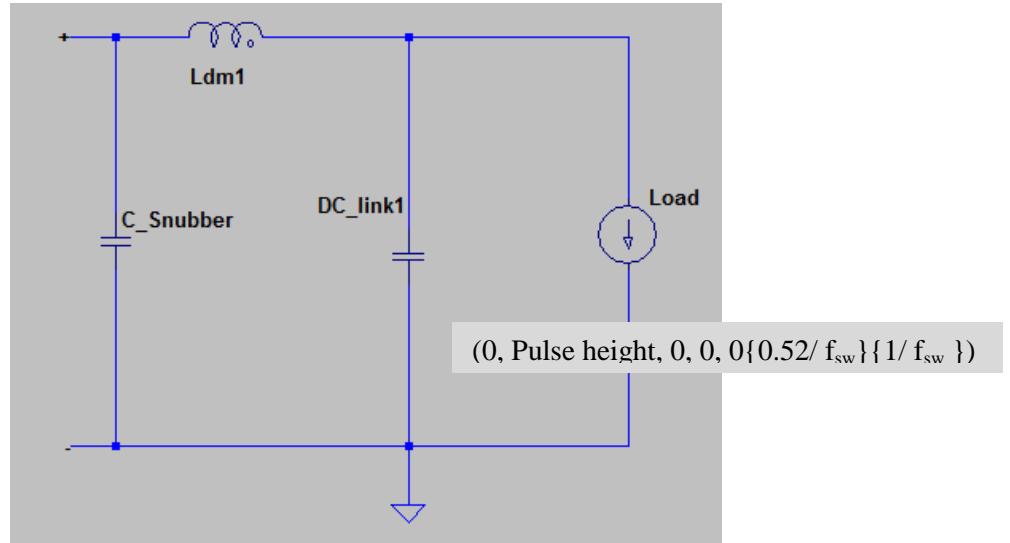
Figure 57 The simulation model of the Air Compressor #VOLVO

5.9 HVAC

The CM choke of the HVAC is updated based on the curve fitting parameters. All of the parameters and the vehicle measurements which the pulsed current load is based on can be seen in the previous chapter. The pulsed current load has been updated based on the current behavior of the HVAC measured in the electric hybrid bus, which in the previous chapter is estimated to be 51.2 %. The height of the current pulse is the result of dividing the mean current by the duty cycle. The simulation model of the HVAC can be seen in Figure 58.
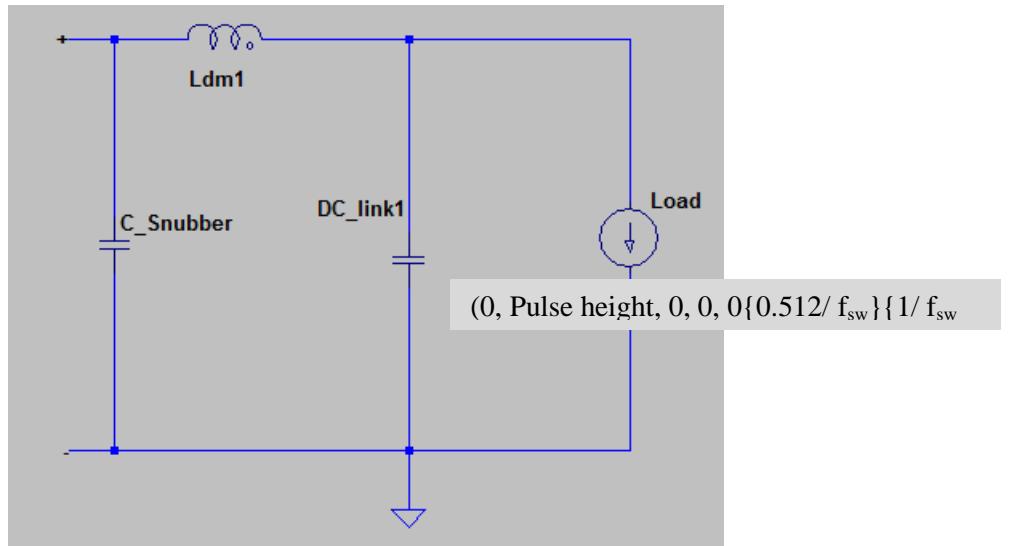
Figure 58 The simulation model of the HVAC #VOLVO

5.10 OnBC

As the on board charger is not active, no current or voltage source is included in the model, as seen in Figure 59. The component is still affected by current ripple, however. All of its CM choke parameters can be seen in the previous chapter.
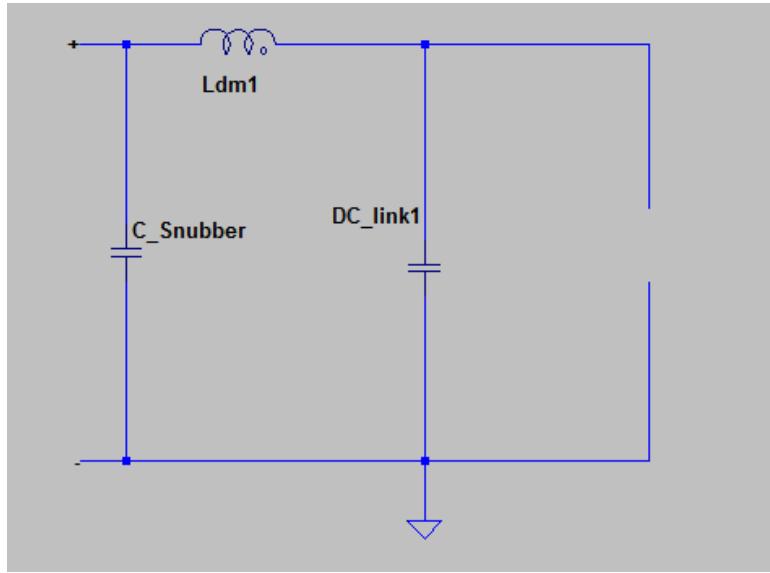
Figure 59 The simulation model of the OnBC #VOLVO

5.11 Battery

The battery model seen in Figure 60 remains relatively unchanged. The series resistance and inductance are based on measurements performed on a single battery cell during the previous thesis project. The voltage level can preferably be changed depending on the voltage level wanted in the system. Other component values are based on specifications provided by Volvo during the previous thesis project.
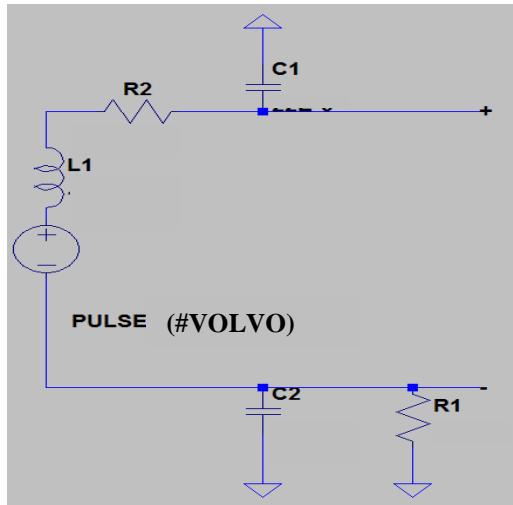
Figure 60 The simulation model of the battery

5.12 Cables

Cable measurements were performed as part of a separate thesis project in which it was also investigated how the placement and connection points of the cables affect its behavior. The existing simulation model was updated based on these values and modeled as a T for all cable types. The cable values were based on the frequency deemed most prominent in the respective TVS they were used in and not based on a curve fitted model.

5.12.1　50 mm²

The model for the 50 mm^2 cable can be seen in Figure 61. The values shown are in per millimeter and hold true for frequencies of #VOLVO kHz.
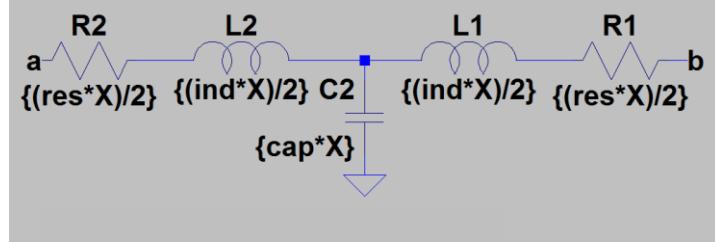
Figure 61 The simulation model of the 50mm² cable

5.12.2　4x2 mm²

The model for the 2x4 mm^2 cable can be seen in Figure 62. The values shown are in per millimeter and hold true for frequencies of #VOLVOkHz.
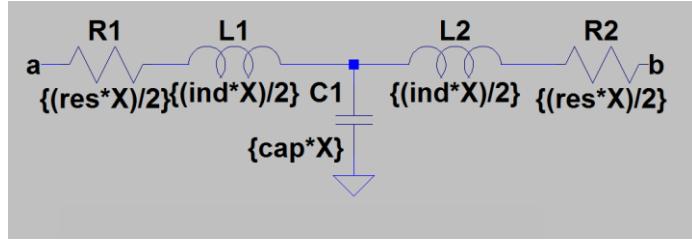
Figure 62 The simulation model of the 4x2mm² cable

5.12.3　70 mm²

The model for the 70 mm^2 cable can be seen in Figure 63. The values shown are in per millimeter and hold true for frequencies of #VOLVO kHz.
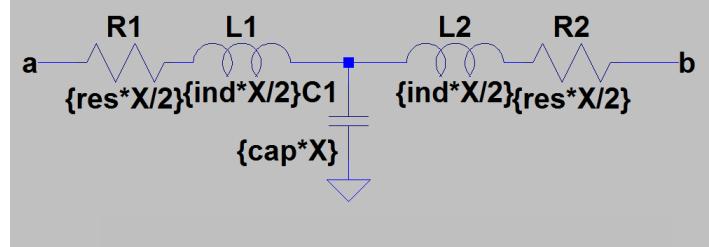
Figure 63 The simulation model of the 70mm² cable

5.13　Heater

The simulation model of the electric heater remains unchanged, as seen in Figure 64.

#VOLVO: Some information, such as figures and values marked with #VOLVO are of specific value to Volvo and not for public. Therefore the figures are replaced and the values are concealed.
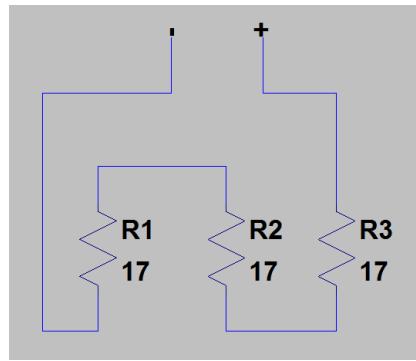
Figure 64 The simulation model of the Heater

5.14 Frequency analysis source

Utilizing the built-in AC analysis tool in LTSpice, a special pulsed current load can be made in order to find the frequency behavior of the simulation model. This load can be seen in Figure 65 along with the operational directive to sweep the frequency from 100 Hz to 100 kHz. To perform the simulation, the pulsed current loads presented earlier in the chapter are exchanged for the AC source and the operational directive exchanged for the one presented in the figure.
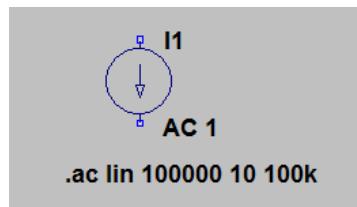
Figure 65 The current source and operational directive used in the AC analysis

6.   Verification

In the verification of the simulation model, many parameters are considered and adjusted for. The battery voltage is set to match the voltage level of the battery in the vehicle at the time of 50 % duty cycle in the case of an accelerating EM. The cable values, received from the other master thesis, are based on the measurements at the most prominent frequency, which is usually the switching frequency of the EMD. Some of the pulsed current loads are, as mentioned in the previous chapter, updated based on the vehicle ripple. To compare the current ripple for different frequencies, an FFT using a flat top windowing function is used for both the simulated and measured values. The AC analyses meant to find current frequencies which can potentially be harmful to components in the DC link of the respective bus models are presented. For the AC analyses, the pulsed current sources are exchanged for AC sources, which are set to sweep the frequency from 100 Hz to 100 kHz.

6.1   Electric hybrid

The visualization of the ripple in the acceleration test can be seen in Figure 66 along with the measured vehicle ripple. The verification for all components in the electric hybrid can be seen in Table 17. A similar verification using a battery model in which the inductance is "tuned" to be accurate when the EMD is active can be seen in Table 18. Note that the measurement probe to the DCDC fell off during the vehicle test. The AC analysis of the electric hybrid is presented in Figure 67.
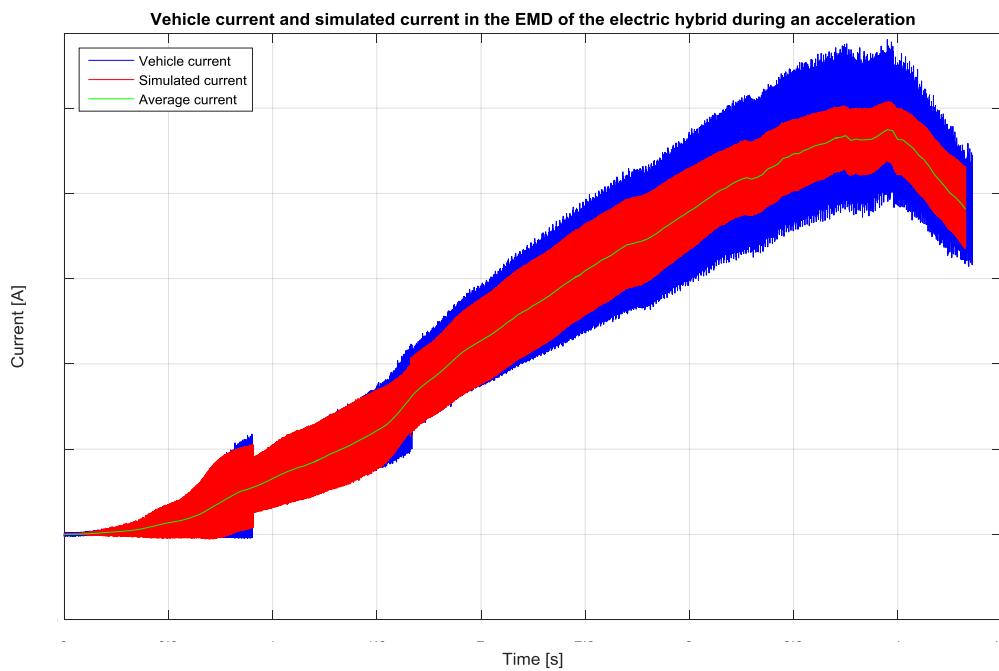
Figure 66 The DC link current ripple measured on the DC terminals of the EMD of the electric hybrid (blue) and the equivalent simulated current ripple (red) during an acceleration at full torque.

65

Table 17 Verification of the current ripple in the electric hybrid.

		EMD active @ #VOLVO kHz	DCDC active @ #VOLVO kHz	HVAC active @ #VOLVO kHz (Not FFT)	Air Com active @ #VOLVOkHz
EMD	Simulation	#VOLVO	#VOLVO	#VOLVO	#VOLVO
	Vehicle	#VOLVO	#VOLVO	#VOLVO	#VOLVO
	Difference	+10.1 %	-42.3 %	+71.4 %	-13.9 % @ #VOLVO kHz -39.0 % @ #VOLVO kHz
DCDC	Simulation	#VOLVO	#VOLVO	#VOLVO	#VOLVO
	Vehicle	#VOLVO	#VOLVO	#VOLVO	#VOLVO
	Difference	NaN	NaN	NaN	NaN
HVAC	Simulation	#VOLVO	#VOLVO	#VOLVO	#VOLVO
	Vehicle	#VOLVO	#VOLVO	#VOLVO	#VOLVO
	Difference	-4.4 %	-60 %	+74.0 %	-35.0 % @ #VOLVO kHz -80.8 % @ #VOLVO kHz +32.0 % @ #VOLVO kHz
Air Comp	Simulation	#VOLVO	#VOLVO	#VOLVO	#VOLVO
	Vehicle	#VOLVO	#VOLVO	#VOLVO	#VOLVO
	Difference	-35.3 %	-33.3 %	-50.2 %	-15.0 %
OnBC	Simulation	#VOLVO	#VOLVO	#VOLVO	#VOLVO
	Vehicle	#VOLVO	#VOLVO	#VOLVO	#VOLVO
	Difference	+26.2 %	-25 %	-15.6 %	+630 % @ #VOLVO kHz -72.7 % @ #VOLVO kHz -76.9 % @ #VOLVO kHz
ESS	Simulation	#VOLVO	#VOLVO	#VOLVO	#VOLVO
	Vehicle	#VOLVO	#VOLVO	#VOLVO	#VOLVO
	Difference	-89.5 %	NaN	-92.5 %	NaN @ #VOLVO kHz -38.4 % @ #VOLVO kHz -97.2 % @ #VOLVO kHz

#VOLVO: Some information, such as figures and values marked with #VOLVO are of specific value to Volvo and not for public. Therefore the figures are replaced and the values are concealed.

Table 18 Verification of the electric hybrid. The battery inductance has been adjusted to #VOLVO H in order to yield a matching current ripple in the battery when the EMD is running.

|		EMD active @ #VOLVO kHz	DCDC active @ #VOLVO kHz	HVAC active @ #VOLVO kHz	Air Comp active @ #VOLVO kHz
EMD	Simulation	#VOLVO	#VOLVO	#VOLVO	#VOLVO
	Vehicle	#VOLVO	#VOLVO	#VOLVO	#VOLVO
					-12.2 % @ #VOLVO kHz
	Difference	-32.6 %	-42.3 %	+50.6 %	-40 % @ #VOLVO kHz
DCDC	Simulation	#VOLVO	#VOLVO	#VOLVO	#VOLVO
	Vehicle	#VOLVO	#VOLVO	#VOLVO	#VOLVO
	Difference	NaN	NaN	NaN	NaN
HVAC	Simulation	#VOLVO	#VOLVO	#VOLVO	#VOLVO
	Vehicle	#VOLVO	#VOLVO	#VOLVO	#VOLVO
					-35 % @ #VOLVO kHz
					-81.5 % @#VOLVO kHz
					+34 % @ #VOLVO
	Difference	-13.3 %	-60 %	+70.5 %	kHz
Air Comp	Simulation	#VOLVO	#VOLVO	#VOLVO	#VOLVO
	Vehicle	#VOLVO	#VOLVO	#VOLVO	#VOLVO
	Difference	-35.3 %	-67 %	-55.2 %	-15.0 %
OnBC	Simulation	#VOLVO	#VOLVO	#VOLVO	#VOLVO
	Vehicle	#VOLVO	#VOLVO	#VOLVO	#VOLVO
					+660 % @ #VOLVO kHz
					-74.5 % @#VOLVO kHz
					-80.2 % @ #VOLVO
	Difference	+26.2 %	-65 %	-38.7 %	kHz
ESS	Simulation	#VOLVO	#VOLVO	#VOLVO	#VOLVO
	Vehicle	#VOLVO	#VOLVO	#VOLVO	#VOLVO
					NaN @#VOLVO kHz
					+28 % @#VOLVO kHz
					-94.3 % @#VOLVO
	Difference	+0.1 %	-92.0 %	-29.3 %	kHz
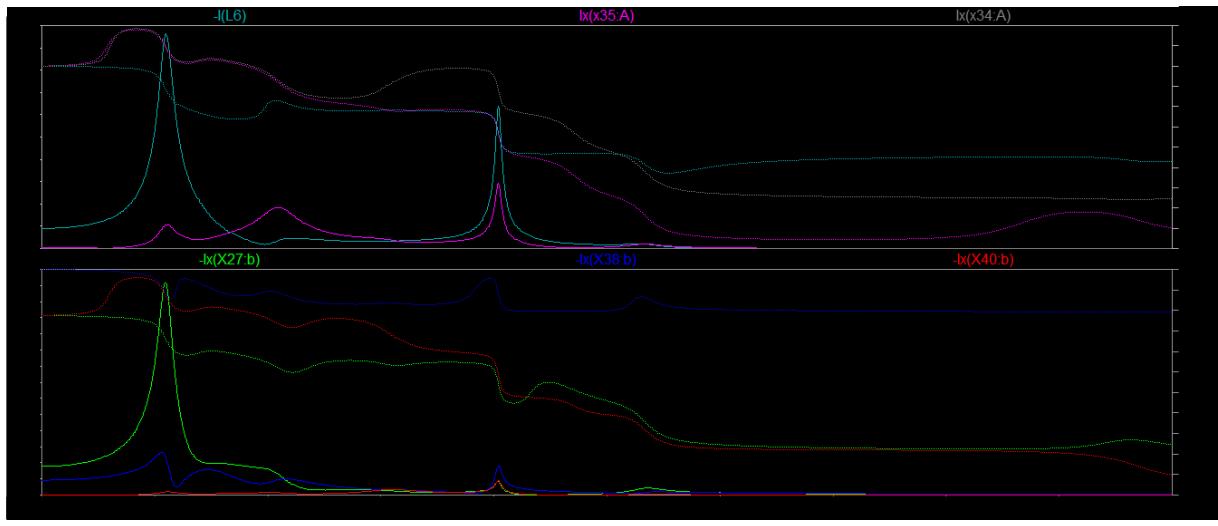
Figure 67 The AC analysis of the electric hybrid. The DC link current as a function of frequency measured at the terminals of the different loads. In the bottom window: EMD type b (green), the air compressor (blue), and the HVAC (red). In the upper window the DCDC (cyan), the OnBC (magenta), and the battery (gray).

Electric

The verification of the electric bus can be seen in Table 19. The AC analysis results can be seen in Figure 68.

Table 19 Verification of the electric bus

		EMD active @ #VOLVO & #VOLVO kHz	DCDC active @ #VOLVO kHz	HVAC active (No file found)	Air Com active @ #VOLVO kHz
EMD	Simulation	#VOLVO	#VOLVO	#VOLVO	#VOLVO
	Vehicle	#VOLVO	#VOLVO	#VOLVO	#VOLVO
	Difference	-96% @ #VOLVO kHz -46.5% @ #VOLVO kHz	-38%		-1%
DCDC	Simulation	#VOLVO	#VOLVO	#VOLVO	#VOLVO
	Vehicle	#VOLVO	#VOLVO	#VOLVO	#VOLVO
	Difference	5% @ #VOLVO kHz 22% @ #VOLVO kHz	-72.6%		30% @ #VOLVO kHz -84% @ #VOLVO kHz NaN @ #VOLVO kHz
HVAC	Simulation	#VOLVO	#VOLVO	#VOLVO	#VOLVO
	Vehicle	#VOLVO	#VOLVO	#VOLVO	#VOLVO
	Difference	NaN @ #VOLVO kHz 10% @ #VOLVO kHz	NaN		NaN
Air Comp	Simulation	#VOLVO	#VOLVO	#VOLVO	#VOLVO
	Vehicle	#VOLVO	#VOLVO	#VOLVO	#VOLVO
	Difference	41.7% @ #VOLVO kHz 1% @ #VOLVO kHz	NaN		-3.2%
OnBC	Simulation	#VOLVO	#VOLVO	#VOLVO	#VOLVO
	Vehicle	#VOLVO	#VOLVO	#VOLVO	#VOLVO
	Difference	20% @ #VOLVO kHz	-84%		NaN
ESS1	Simulation	#VOLVO	#VOLVO	#VOLVO	#VOLVO
	Vehicle	#VOLVO	#VOLVO	#VOLVO	#VOLVO
	Difference	-	-		
ESS2	Simulation	#VOLVO	#VOLVO	#VOLVO	#VOLVO
	Vehicle	#VOLVO	#VOLVO	#VOLVO	#VOLVO
	Difference				
ESS3	Simulation	#VOLVO	#VOLVO	#VOLVO	#VOLVO
	Vehicle	#VOLVO	#VOLVO	#VOLVO	#VOLVO
	Difference				
ESS4	Simulation	#VOLVO	#VOLVO	#VOLVO	#VOLVO
	Vehicle	#VOLVO	#VOLVO	#VOLVO	#VOLVO
	Difference				

#VOLVO: Some information, such as figures and values marked with #VOLVO are of specific value to Volvo and not for public. Therefore the figures are replaced and the values are concealed.

The peak at #VOLVO kHz corresponds to the ripple before the change in switching frequency (0.1117 % duty cycle). The few decimals are due to dewesoft not providing more.
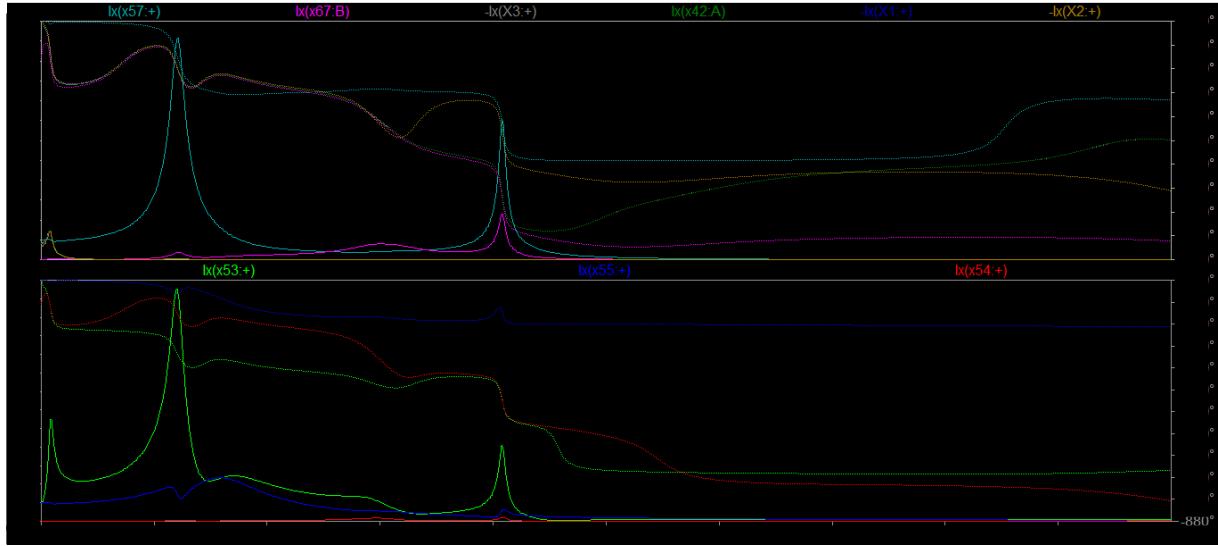
Figure 68 The AC analysis of the electric bus. The DC link current as a function of frequency measured at the terminals of the different loads. In the bottom window: EMD type c (green), air compressor (blue), HVAC (red). In the top window: DCDC (cyan), OnBC (magenta), Batteries 1-4 (gray, dark green, dark blue, brown).

6.2   TWIN MOTOR BUS1

The verification of the TWIN MOTOR BUS1 when the EMD-loads are in perfect sync can be seen in Table 20Table 20 Verification of the TWIN MOTOR BUS1. The results of the AC analysis can be seen in Figure 69. The AC analysis of the TWIN MOTOR BUS1 with the DCDCs removed can be seen in Figure 70 and Figure 71.

Table 20 Verification of the TWIN MOTOR BUS1

Motors in sync		EMD:s active @ #VOLVO kHz	DCDC:s active @ #VOLVO kHz		Air Comp active @ #VOLVO kHz
EMD left	Simulation	#VOLVO	#VOLVO	#VOLVO	#VOLVO
EMD right	Simulation	#VOLVO	#VOLVO	#VOLVO	#VOLVO
DCDC roof	Simulation	#VOLVO	#VOLVO	#VOLVO	#VOLVO
DCDC motor room	Simulation	#VOLVO	#VOLVO	#VOLVO	#VOLVO
Air comp.	Simulation	#VOLVO	#VOLVO	#VOLVO	#VOLVO
OnBC	Simulation	#VOLVO	#VOLVO	#VOLVO	#VOLVO
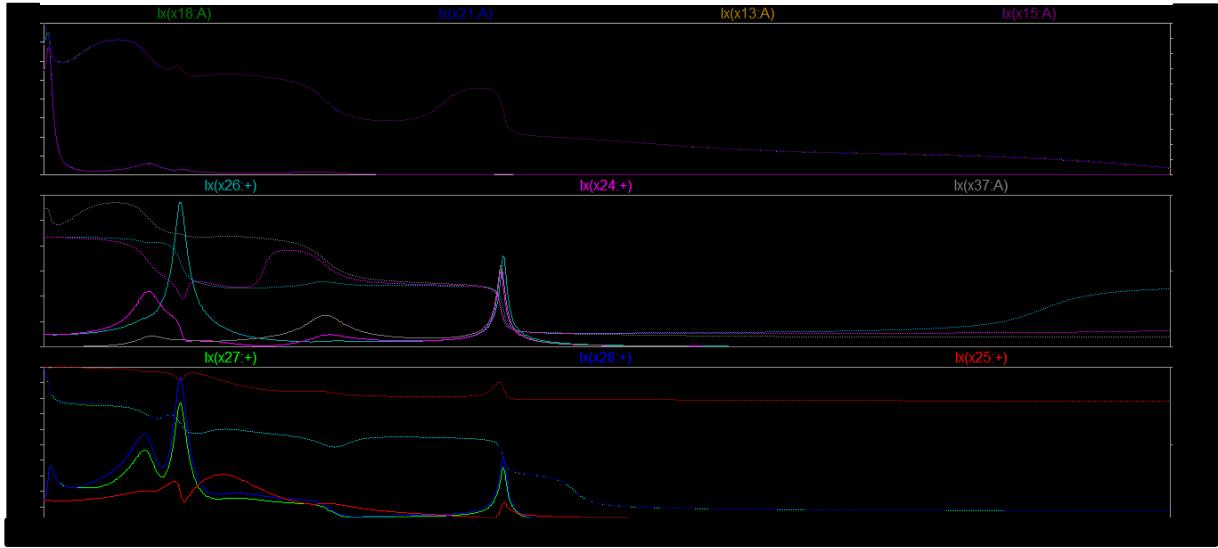
Figure 69 The AC analysis of the TWIN MOTOR BUS1. The DC link current as a function of frequency measured at the terminals of the different loads. Ignoring the battery measurements in the top window. In the bottom window: EMD1 (green), EMD2 (blue), air compressor (red). The middle window: DCDC1 (cyan), DCDC2 (magenta), OnBC (gray).
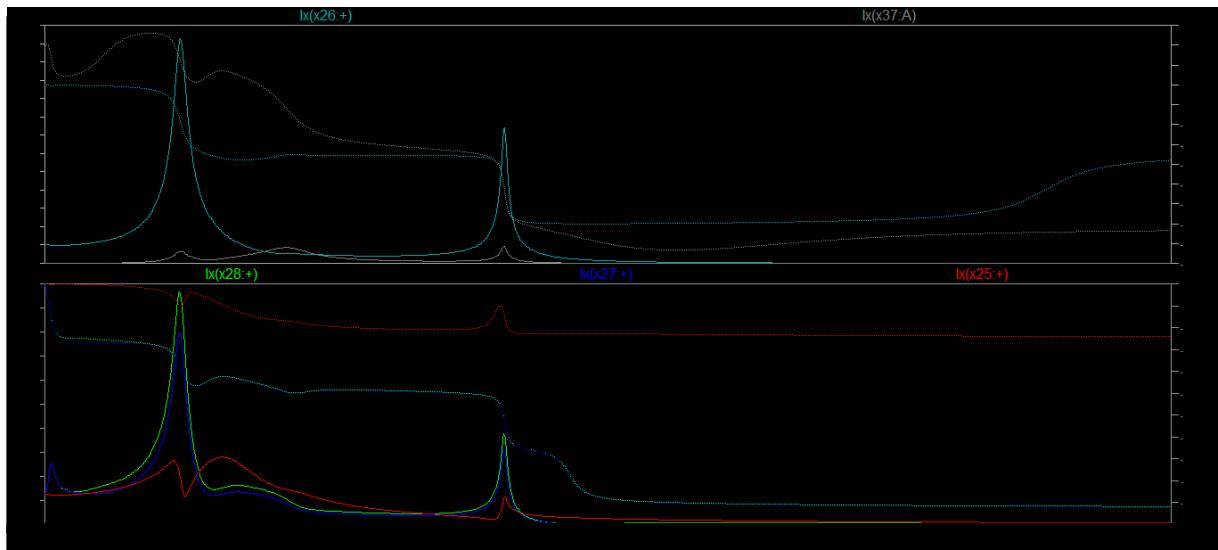
Figure 70 The AC analysis of the TWIN MOTOR BUS1 with one DCDC removed. The DC link current as a function of frequency measured at the terminals of the different loads. Bottom window: EMD1 (green), EMD2 (blue), air compressor (red). Top window: DCDC1 (cyan), OnBC (gray).
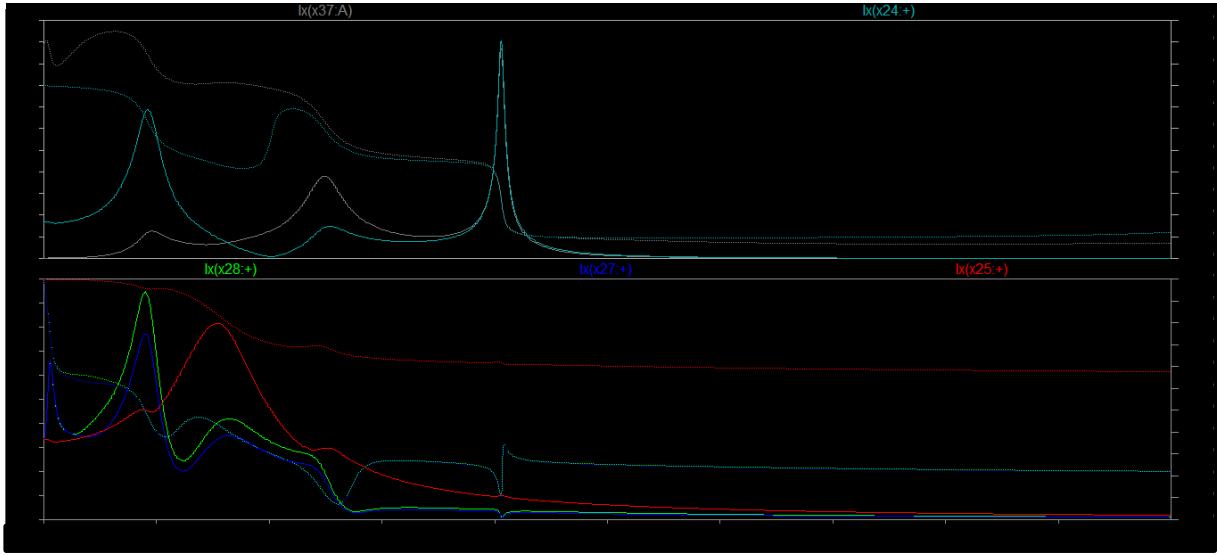
Figure 71 The AC analysis of the TWIN MOTOR BUS1 bus with one DCDC removed. The DC link current as a function of frequency measured at the terminals of the different loads. Bottom window: EMD1 (green), EMD2 (blue), air compressor (red). Top window: DCDC2 (cyan), OnBC (gray).

6.3 TWIN MOTOR BUS2

There are no measurements to compare the TWIN MOTOR BUS2 model to. The AC analysis of the model results in the behavior seen in Figure 72.
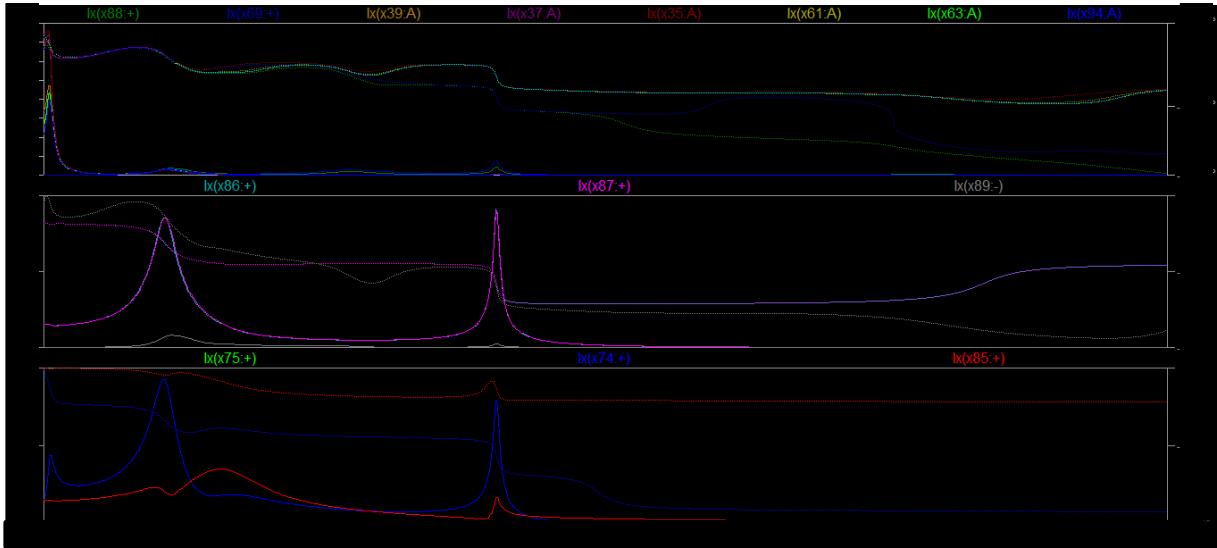
Figure 72 The AC analysis of the TWIN MOTOR BUS2 model. The DC link current as a function of frequency measured at the terminals of the different loads. Ignoring the battery and HVAC measurements in the top window. Bottom window: EMD1 (green), EMD2 (blue), air compressor (red). Middle window: DCDC1 (cyan), DCDC2 (magenta), OnBC (gray).

The acceleration test, in which the current load source of the electric hybrid bus was set to mimic the switching frequency and duty cycle of a real acceleration, is to be taken with a grain of salt. While it appears in Figure 43 as if the simulated current ripple deviates by a large amount for higher speeds, the truth of the matter is revealed when zooming in on the ripple measured in the bus. The real ripple at #VOLVO kHz rather well mimics the shape

72

vaguely appearing in the simulation. However, there are other, lower frequencies, which also come into play at higher speeds. These can be seen in the zoomed in 3D plot of the EMD current plotted against time and frequency in Figure 44 as increasing in frequency. The frequencies of the peaks are likely tied to the speed of the electric motor.

The simulated current ripple values did, as can be seen in Table 17,Table 19 and Table 20, not fall within the 10 % margin of the measured values when the models were based solely on the measured values. The pulsed current loads did not always result in the same behavior as seen in the vehicle measurements with regards to mean current and ripple amplitude either. As some of the components have not been measured at all, namely the battery, this is not very surprising. While probably accurate for the measured frequencies, the frequency dependency of the cables has not been modeled either. As made clear by the verification of the experimental battery inductance tests, tuning the models by simply changing the inductance of the components is likely not possible. Instead, measurements which result in a curve fitted impedance based on a more complex model are required. Until then, tuning of the load models and further in depth verification of the current ripple is wasted.

Verification of the AC analysis model was made by comparing it to one single known value: #VOLVO kHz. The previous EMD switching frequency of #VOLVO kHz had to be removed because its ripple (at #VOLVO kHz) would destroy the DCDC. The AC analysis does offer some insight as to why that is, as the current peaks of either one of the two types of EMD and the DCDC reach a peak around #VOLVO kHz. A similar behavior can be seen at around #VOLVO kHz involving the EMD type c, the DCDC, the on board charger, and to some extent the air compressor. The AC analysis model is likely more accurate than the transient model, in part due to the fact that mainly qualitative analysis of which frequencies are dangerous is needed. The sensitive frequencies also seem to be affected mostly by the components affected in turn by the resonance. In other words, if resonance of some sort occurs between the EMD and the DCDC, as seen in the electric hybrid, the influence of, for instance, the battery is diminished. This hypothesis is somewhat confirmed by removing components. Unless a removed component is involved in the resonance, the resonance remains at about the same frequency and amplitude. What seems to influence the resonance, however, is the distance between the components, as seen when the different DCDCs are removed in the TWIN MOTOR BUS1. Worth noting is also that a source not involved in the resonance itself can still cause resonance elsewhere in the system, although the effect will be slightly attenuated. Practically this means that no component which creates ripple at #VOLVO kHz or #VOLVO kHz can be used in the same system as the components in use today. To sum up, the AC analysis can probably be made even more accurate by adjusting the cable measurements based on some sort of curve fitting, as the resonance seems to be affected by the distance between the resonating components (and therefore the cable parameters). The unfinished battery model, however, does not seem to influence the AC analysis noticeably either when altered slightly or removed completely. For this reason, the AC analysis model is likely to be more useful as of right now than the transient analysis model.

7.   Conclusion

7.1   Results conclusion

Although the verification of the model in general does not point to any major advancement with regards to model accuracy, the project still brought with it some useful results.

Using an LCR meter together with a curve fitting script yields promising results and can be done easily when acquiring new components in the future. Looking into the current dependency of the components, some components clearly appear more susceptible than others. Modeling for this dependency is hard using LTSpice, and the true effects of current dependency in a real vehicle may not be accurately represented by a model based on single component measurements.

As for the simulation model itself, there is still a way to go before the ripple simulations are accurate enough to be useful in the context of placement optimization and component lifetime calculations. Using the model to provide an approximation of which frequencies are likely to cause problems in any similar systems is something that it likely can be used for, however, as the components which influence such an analysis are up and running to a large extent.

7.2   Future Work

The battery measurements serve as a bottleneck for future development of the simulation model, and should therefore be a first priority in taking the next step. Following that, a further model tuning with regards to especially the pulsed current loads and voltage spread should be looked at, as the current ripple is greatly impacted by these factors.

A curve fitting based model, or any model which takes the frequency dependency of the cables into account, would likely also benefit the model. This can probably not be done based on the measurements performed by the separate thesis project and remains as the biggest error source of the AC analysis model.

If a margin of error of less than 10 % is ever required, there are many components to look at in the different systems. Provided Volvo develops a habit of measuring the properties of new components, all components in the existing subsystems would likely benefit from a more thorough model such as the ones described in this report. Taking it even further, even stray elements in the conducting paths of the circuit boards can be examined.

The pulsed current sources are another potential source of error. Seeing how different frequencies come into play for higher speeds in the acceleration test, it might be needed to go to the bottom with this behavior in order to accurately model the loads and simulate the current ripple. This likely involves looking into the control and behavior of the electric motor.

In the end, the model can hopefully be used to determine the optimal input stages of new components with regards to placement and component values, which can then be specified to the manufacturers directly. Looking into how the model can be used for this purpose should be one of the steps in fully utilizing the results of the ongoing chain of thesis projects.

9. References

[1] Abdelbagi, Hamdi Altayib. 2007. SKIN AND PROXIMITY EFFECTS IN TWO PARALLEL PLATES. Master theisis. Wright State University. https://etd.ohiolink.edu/rws_etd/document/get/wright1190054809/inline (Retrieved 2017-06-05)

[2] Alaküla, Mats., Karlsson, Per. (2015 ver 1). Power Electronics. Lund: Department of Industrial Electrical Engineering and Automation.

[3] Alexandersson, Sabine. 2008. Automotive Electromagnetic Compatibility-Prediction and Analysis of Parasitic Components in Conductor Layouts. Diss., Lund University.

[4] Bergman, Mårten; Annerberg, Lars; Grönlund, Anna; Back, Stefan; Nilsson, Petter; Sunér Fleming, Maria. 2016. En klimatneutral och hållbar transportsektor. https://www.svensktnaringsliv.se/migration_catalog/Rapporter_och_opinionsmaterial/Rapporter/en-klimatneutral-och-hallbar-transportsektorpdf_650506.html/BINARY/En%20klimatneutral%20och%20h%C3%A5llbar%20transportsektor.pdf (Retrieved 2017-06-06)

[5] Cheng, David. K. 2013. Field and Wave Electromagnetics. 2nd Edition, Pearson New International Edition. Edinburgh: Pearson Education Limited.

[6] Dowell, P.L. 1966. Effects of eddy currents in transformer windings. Proceedings in the Institution of Electrical Engineers., vol 113, no. 8. http://ieeexplore.ieee.org/document/5247417/ (Retrieved 2017-06-05)

[7] Hambley, Allan R. 2011. Electrical Engineering- Principles and applications. 5th edition. New Jersey: Prentice Hall.

[8] Hioki. 2017. Hioki E.E.Corporation https://www.hioki.com/en/products/listUse/?category=10 (Retrieved 2017-03-07)

[9] Konstantin Kostov and Jorma Kyyrä. 2009. Common-Mode choke coils characterization. In: Proceedings of the 13th European Conference on Power Electronics and Applications (EPE 2009). Publication VII. Spain: Barcelona. 2009.

[10] Lineberger, Lewis. 2011. L Inductor. LT-Wiki. http://ltwiki.org/index.php5?title=C_Capacitor (Retrieved 2017-05-12)

[11] Lineberger, Lewis. 2011. C Capacitor. LT-Wiki. http://ltwiki.org/LTspiceHelp/LTspiceHelp/L_Inductor.htm (Retrieved 2017-05-12)

[12] Lugnberg, Christian; Wenander, David. 2017. Current ripple simulation in DC traction voltage system of an electric bus. Master Thesis. Lund University.

[13] MuRata. 2009. Differntial and common mode noise. Noise Suppression Techniques. http://www.murata.com/~/media/webrenewal/products/emc/emifil/knowhow/26to30.ashx?la=en-gb (Retrieved 2017-02-20)

[14] Nelson, Garcia. 2012. Power inductors and peak-current handling capability. Power Systems Design. https://www.powersystemsdesign.com/power-inductors-and-peak-current-handling-capability/22 (Retrieved 2017-06-05)

[15] Puls Electronics. 2017. Understanding common mode noise. Pulse Electronics. http://www.power.pulseelectronics.com/hubfs/CM_Chokes/Pulse-Power-BU-Understanding-Common-Mode-Noise.pdf?t=1496769774758 (Retrieved 2017-02-20)

[16] Schultz, Charlotta von. 2015. Volvos första elbuss rullar i trafiken. NyTeknik. http://www.nyteknik.se/fordon/volvos-forsta-elbuss-rullar-i-trafiken-6393682 (Retrieved 2017-06-06)

[17] Vandelac, J.-P., Ziogas, P.D. A novel approach for minimizing high-frequency transformer copper losses. IEEE. http://ieeexplore.ieee.org/document/17944/ (Retrieved 2017-06-05)

[18] Zadeh, Nadia; Hjert, Andreas; Renukaiah, Navya K; Maheshwar, Shivadeep; Murthy, Sri V.G.N; Shukla, Tanmay M. 2017. Injection Transformer Equipment for Battery Characterization Tests. Power Engineering Design Project. Chalmers University of Technology.

List of abbreviations

CM – Common Mode

DM – Differential Mode

EIS - Electrochemical Impedance Spectroscopy

EMD – Electric Motor Drive

ESS – Electrical Storage System

HVAC – Heat Ventilation Air Condition

MDS – Motor Drive System

PEC – Power Electronic Converter

TVS – Traction Voltage System

List of figures

List of tables

Appendix A - Matlab script- curve fitting

Make a curve fit of the measured impedance of a component to determine the equivalent component parameters of the measured component by defining the total impedance as a function of all its equivalent components.

The function fminsearch(FUN,X0) is a standard matlab function for multidimensional nonlinear minimization. The input value Xo is the start value that the function FUN uses to calculate the minimizer. More about fminsearch; press 'help fminsearch' in Matlab.

The function fun() compares the calculated values and the measured values for the impedance, and returns the difference to fminsearch. Fminsearch then controls if the minimum tolerance is reached.

When the tolerance is reached the function fminsearch returns a vector or matrix of the same dimension as the start value.

With the fminsearchbnd function it's possible to set limitations, both upper and lower. To make sure the parameter values are positive the lower limitation should be zero. Fminsearchbnd runs the fminsearch with the given functions and controls that the returned value meet the limitations before it returns the value. The script of fminsearchbnd can be found on mathworks.com.

Ex. To represent the CM-choke, an Inductor can be used. Schematic for the inductor with the parasitics can be seen in Appendix figure 1.
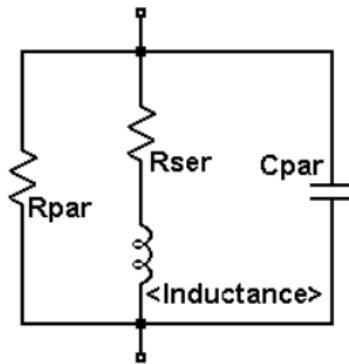
Appendix figure 1 Equivalent circuit of an inductor

The total impedance of the inductor is then represented as z:

$$z = (\frac{1}{R_{par}} + \frac{1}{z_{ser}} + \frac{1}{C_{par}})^{-1}$$

Where z_{ser}:

$$z_{ser} = R_{ser} + Inductance$$

fitToCurve.m

```matlab
f = […]; %Vector with the measured frequency

z = […]; %Vector with the measured impedance


figure(1)

plot(f,z) % Make a plot of the measured impedance as a function of the
frequency
hold on


%% Make initial guesses of the unknown parameters

x1(1) =[0.001];       % Rs
x1(2) =[2*10^-6];     % L
x1(3) =80*10^10;      % Rp
x1(4) = 10^-12;       % Cp


title('Impedance as a function of frequency for the CM-choke in EMD_B')
xlabel('Frequency [Hz]')
ylabel('Impedance [Ohm]')


for i = 1:3

    Rs2 = x1(1);
    L2 = x1(2);
    Rp2 = x1(3);
    Cp2 = x1(4);


    x = fminsearchbnd(@(pp) fun(f,z,pp),[Rs2,L2,Rp2,Cp2], [0, 0, 0, 0],
[],optimset('MaxFunEvals',1e7,'MaxIter',1e7)) % Gives an vector x, with the
parasitics


    % z for an inductance with the parasitics
    z3 = (x(1) + j*2*pi.*f.*x(2));
    z4 = abs((1./x(3) + j*2*pi.*f.*x(4) +1./(z3)).^-1);
    plot(f,z4) % Make a plot of the calculated impedance as a function of
the frequency

end

legend('Measured z','Curve fitting 1','Curve fitting 2', ' Curve fitting
3',' Curve fitting 4')
```

fun.m

```matlab
function err= fun(f,z,pp)

        Rs=pp(1);
        L=pp(2);
        Rp= pp(3);
        Cp= pp(4);


        %The function that is compared to the measured impedance must be
        the same as in the fitToCurve-script.

        z1 = (Rs + j*2*pi.*f.*L);
        z2 = abs((1./Rp + j*2*pi.*f.*Cp +1./(z1)).^-1);
        er = z-z2;


        err=sum(abs(er));

end
```

Appendix B - Simulation model manual

For basic instructions on how to organize your file library and get started with building the main structure of a model, please see the previous thesis. This model manual is focused mainly on two subjects:

- Pulsed current load design of an accelerating bus
- AC analysis model design

In order to model the pulsed current load of an accelerating bus, knowing the different switching frequencies and approximately when the change from one switching frequency to another occurs is essential. The other thing that is changing during acceleration is the duty cycle. In order to model all of this, an arbitrary behavioral current source can be used. Such a source can be found in the standard LTSpice library under the name "bi" and it outputs a current based on the function it is given. In the figure below, the current source marked EMDLoad is an arbitrary behavioral current source. Its output is determined by the line of code next to it. The "if" statement will output a 0 or a 1 depending on whether the voltage level of the different triangle waves generated by V1, V2, or V3 is currently higher than the duty cycle, which goes from 0 % to 100 % during an acceleration. Whether the voltage of V1, V2, or V3 is used to determine if the total output should be 1 or 0 is also determined by the duty cycle, as the change in switching frequency represented by the different voltage source frequencies changes when the motor speed (duty cycle) reaches a certain level.

If the exact acceleration of a vehicle is to be simulated, as in the simulation test, the voltage source labeled Duty_cycle_voltage can be set to mimic the duty cycle of a real acceleration by using the mean current of the vehicle measurement divided by the pulse height as input to the Duty_cycle_voltage source. This can be done by assigning the source a PWL input and read the data points from the real duty cycle and the points should range from 0-1. If a constant increase in duty cycle is preferred, this can be simulated simply by setting the PWL source to go from 0 to 1 over the course of time the acceleration should take.

The result of the "if" statement is then multiplied with the total pulse height at the end in order to simulate the current ripple accurately.
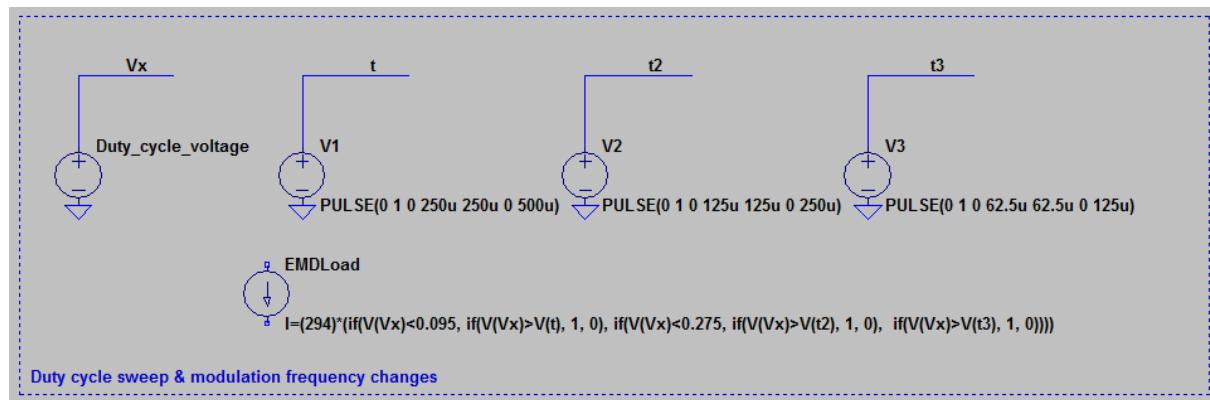

Appendix B- Figure 1 Accelerating EMD

The AC analysis is far simpler. What is required for it to work is to exchange the pulsed current loads which are to be active in the analysis for AC sources and remove the others. An AC source is a simple current source which can be set to perform a sweep across all frequencies in order to see if any stand out. To do so, no particular function needs to be used, but the AC Amplitude in the AC analysis window to the right in the figure below has to be set to 1. This allows for the current source to be controlled by the operational directive. An example of such can be seen in the second figure below.

When all is modeled properly, simply click Simulate as usual. Then click the nodes of the different components to get the results presented in this report.
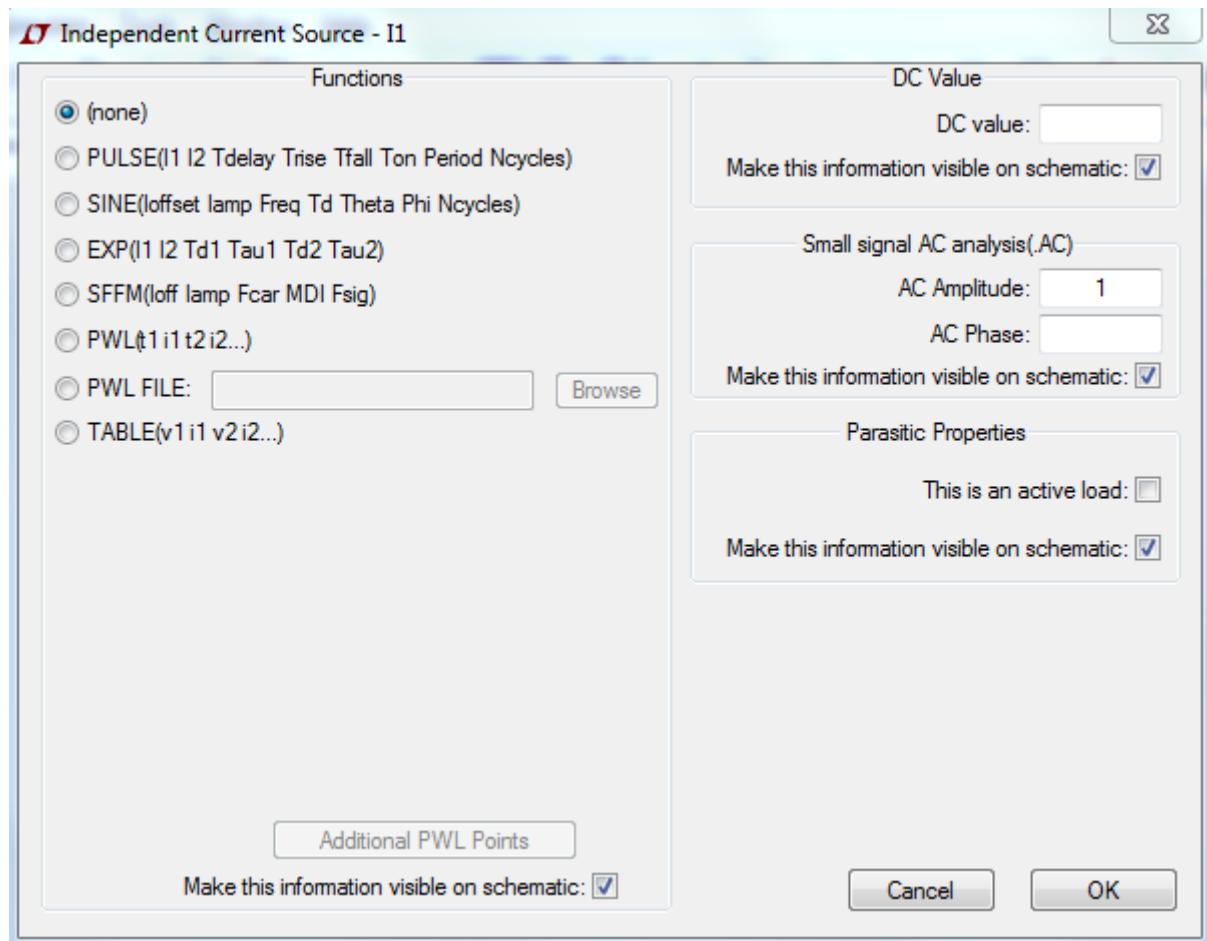
Appendix B- Figure 2 The AC source setup
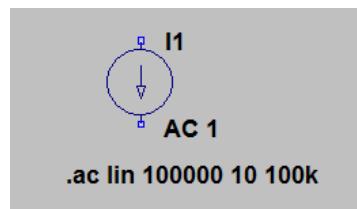
Appendix B- Figure 3 Current source and operational directive used in the AC analysis